Public Report

Project no. **019830**

Project acronym: **SOLHYCO**

Project title: ***Solar-Hybrid Power and Cogeneration Plants***

Instrument: SPECIFIC TARGETED RESEARCH OR INNOVATION PROJECT

Thematic Priority: 6.1.3.2.3 "New and advanced concepts in renewable energy technologies"

Final Public Report

Period covered: from 01.01.2009 to 30.06.2010

Date of preparation: 21.03.2011

Start date of project: 01.01.2006

Duration: 54 months

Project coordinator name: Dr. Peter Heller
Project coordinator organisation name: Deutsches Zentrum für Luft- und Raumfahrt e.V. (DLR)

Revision [3]

1 Executive summary

1.1 Summary of work performed and results achieved

The SOLHYCO project started on 1st January 2006 and finished on 30th June 2010.

The scientific and technological objective of the SOLHYCO project was to develop and test a highly efficient, reliable and economic solar-hybrid cogeneration system based on a 100 kW microturbine, able to operate in parallel on varying contributions of solar power input and fuel.

Development of an innovative absorber tube technology

As key component, an innovative solar receiver should have been developed based on an innovative profiled multi layer (PML) tube concept. This technology would enhance the heat transfer from the irradiated tube wall to the gas and allow for reduced temperature differences on the circumference of the tube, thus reducing stress and leading to higher life time. During the course of the project, the manufacturing of such tubes was developed and first samples and test tubes up to a length of 1.3 m were tested in a laboratory setup. It could be shown, that the temperature difference on the tube circumference could be reduced from 73.7 °C to 14.1 °C or 80.9 % respectively. Although a great success, it was also noted that the durability of the intermetallic connection was not yet sufficiently withstanding temperature cycling.

Due to time delays in the development of the manufacturing method for the solar receiver it was decided to built the receiver for the prototype microturbine system from mono-layer tubes. The receiver has the same design as with PML tubes, such allowing a later replacement of the tubes.

Solar component qualification test

To elaborate the use of bio-diesel for 100% renewable operation of such plant, a study was realized and necessary modifications for a turbine system developed. The operation with biodiesel was then implemented in the former SOLGATE test setup consisting of a 250 kW airborne gas turbine with three solar receivers. During this project the solar hybrid operation had been successfully demonstrated in 2003, but with kerosene as backup fuel. Now this system was modified and equipped for biodiesel operation. In the test phase from March 1st 2008 until March 13th 2009 approx. 100 hours of turbine operation were achieved, of which 57 hours of solar operation could be accumulated. The system was successfully operated at 100% power from renewable energy sources. Tests were accomplished with even higher receiver air outlet temperature (843 °C) than planned and electric power generation reached almost 220 kW. Data evaluation showed that the performance of the system did not significantly change between kerosene and biodiesel operation. The control system worked very well, solar hybrid operation was successfully demonstrated.

In April 2009 the complete system was dismantled.

Development of solar-hybrid microturbine cogeneration unit, system test and evaluation

The design of the Turbec T100 microturbine had to be modified from the original cogeneration unit since the operation conditions as solar-hybrid unit are quite different. The solar receiver adds additional volume and acts as heat sink during start-up which requires modifications of the control system. The flow paths had to be improved and pressure losses in

the system optimized. The combustor had to be modified due to the different cooling necessities stemming from higher temperatures due to the solar receiver.

The solar receiver for the Turbec T100 microturbine was manufactured in spring 2009. The test bed in the CESA-1 tower was prepared and a test plan defined. The receiver cavity was designed, manufactured and assembled. In summer 2009 the complete system could be built up in the test facility. Electrical wiring was completed and the flux measurement system prepared. A data acquisition system had to be installed and programmed. First system tests started in autumn 2009 showing still major initial problems with the turbine operation and control which could not been solved before spring 2010. Then, the system was successfully tested through a period of more than 165 hours of turbine operation whereof 100 hours were solar operation. The system was operated at design conditions of 800 °C receiver outlet temperature. Unfortunately the receiver efficiency could not been measured with the desired accuracy, since the receiver cavity showed defects already after a few testing hours. This led to major heat leaks which could not been precisely determined. Nevertheless the complete system behaved very good and solar hybrid operation could be demonstrated successfully. Also the first solar-only gas turbine operation worldwide of two hours of operation was achieved. Additionally, it could be shown that a receiver window has a positive effect on the system performance, especially for setups with receivers not facing vertically downwards.

Commercial system layout and cost analysis

Different design variations for cogeneration systems and Combined Cycle systems were analyzed and the cost for electricity generation evaluated. For the small cogeneration systems (100 kWe) the final receiver design resulted in a more expensive layout leading to overall system cost of 3,440 €/kW. The cost study shows that with this layout the cost for electricity generation for a good solar site in Algeria is 0.101 €/kWh in an operating scheme with 25 % solar share. To be fully competitive, the system must reduce the Levelized Electricity cost (LEC) by only 20% which seems to be feasible. For the large CC systems a 21 MW system was selected and evaluated. The LEC of such system is 0.078 €/kWh being operated in base load configuration with a solar share of 18 %. For solar shares of 35 % the LEC will be 0.094 €/kWh. This plant would be operated in mid load for 4000 hours per year. It could be shown that the solar hybrid CC system can provide dispatchable power at a high conversion efficiency of 48 %.

Market assessment

The Mediterranean market was studied in detail to elaborate the market potential for the SOLHYCO technology. The market assessment showed that in most countries the market for hybrid systems is not very well prepared since feed-in regulations, if existing, prefer storage against hybrid solutions. However, the Algerian market, providing also a great solar resource, is offering adequate feed-in regulations for hybrid systems and is identified as the preferred actual market in the Mediterranean. This is especially valid for the big CC plants, since the generation cost and such the profitability is advantageous. If the above mentioned CC plant of 21 MW is operated with a 25 % solar share, the LEC is 0.085 €/kWh and thus close to be profitable in the Algerian market.

For the Brazilian market assessment three cases for different cogeneration applications with the solar-hybrid gas turbine were studied. An analysis of the solar radiation potential in Brazil was realized and the data provided for the case study. It is expected that the internalization of the technology and the development of local providers for several items of the system could cause a considerable improvement on the LEC value, which would allow its settlement as a competitive alternative for clean energy generation in the country. Dissemination activities

were accomplished on the Brazilian National Solar Congress, on the Brazilian Symposium on Agroenergy and by the conduction of two SOLHYCO-workshops.

The market potential assessment for solar hybrid cogeneration systems in Mexico was issued. The market value for the industrial and rural sector was discussed. The market for cogeneration systems in rural areas, which was identified as being most attractive and near-term, has the size of approx. 1000 SOLHYCO units with an investment of almost 400 million Euros. It was concluded that the SOLHYCO technology is close to being competitive in these markets, where today Diesel generators are providing electricity. Also, a workshop on solar-hybrid cogeneration systems in Mexico was carried out.

Dissemination

As dissemination activities, for the SOLHYCO project three web sites were created in English, Spanish and Portuguese language. These web sites are containing the project results and much information on the technology. During the course of the project also intermediate progress on the development of the SOLHYCO technology was published in a total of 15 papers or articles.

2 Project objectives and work performed

2.1 General project objectives

The SOLHYCO project started on 1st January 2006 and finished on 30th June 2010.

The scientific and technological objective of the SOLHYCO project was to develop and test a highly efficient, reliable and economic solar-hybrid cogeneration system based on a 100 kW microturbine, able to operate in parallel on varying contributions of solar power input and fuel. A new receiver concept, based on an innovative receiver tube configuration, shall improve performance and reduce system cost. Enhancing the combustion system to multi-fuel capability including bio-fuels shall allow operation with up to 100 % renewable energy sources. Such small systems are intended for early market introduction of solar-hybrid systems, preparing the way for highly efficient Combined Cycle plants in the long term. Figure 1 shows the schemes of a solar-hybrid cogeneration and a Combined Cycle system.

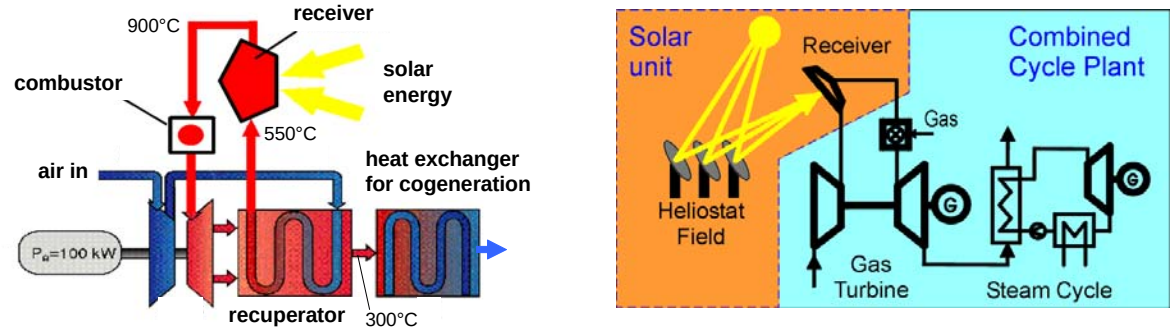

Figure 1 Schemes of a solar-hybrid cogeneration (left) and a Combined Cycel plant (right)

The specific technical objectives of SOLHYCO to be achieved within this project were:

- Design and manufacture a prototype solar-hybrid cogeneration unit by modification of a commercial 100 kWe microturbine and integration with a tube receiver; demonstrate operation with 80 % solar share;
- Develop an innovative "profiled multilayer tube" receiver concept for temperatures > 800 °C with 85 % efficiency;
- Develop and test a solar-hybrid combustion system for bio-Diesel with combustor air inlet temperatures of 800 °C for 100 % renewable operation of the test system;
- Evaluate performance and economic data for optimized solar-hybrid cogeneration systems (100 kWe to 5 MW) and large solar hybrid Combined Cycle (CC) power plants (> 20 MW) to verify the long term cost reduction goal of 0.05 €/kWh (CC);
- Prepare market introduction for solar-hybrid cogeneration systems by identification of initial niche applications in the Mediterranean region, Brazil and Mexico.

State-of-the-art

Solar-hybrid systems are considered as a promising option to integrate solar power into the grid while maintaining the dispatchability of conventional power plants. In addition, such plants offer a significant cost reduction potential for solar power, i. e. the power fraction generated by solar energy. State-of-the-art is the introduction of solar heat into steam cycle power plants, which can only offer a limited conversion efficiency of 30 – 40 % at the foreseen power levels. In contrary, the introduction of solar heat into highly efficient Combined Cycles, using modern gas turbines, can significantly increase the conversion

efficiency (up to 55 %). At smaller power levels, cogeneration of heat and power is an attractive option by making use of the high exhaust temperature of the gas turbine, thus getting an additional benefit.

Solar Receivers: Introducing solar energy into gas turbine cycles requires solar receivers that can heat the pressurized air after the compressor to high temperatures using the absorbed solar power (see Figure 2). This technology has been investigated and developed in recent R&D projects. In a first project, REFOS, the feasibility of the pressurized receiver technology was proven. Within the consequent SOLGATE project (co-funded by EC) the combination of the key components, a gas turbine and a solar receiver, was successfully demonstrated at a power level of 230 kWe. Three receiver modules in serial connection, operating at increasing temperature levels, were used. The first receiver module was a tube receiver operating up to 600 °C, the next two stages were pressurized volumetric receiver modules that achieved air exit temperatures up to 800 °C and 960 °C. In a follow-on project (HST) the previous receiver setup was modified, and the receiver was tested up to 1030 °C.

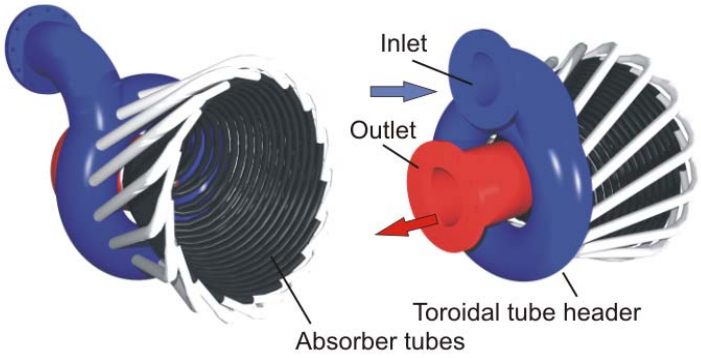

Figure 2 Solgate tubular receiver for 600 °C air outlet temperature

During the development of the low temperature tube module in the SOLGATE project (Figure 2), investigations were made to evaluate the upper limit of tube receivers for solar-hybrid gas turbine systems. Typical for this application is the strongly inhomogeneous heat load on the absorber tubes (solar fluxes up to 500 kW/m^2 on the front side; low fluxes on the backside of the tubes). Two limiting factors were identified: the low heat conductivity of high temperature metal alloys and the poor ratio between heat transfer coefficients and pressure drop.

Finite element calculations of the temperature and stress distribution at the cross-section of the absorber tubes showed high temperature gradients in the tube walls (up to 220 K). The high temperature gradients are caused by the low thermal conductivity of the tube material and the relatively low heat transfer coefficient between tube wall and air at the inner side of the tube. This leads to high and inhomogeneous stresses (reduced life time) and a relatively low air outlet temperature compared to the maximum allowed surface temperature.

Microturbine systems for cogeneration are available on the market since several years. They offer high overall efficiency of up to 80 %, combined with a good electric efficiency of 30 %. Such systems are often applied for combined power and heating and/or cooling. Cooling is obtained by using the hot exhaust gas of the microturbine to drive an absorption chiller.

From the testing experience and the results of accompanying studies the following conclusions were drawn:

- basic technological components are developed and demonstrated
- tube receiver technology has significant potential for improvement
- potential for solar-hybrid gas turbine power plants exists

- market introduction preferably at low power levels (e.g. microturbine)
- later up-scaling to Combined Cycle plants has the potential to reach competitive electricity cost

Based on these conclusions the SOLHYCO project was initiated by the following partners (Table 1) and the work was proposed to be structured as can be seen in Table 2.

Table 1: Partners of the SOLHYCO project

Participant name	Participant short name	Country
Deutsches Zentrum für Luft- und Raumfahrt e.V.	DLR	Germany
Turbec AB	TURBEC	Sweden
Centro de Investigaciones Energéticas, Medioambientales y Tecnológicas	CIEMAT	Spain
CEA/GREThE	CEA	France
ORMAT Systems	ORMAT	Israel
Abengoa Solar New Technology	Abengoa	Spain
FTF	FTF	Germany
New Energy Algeria	NEAL	Algeria
Technika Cieplna Sp. Z o.o	GEA	Poland
Fundação de Apoio a Universidade de São Paulo	FUSP	Brazil
Vitalux Eficiencia Energética Ltda.	Vitalux	Brazil
Instituto de Investigación Electrica	IIE	Mexico

Table 2: Overview on work packages

Work package	Work package title
WP 1	Development of solar-hybrid receiver components
WP 2	Development of solar bio-fuel system
WP 3	Solar component qualification tests
WP 4	Development of solar-hybrid microturbine cogeneration unit
WP 5	Cogeneration unit system test and evaluation
WP 6	Commercial system layout and cost analysis
WP 7	Market assessment Mediterranean
WP 8	Coordination and Management
WP 9	Technological assessment - Brazil
WP 10	Market Assessment Brazil
WP 11	Market Assessment Mexico

2.2 Development of an innovative absorber tube technology

To reduce the temperature gradients between the irradiated front side and the non-irradiated back side of the absorber tubes the concept of the "profiled multilayer tube" (PML tube) technology should been developed. It consists of using three metallic tube layers: a high temperature alloy at the outer side, copper as intermediate layer and another high temperature alloy layer at the inner side of the tube (see Figure 3). The function of the copper with its much higher heat conductivity is to distribute the heat by conduction throughout the circumference. The outer layer provides the structural strength. The inner layer protects the copper from corrosion at high temperatures. In addition, a spiral profile can be implemented on the inner surface to improve the heat transfer coefficient.

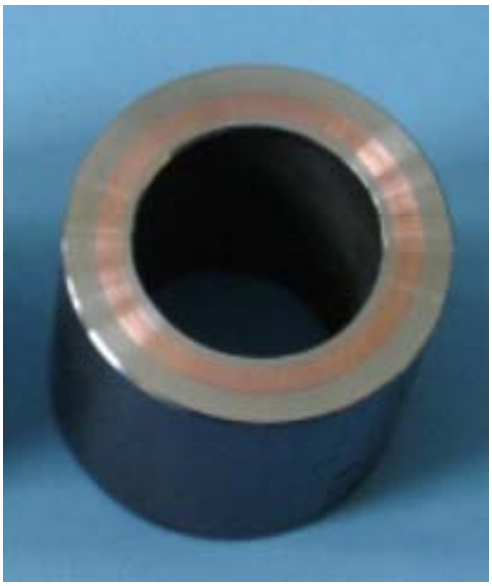

Figure 3 Multi-layer tube sample

Preliminary calculations for a solar receiver showed that the temperature gradient in the tube wall could be significantly reduced, as well as the maximum temperature of the tube. Figure 4 shows the simulated temperature distribution in standard (left) and multi-layer absorber tubes (right).

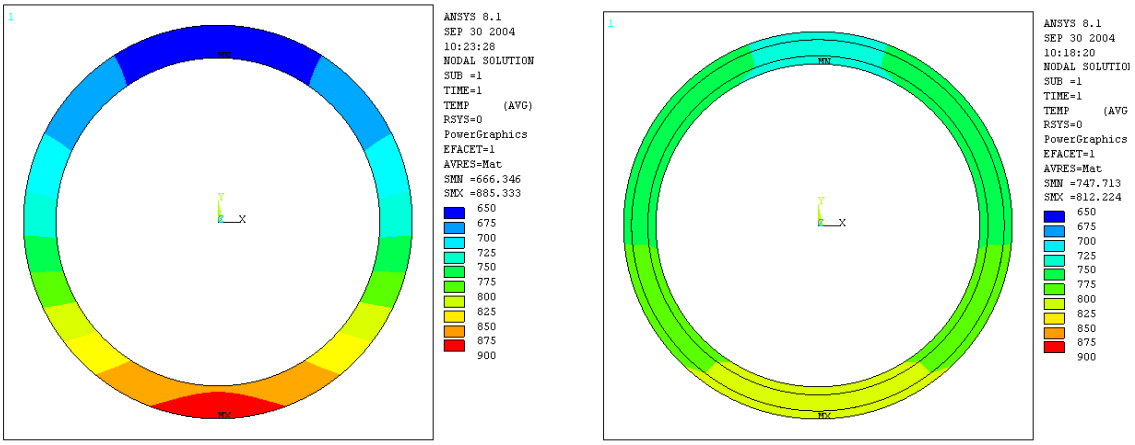

Figure 4 Temperature distribution in an irradiated standard tube (left) and a multi-layer tube (right)

With a solar absorber using profiled multi-layer tubes, air exit temperatures exceeding 800°C were predicted. This work package was focusing on the concept verification and the evaluation of the performance characteristics as basis for the absorber layout. In a first phase sample tubes of 10 cm length were manufactured to develop and test the manufacturing process. In the second step the manufacturing technology was extended to representative dimensions (1.3 m). Several tube variations were manufactured in order to evaluate the thermo-hydraulic characteristics for different profile geometries.

Work:

- definition of sample tubes for material and manufacturing tests
- FEM analysis on inner profiling manufacturing
- sample manufacturing
- sample testing and evaluation (layer interconnection, metallurgical analysis)
- CFD analysis on heat transfer improvement by profiling
- definition of test tube specifications
- manufacturing of test tubes
- modification of CEA hot air test loop
- test and analysis of thermo-hydraulic performance of test tubes

2.2.1 Definition of sample tubes for material and manufacturing tests

Different high temperature materials have been evaluated. A nickel based alloy was chosen because of its good mechanical resistance at high temperatures. It was difficult to get thin wall tubes. For the PML design it was foreseen to have a wall thickness of about 1mm for the outer tube and 0.5mm for the inner tube. After long term searching for cold drawn tubes without success, coil material had to be chosen. The tubes were manufactured by welding (Figure 5).

Figure 5 Welded tubes of a nickel based alloy

2.2.2 Sample manufacturing

Because of the complex manufacturing process of the PML design the development was done in several steps.

Primarily tests with normal steel and copper tubes without profile

In order to demonstrate the manufacturing process in principal several samples were produced by using the manufacturing technology of the partner FTF. The result of the first samples showed the need to improve the hydro-forming machine. The maximum pressure of the hydro-forming process was not high enough. Furthermore the fixing of the tubes in the

machine was problematic. These problems had been solved by further developing the process and the machine. Figure 6 shows a sample of a PML tube.

Figure 6 PML tube sample of normal steel and copper

Test samples with nickel based alloy material
The aim of this step was to test the influence on the manufacturing process using the selected nickel based alloy material. A few samples had been manufactured with the result that the material is principally well suited for the manufacturing process. Nevertheless it was found, that the samples could not been manufactured without cracks stemming from overstressing the material.

2.2.3 Sample testing and evaluation

For this reason PML samples of the primarily done manufacturing had been used to test the principal behavior of the inter-metallic material connection by microphotograph analysis. In the first part of the work, a metallurgical evaluation of PML tubes was performed for non thermal treated and thermally aged tubes.

.

Metallographic examinations of INCONEL/copper interfaces were performed after 15 h, 100 h and 500 h of thermal ageing at 900 °C and 950 °C. After ageing, the inter-diffusion of chemical elements was studied by SEM-EDX (Scanning Electron Microscopy with Energy Dispersive X Ray analysis).

After the hydro-forming process small cracks and porosities were observed at the interfaces between INCONEL and copper. The cracks were often filled with copper oxides. After ageing, we observed diffusion. For the ageing at 950 °C, large porosities appeared in the copper close to the interface for ageing times higher than 100 h.

The estimated lifetime was calculated by comparison of mechanical stresses and design stresses. Mechanical stresses were calculated by a FE analysis of tubes subjected to internal pressure and thermal gradients (CAST3M CEA code).

Design stresses were obtained in accordance to ASME design codes for high temperature components. Materials data were obtained by a literature review and also by tensile tests performed at CEA on INCONEL and copper. Tensile tests were performed on both materials

at 20, 400, 700, 800, 850, 900 and 950 °C with 2 specimens per test temperature. Tests were performed in air atmosphere, except for high temperature tests on copper specimens.

After the completion of the design rules, lifetime estimations were performed for INCONEL tubes and multilayer INCONEL/Cu/ INCONEL tubes for stationary conditions (no transients).

2.2.4 Manufacturing of test tube samples

On the one hand it was decided to use a tool supported forming technology and on the other hand to make burst tests in order to know the plastic behaviour of the tube material. The results showed that the probe would crack in the welding seam without a previous annealing process. Thereby an adequate elongation could be reached so that the first successful formed tubes could be manufactured by the new technology. These probes were then foreseen for the thermal cycling tests, the photomicrograph and finally the hydraulic tests in the laboratory.

2.2.5 Laboratory tests of profiled absorber tube samples

A wire-coil insert in the absorber tube results in a lower outer wall temperature and thus lower thermal radiation losses. Compared to an average driving temperature difference between the tube wall and the fluid of 91 K for a tube without enhancement the wire-coil insert needs only 67 K temperature difference for the same pressure loss of 75 mbar. The heat transfer and pressure drop in the wire-coil inserted absorber tubes was calculated in the design process. These correlations were derived for a homogeneous tube wall temperature[1]. To be able to verify the simulation results a test rig for heat transfer and pressure drop measurements under inhomogeneous heating was developed at CEA in Grenoble, France. Figure 7 shows the CLAIRETTE test loop containing the tube test rig shown in Figure 8. The test rig is composed of an open compressed air loop. An electrical heater allows adjusting the inlet temperature of the test section up to 750 °C. In order to set both pressure level and required flow rate, two regulation loops have been implemented (one using pressure sensor and valve; the other using mass flow meter and valve). The sample tube is inserted inside an oven which consists of SiC-tubes arranged in two layers above and below the sample tube. Screens have been used to separate the two sides of the sample tube and the electrical heating system. The two layers of the heating system can be operated separately allowing heating from one or both sides.

For the measurement of the sample tube wall temperature a pyrometer measurement device was used to decrease the measurement uncertainty compared to e.g. thermocouples. To reduce significantly the influence of reflected radiation on the pyrometer a screen tube was installed in-between the sample and the pyrometer. Wall temperature was than measured by measuring the emitted thermal radiation. The complete device is moved into the test rig with a pneumatic drive system for a short time and then the screen tube blocks all reflected (solar) radiation to the measurement point and the pyrometer only receives emitted thermal radiation from the measurement point. A calibration of the pyrometer device was done with the same inlet and outlet temperature of the sample tube and the oven power to compensate the heat losses through the insulation.

[1] Zhang,Y.F.; Liang, Z.M.; 1991. ”Heat transfer in spiral-coil-inserted tubes and its application”, in Advances in Heat Transfer Augmention, M.A. Ebadin, D.W. Pepper and T.Diller, Eds., ASME Symp. Vol. HTD, 169, 31-36.

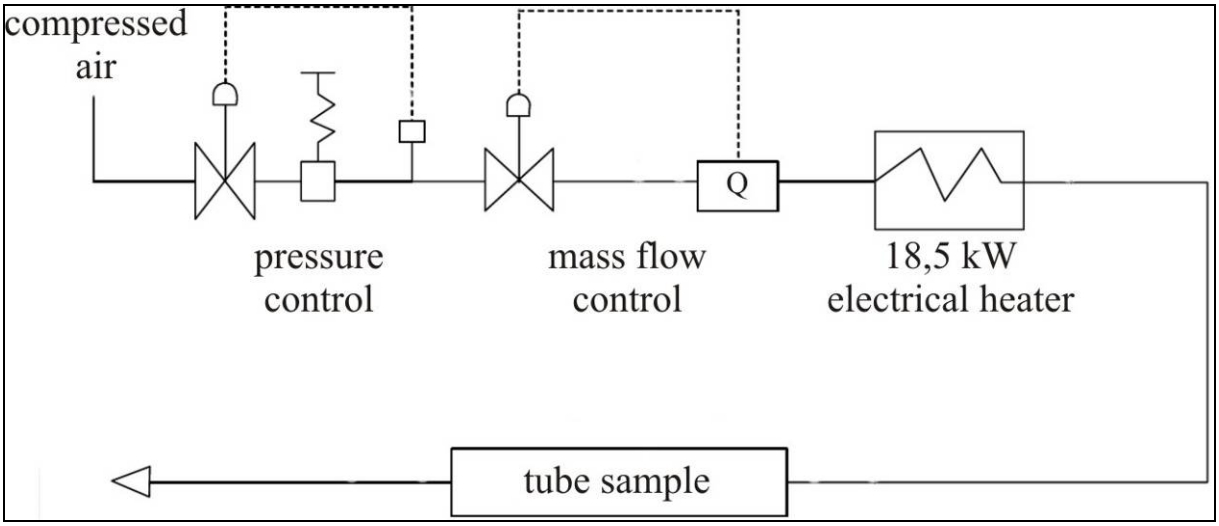

Figure 7 CLAIRETTE Loop

The wall temperature of the sample tube was measured at five positions along the test rig through holes in the casing. The heat transfer coefficient was calculated from the inlet and outlet temperature and the wall temperatures along the sample tube using a polynomial fit of the five measured temperatures.

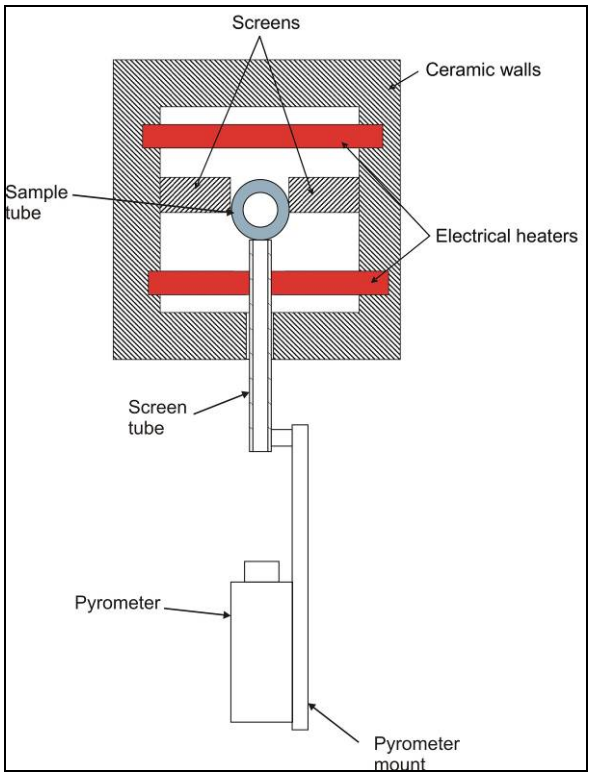

Figure 8 Test rig for heat transfer and pressure drop measurements

Table 3 and Table 4 show the results of the measurements at a Reynolds number similar to the SOLHYCO configuration. The inner tube diameter is 22.48 mm and the wire-coil insert has a diameter of 2 mm with a pitch of 55 mm. Ongoing oxidation of the sample tube was the reason for uncertainties in the emissivity of the sample tube and therefore uncertainties in the heat transfer coefficient which was measured with the calibration procedure.

The heat transfer with radiation from both sides was in the range of 80 % of the value calculated from the correlations. An error of 20% is acceptable for the heat transfer measurements as here errors of two measurements are accumulated, the measurements for the design correlation[2] and the measurements done in the Solhyco-project. The design of the SOLHYCO receiver permits a 20 % lower heat transfer coefficient with acceptable higher stresses. Under radiation from one side the overall heat transfer coefficient was higher hence the temperature distribution of the absorber tube better, indicating a positive effect of the swirl caused by the wire-coil insert. The measured pressure drop is similar to the calculated value

[2] Zhang,Y.F.; Liang, Z.M.; 1991. ”Heat transfer in spiral-coil-inserted tubes and its application”, in Advances in Heat Transfer Augmention, M.A. Ebadin, D.W. Pepper and T.Diller, Eds.,ASME Symp. Vol. HTD, 169, 31-36.

from the correlation. It could be concluded that with the thermo-hydraulic tests of the absorber tube the design basics could be validated.

Table 3. Heat transfer results

Measurement	Re	Measured heat transfer coefficient [W/m^{2}K]	Measured heat transfer coefficient with error of calibration [W/m^{2}K]	Heat transfer coefficient from Nussel-correlation [W/m^{2}K]	Ratio measured/ calculated heat transfer coefficient	Ratio measured with calibration error/ calculated heat transfer coefficient
Radiation from both sides	25624	324	291	384.0	0.844	0.758
Radiation from one side	28108	423	381	420.6	1.006	0.906

Table 4. Pressure drop results

Measurement	Re	Measured pressure drop [mbar]	Pressure drop from correlation [mbar]	Ratio measured/ calculated pressure drop
Radiation from both sides	25624	95.65	97.37	0.982
Radiation from one side	28108	107.2	111.50	0.961

2.2.6 Manufacturing and testing of tubes

In February 2009 the hydro forming tool for the PML-tubes was developed. The 150 mm long samples for thermo-cycling and photomicrograph as well as the 1.3 m long samples for the thermo-hydraulic tests were successfully manufactured. All planned tests were done as foreseen.

The following Figure 9 shows the temperature distribution of common mono tubes with wire-coil insert and the temperature distribution of PML tubes.

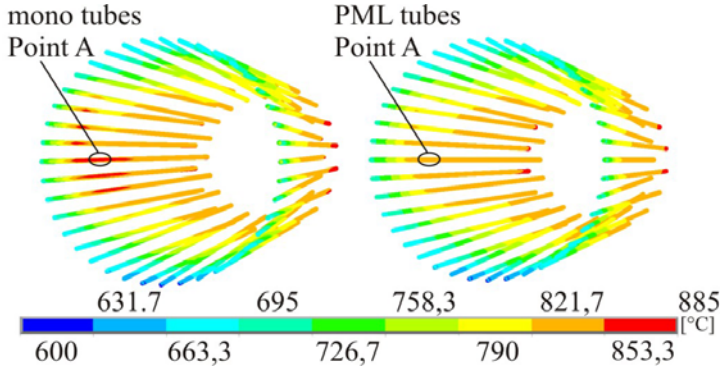

Figure 9 Overall temperature distribution [°C]

To determine the temperature difference between irradiated and unirradiated side the tube section with the highest thermal gradient was evaluated (Point A in Figure 9). The results are shown in Figure 10. The red curve represents the temperature distribution along the circumferences of the mono tube and the blue curve shows the distribution for the PML tube.

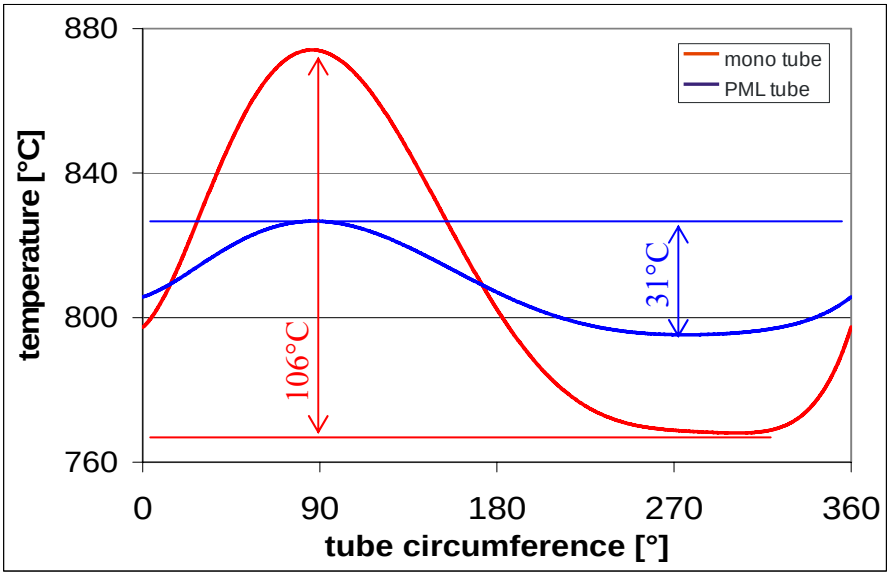

Figure 10 Local temperature distribution

The results show that the temperature difference can be reduced from 106 °C to 31 °C. The application of PML tubes instead of common mono tubes leads to a noticeable decrease of the maximal overall temperature and also to a significant reduction of the temperature gradient relating to the tube circumference and, hence, to a reduction of the internal stresses.

Manufacturing PML-tubes

The PML tubes were manufactured by a tool supported hydro forming process: Three separated tubes (INCONEL-copper-INCONEL) were put into each other and positioned in a divided mold.(Figure 11) The mold was closed during the hydro-forming process by hydraulic force. To get a tube composite two axial cylinders sealed the tube ends in order to fill them up with water until the required pressure (approx. 2000 bar) for the plastic deformation was reached. In order to shape the structure to the inner layer of the PML tube the wire-coil was inserted before the manufacturing process between the inner and middle layer.

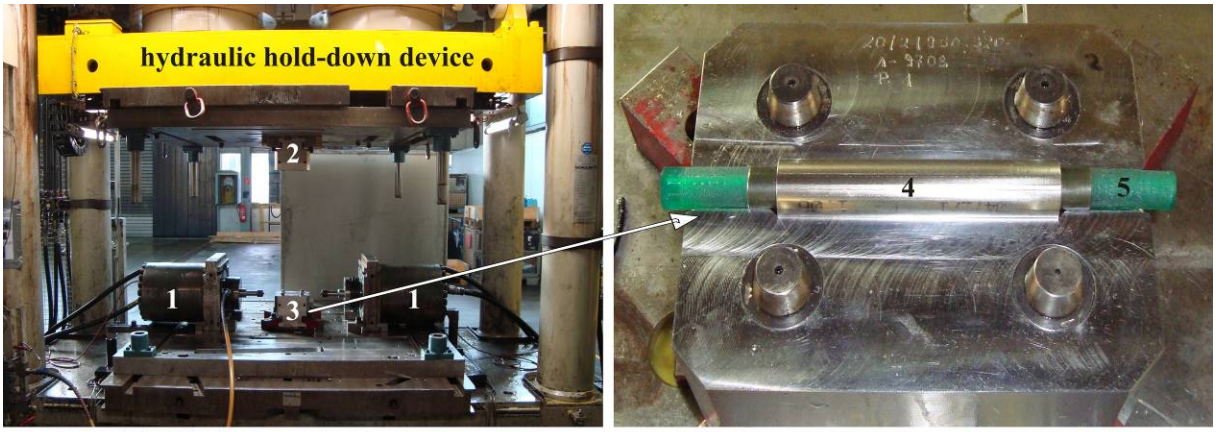

Pos.1 = axial cylinder
Pos.2 = divided mold top
Pos.3 = divided mold bottom

Pos.4 = PML tube
Pos.5 = flexible tube

Figure 11 Hydro-forming process

The problematic with the water inclusions was solved by using a flexible tube in order to displace the sealing end from the metallic tube to the flexible tube. For the thermal cycling tests and the photomicrograph tube samples with 150 mm (Figure 12) were used.

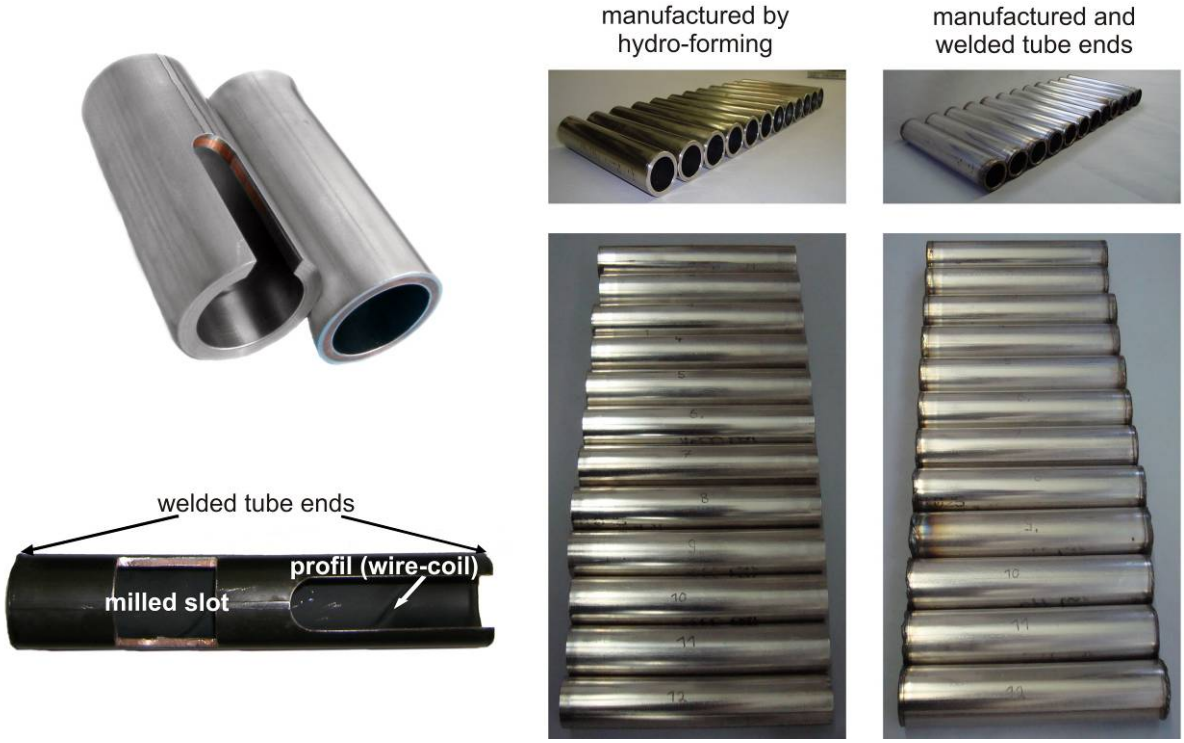

Figure 12 150 mm PML-tube samples

Thermo-cycling tests

After the hydro forming process the tube ends were closed by welding. To investigate the effect of the different thermal expansion coefficients of INCONEL and copper, thermal cycling tests under representative conditions were done. The tube samples were put into a furnace at a temperature of 900 °C for 10 minutes. Afterwards the tubes were cooled down to 600 °C outside the furnace (see Figure 13).

The connections between the inner and outer layer were investigated by microphotograph (see Figure 14).

For rapid cooling an active cooling system was installed around the tube. It consists of a ring with holes directing pressurized air. At a temperature of 600 °C the tube was put back into the furnace and a new cycle started. The results showed an unchanged or even better contact at the outer layer independent on the number of cycles. But at the inner layer the contact was disordered by cracks that grew with the number of cycles (see Figure 15 and Figure 16).

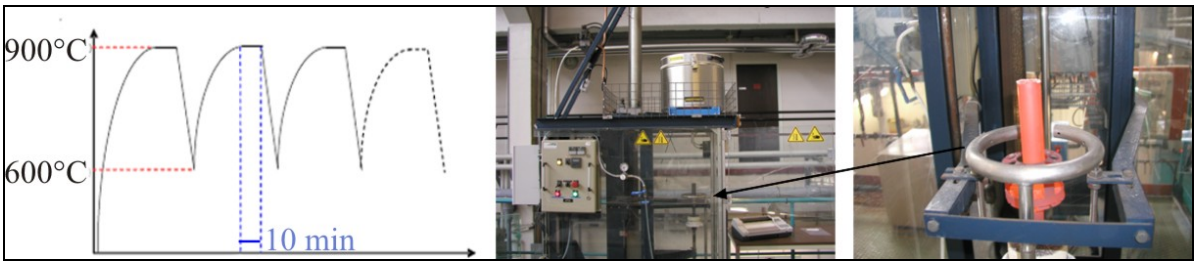

Figure 13 Cycling period (left) furnace (middle) tube outside the furnace (right)

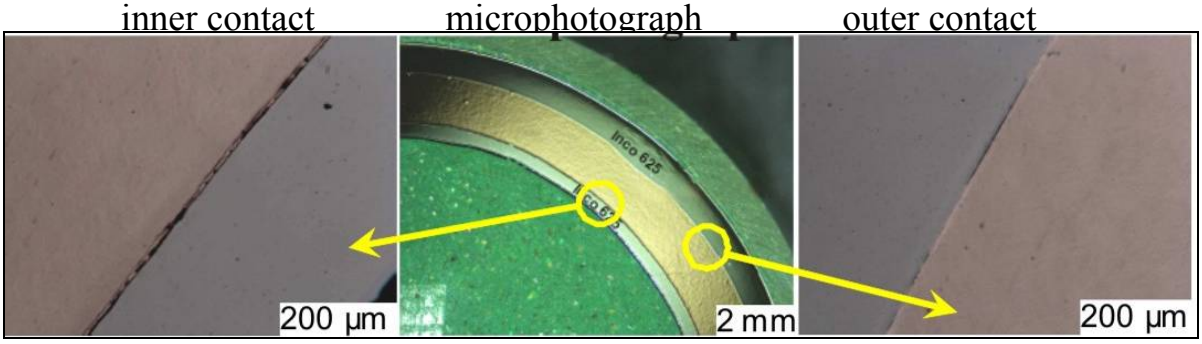

Figure 14 Microphotograph after manufacturing

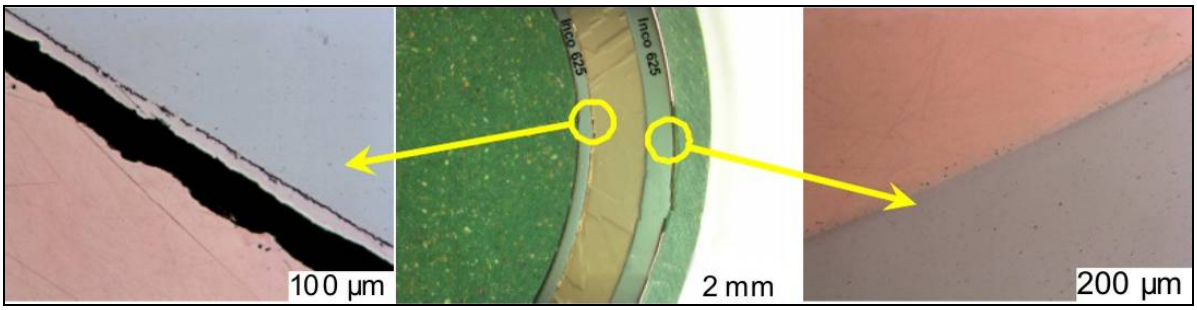

Figure 15 Microphotograph after 50 cycles

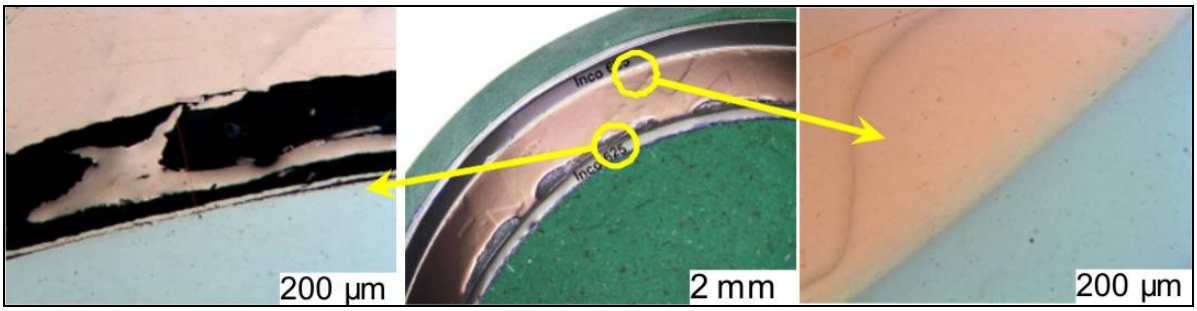

Figure 16 Microphotograph after 500 cycles

Thermo hydraulic measurements

For the thermo hydraulic measurements, PML tubes with a length of 1.3 m were required in order to obtain reprehensive conditions during the measurement campaign. The following Figure 17 shows the 1.3 m long PML-tubes.

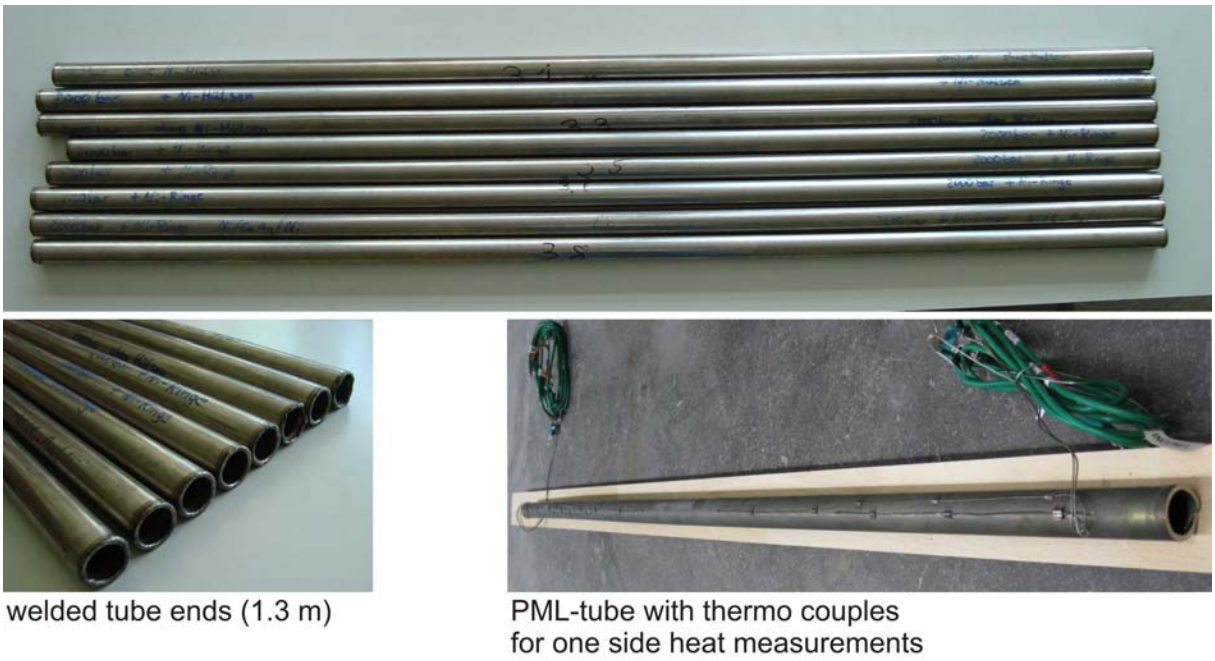

Figure 17 PML-tube samples (1.3 m length)

To demonstrate the performance of the PML tubes and to determine the heat transfer and the temperature distribution, the CLAIRETTE test loop was used (see Figure 18).

A total of five temperature measurements with the pyrometer were done along the tube length in regular distance. In order to obtain the wall temperatures on the non-irradiated side of the tubes thermocouples were installed. The thermocouples were placed on th1e opposite of the five pyrometer positions. Before testing the tube surfaces had to be oxidized in order to obtain a defined emissivity. The emissivity should be as homogeneous as possible to avoid significant changes during the measurement. Therefore the tubes were heated in a furnace at high temperatures for several hours (up to 900 °C for at least 32 h).

Furthermore a calibration of the pyrometer was realized to determine the emissivity of the tube. Therefore a first value of the emissivity was assumed as a constant value along the tube length. Therefore the heater and pre-heater were adjusted until the same fluid temperature at the tube inlet and outlet was reached. In the next step the wall temperature was measured by using the estimated emissivity. Afterwards the real emissivity was calculated by solving the energy balance and assuming that the average tube temperature is equal to the inlet and outlet temperature. Calibration and measurements were accomplished under steady state conditions, i.e. inlet and outlet temperature at all measuring points were constant. When steady state was reached five repetitions for each measuring point were registered and the average value was used for the analysis.

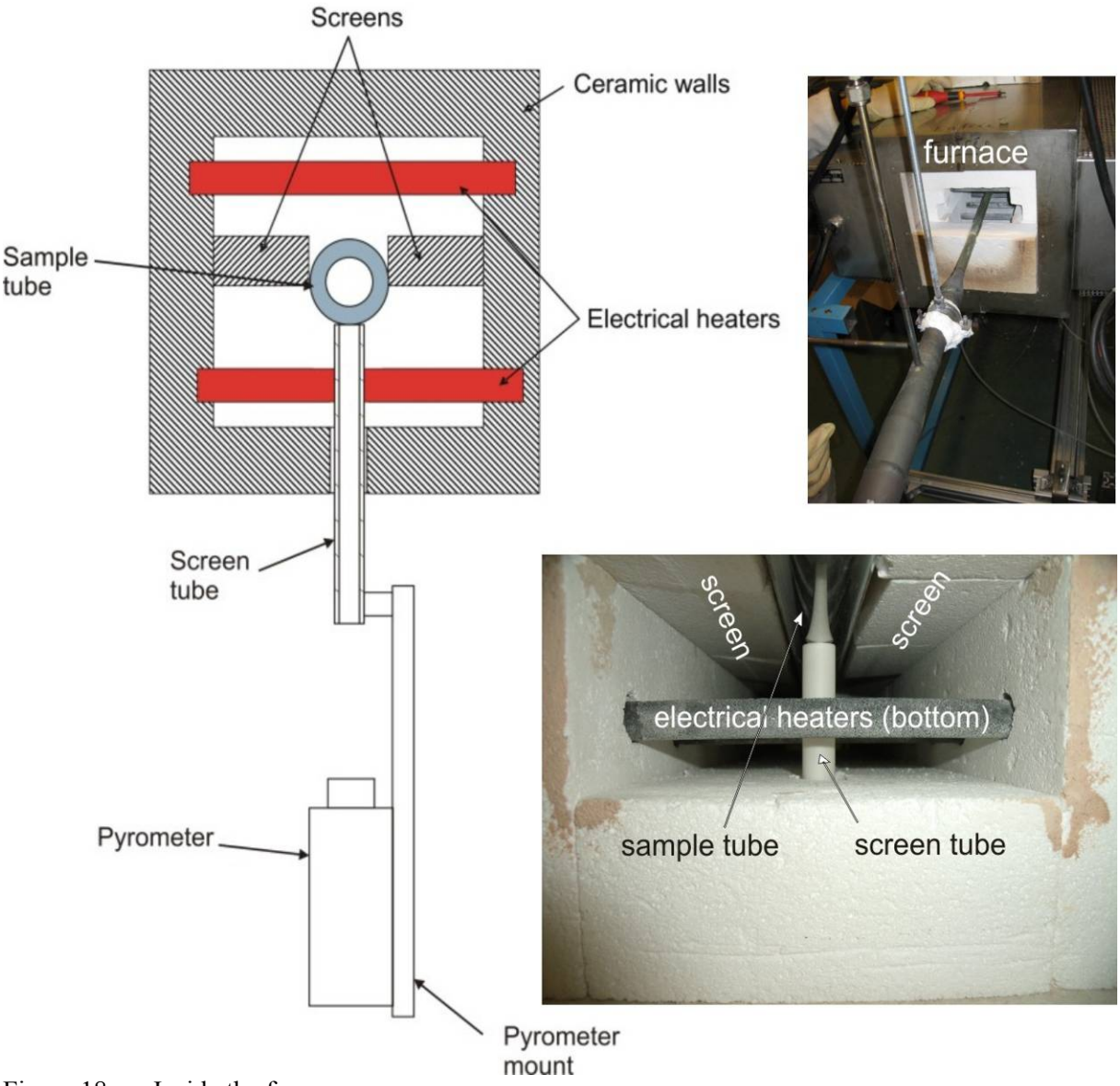

Figure 18 Inside the furnace

Results of thermo hydraulic measurements

To demonstrate the effects of the PML-technology three different tubes with a length of 1.3 m were tested under similar conditions. The first was an INCONEL tube with an inner diameter of 22.48 mm and a wall thickness of 2.11 mm (mono tube). The second one was a multi-layer tube with an inner diameter of 22.5 mm and a wall thickness of 3.5 mm. (0.5 mm inner layer; 2 mm middle layer; 1 mm outer layer) The third tube was a profiled multi layer tube with the same dimensions as the second one plus a shaped wire-coil structure with a wire diameter of 0.5 mm and a pitch of 12.5 mm. Furthermore an additional silver coating (10 µm) was applied around the copper layer in order to improve the inter-metallic connection.

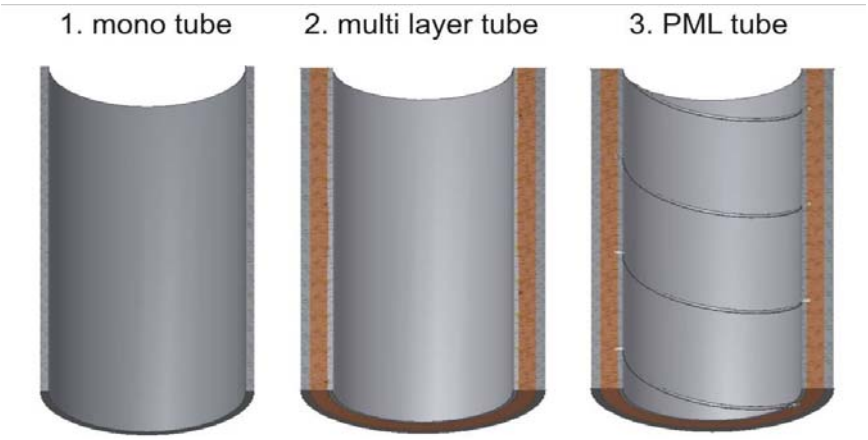

Figure 19 Half- section of the test tubes

The test conditions were similar to the real solar receiver as the heat was applied only to one side. Two measurements per tube with two different Reynolds numbers (Re) were done. The Re of around 1.7e4 and 3.4e4 were determined by different volume flow rates in the loop at an average fluid temperature of approx. 600 °C. The thermodynamic conditions of the measuring campaign are presented in Table 5.

Table 5. Thermo hydraulic conditions

values \ case	IN_Re1	IN_Re2	ML_Re1	ML_Re2	PML_Re1	PML_Re2
tube	mono	mono	multi layer	multi layer	PML	PML
heating	one side	one side	one side	one side	one side	one side
vfr [m^3/h]	12	16	12	16	12	16
p_loop [bar]	3	5	3	5	3	5
T_loop [°C]	29	29	29	27	29	28
p_in [bar]	3	4	3	4	3	4
T_in [°C]	552	551	554	555	554	553
T_out [°C]	661	661	657	658	658	658
emissivity [%]	86,60	86,70	75,40	75,60	89,60	88,90
Re	17430	33349	17062	34422	17585	33738

The following Figure 20, Figure 21, Figure 22 show the temperature for different tube configurations at the tube bottom and the tube top versus the tube length as well as the fluid temperatures at the tube inlet and tube outlet. The figures on the left side show the results for the lower Re, on the right side for the higher Re, respectively.

Comparing the results between low and high Re it can be noticed that the temperature difference between the bottom and top is larger at high Re. This is caused by higher heat power which is necessary to obtain the same fluid temperature at the tube outlet due to increased mass flow rate. The results show the positive effect of the PML tube reaching smaller temperature differences between the bottom and top side. This effect results from the high conductivity of the copper layer which is also responsible for the decreased maximum tube temperature. The comparison of mono tube and PML tube shows a clearly reduced maximal overall temperature (47 °C) and a reduced temperature between radiated an irradiated site of the tube (60 °C).

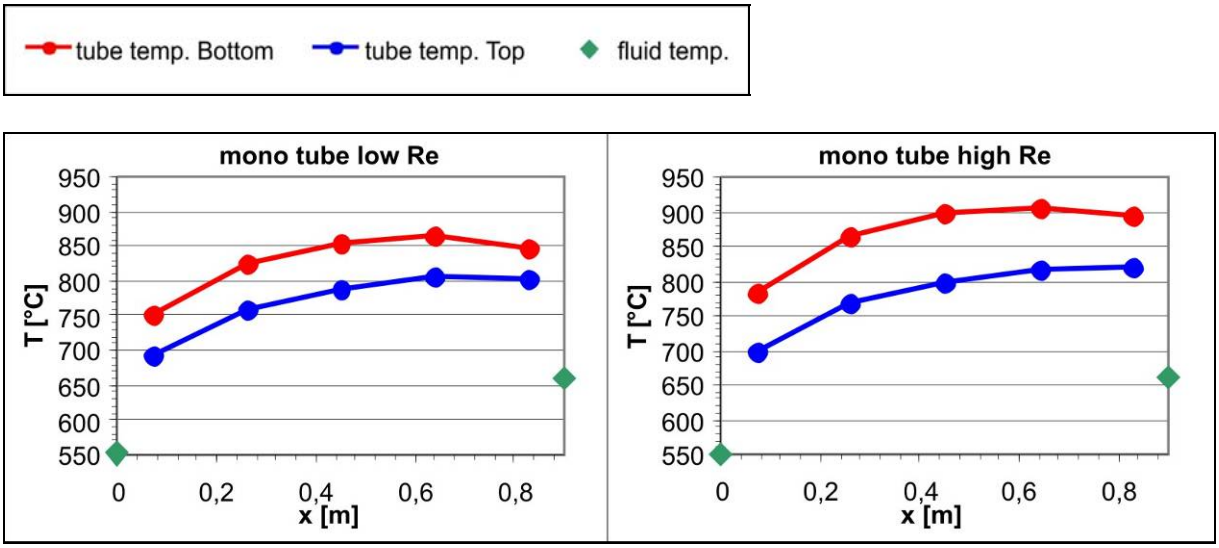

Figure 20 Temperature distribution mono tube

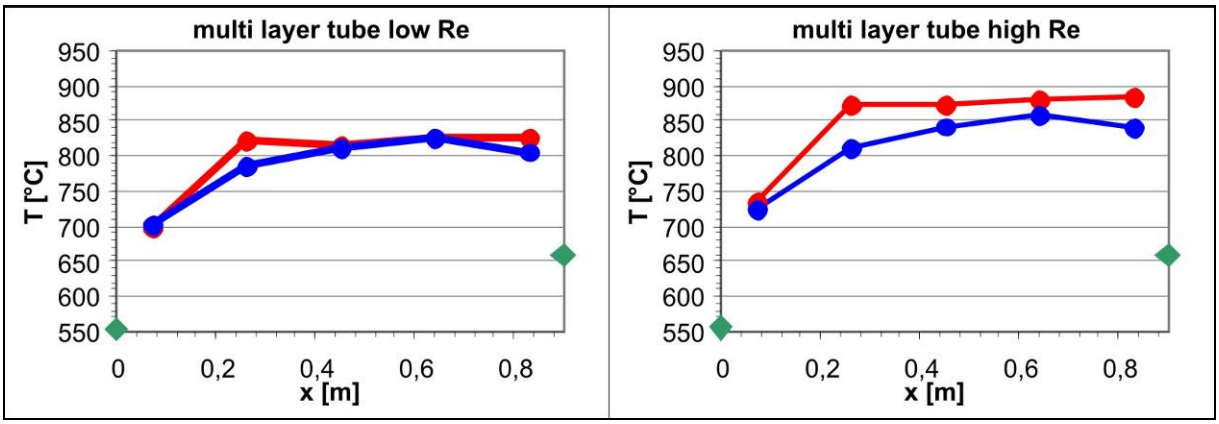

Figure 21 Temperature distribution multi layer tube

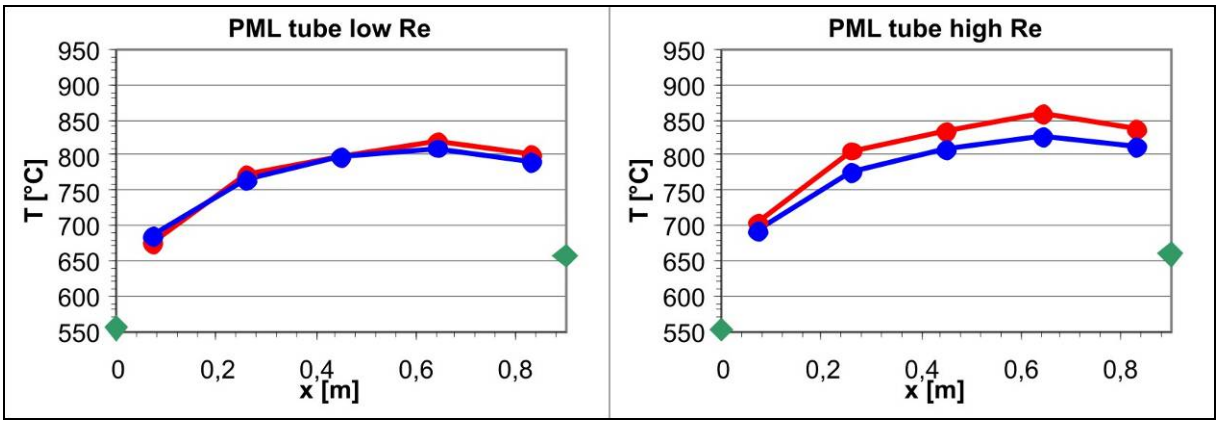

Figure 22 Temperature distribution PML tube

Table 6. Experimental results

	Experimental results*		
	mono tube	PML tube	reduction
max overall temp.	885,45°C	838,51°C	5,30%
max. ΔT	73,72°C	14,096°C	80,88%

* averaged values of both Re

As shown in Table 6 the experimental results verify that the maximum tube temperature as well as the temperature gradient along the tube circumference can be reduced notably, namely, about 5% of the maximum tube temperature and about 80% of the maximum temperature gradient. Hence, the PML-technology leads either to longer lifetime, or to higher acceptable operating temperatures. Both finally lead to lower lifecycle costs. These experimental results verify the theoretical assumptions and justify the further development of the PML-technology.

Measurement uncertainties

Due to measurement uncertainties it is not possible to compare the results between the multi-layer and the profiled-multi-layer tubes accurately. Both tubes show similar results in terms of temperature differences (Figure 21 and Figure 22). It should be noticed that the oxidation of the multi layer tube was not homogeneous along the length and the surface. Temperature measurements using pyrometers are difficult to accomplish exactly. In the process it is essential to set up the true emissivity of the measured surface and also to find the right position of the pyrometer to be sure that no other bodies are captured by the sensor. The emissivity of the tubes depends on the surface properties and temperature. While estimating the emissivity a constant value is assumed along the length of the tube. Due to this inhomogeneous oxidation the emissivity average can differ from the local emissivity at some regions, leading to inaccurate temperature values.

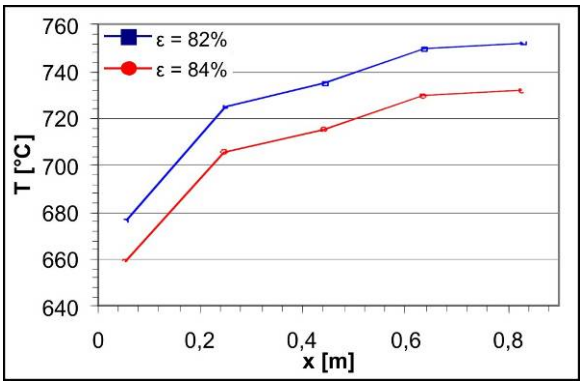

Figure 23 Effect of emissivity on temperature values

Figure 23 shows the influence of an error in the estimated emissivity value on the temperature measurement. The value was changed from 82% to 84% which leads to a temperature deviation of 20 °C. The uncertainty of the emissivity has a big influence on the determination of the heat transfer coefficient and has to be reduced in order to obtain tube temperatures for a more reliable calculation. Therefore further measurements with a better determination of emissivity are necessary. Problems with variations of the emissivity due to the inhomogeneous oxidation could be avoided by painting the test tube with Pyromark (high temperature paint).

2.3 Development of Solar Bio-Fuel System

2.3.1 Objectives

- Increase the share of renewables of solar-hybrid gas turbine system to 100%
- Development of a combustion technology for liquid bio-fuels in combination with solar air heating to high temperatures (800°C).

2.3.2 Background and Description of work

Since solar energy is continuously changing not only because of site geographical position or time of day and season, but also because of cloudiness, it is only obvious that continuous power supply can be based only on hybrid power supply of solar-fuel combination. Since start-up failures may occur in gas turbines it was decided that in this demonstration of technology project, the engine will not be completely shut down but kept on minimum fuel supply even during sufficient solar heat supply. This way a reliable and controllable solar power conversion systems is achieved, based on gas turbine in single or combined cycle.

The use of fossil fuel in most hybrid systems is limited to certain small percentage of the total energy, because of the requirements for the subsidy given to green power and maybe the hesitation from combined use of regular and green fuel which opens the door to use more regular fuel than what the regulations allowed originally. This issue has been solved here since the use of green fuels such as biodiesel fuel, instead of fossil fuel makes the whole system 100 per cent renewable. However, since bio-fuel differs from fossil fuels and it is usually blended with ordinary fossil fuel and because in this project it was designed as the sole supplement fuel in the combustion process, there were few unknowns to be investigated. Therefore, the aim of the present work was to study the various problems and alterations of the bio-fuel combustion process, select a solution and implement it into the hybrid turbine test system in PSA. The potential interaction of fuel system components with more corrosive, less homogenous and more viscous bio-fuels has been evaluated to identify critical issues and to determine the required changes on the fuel piping and control systems. Additionally, the combustion system of the existing gas turbine has been checked to find if it should be modified to enable stable operation in a very wide range of air to fuel ratio with air ingression to the combustion chamber at elevated temperatures up to 800 °C supplying most of the power.

While preparing the system for operation we encountered start-up problems with the fuel-metering valve. It seemed that the problems resulted from fuel residues which bonded the metering valves parts together after it had been used in the SOLGATE project in 2004 and past long term conservation process and then undergone restart trials in 2006. The PCU fuel system was equipped with a Nitrogen purging system that should maintain the injector unclogged but it did not clean the metering valve that lays upstream of the injectors system.

Bio-fuel effects study

A comprehensive study on biofuel-effects was performed, initial conclusions said that besides the difference in calorific value, higher viscosity etc, there is the problem of residues content of various materials which are more likely to stick to the structure material surface, corrode certain metals and harm some non metallic pipe materials and altogether can slowly deteriorate the performance of an engine. This is also a problem that may persist with longtime storage, which has actually not been recorded for length of time. There are the usual solutions which are mainly based on blending of Biodiesel with Kerosene or regular Diesel fuel, solutions that are outside the scope of the present project.

We can summarize the published info as follows:

- Biodiesel offers slight difference in calorific value compared to diesel fuel. One of the major advantages of Biodiesel is the fact that it can be used in existing engines and fuel injection equipment with little impact on operating performance. With gas turbines there is still the need for exact setting of fuel metering valve and control system properties and checking/modifying of injection components

- Biodiesel has lubricating effects. Comparison of lubricity between Biodiesel and petroleum diesel indicate that there is a marked improvement in lubricity when Biodiesel is added to conventional diesel fuel. Even Biodiesel levels below one percent can provide up to a 65 per cent increase in lubricity in distillate fuels. The lubrication effect was not checked with gas turbines and it should be evaluated during the turbine operation on heat from solar and Biodiesel.

- Compatibility of Biodiesel with engine components. In general, Biodiesel will soften and degrade certain types of elastomers like natural rubber compounds and others over time. Using high percent blends can impact fuel system components (primarily fuel hoses and various seals) that contain elastomeric compounds incompatible with Biodiesel. Manufacturers recommend that natural or butyl rubbers will not be allowed to come in contact with pure Biodiesel. Biodiesel will lead to degradation of these materials over time, although the effect is lessened with Biodiesel blends but that is not our case since we did not use blend fuels.

- Biodiesel in low temperature. Low temperature can cloud and even gel any diesel fuel, including blended Biodiesel. Unblended Biodiesel will gel faster than petroleum-diesel in cold weather operations. Solutions for operability with neat (100%) Biodiesel are much the same as that for low-sulfur #2 diesel i.e., blending with #1 Diesel or utilization of fuel heaters. These solutions work also well with Biodiesel blends, as do the use of cold flow-improvement additives. Of the above possible solutions the use of fuel heaters was selected for the SOLHYCO project, see further details below.

- Biodiesel storage. Biodiesel does not require special storage. Biodiesel can be stored wherever petroleum Diesel is stored, except in concrete-lined tanks. Acceptable storage tank materials include aluminum, steel, fluorinated polyethylene, fluorinated polypropylene and Teflon. The fuel should be stored in a clean, dry, dark environment. Due to heating needs, one should be sure to verify compatibility with materials exposed to the heaters and heated neat Biodiesel.

- Long term storage. As Biodiesel has not been commercially used for more than a few years, there is hardly any report on long-term storage effects on Biodiesel fuel. In case long term storage would be required the Biodiesel vendor will be consulted regarding deterioration or change of specifications.

Development

a. The SOLHYCO project is a follow-up on the successful SOLGATE project, thus the SOLGATE PCU systems were utilized with the minimal required changes to switch from solar jet fuel to solar and Biodiesel hybrid operation.

b. Experts have been consulted to determine the required modifications of the PCU system components to utilize Biodiesel instead of fossil jet-fuel. The findings show that beside the already made changes in the combustion chamber design that were done for its “solarization”, there is no other required modification in the main “solarized” components of the combustion system including the high temperature super alloy combustion chamber, special injector and igniter themselves.

c. The fuel system piping requires no modifications as it contains no elastomers that are sensitive to Biodiesel and the system had already been tested with hot air coming into the un-insulated combustor.

d. Control system parameters had to be modified to accommodate for the slightly higher fuel flow due to the lower calorific value.

e. After some research, it seems that changes resulting from the fuel properties are not expected to require recalibration of the metering valve as the modifications in the control system should be sufficient.

f. Other modifications relate to valves and filters sealing materials that should comply with Biodiesel requirements as mentioned above. A checklist has been prepared to check all components compatibility with requirements.

2.3.3 Design of Solar bio-diesel system

A scheme of the modifications and addition components was prepared for the fuel system considering the use of neat (100%) biodiesel fuel while using jet fuel for startups only (see Figure 24). This includes the heating system and the change of all fuel pipes that may not be compatible with the Biodiesel requirements for long-term operation. It also included addition of a jet fuel tank for start-up.

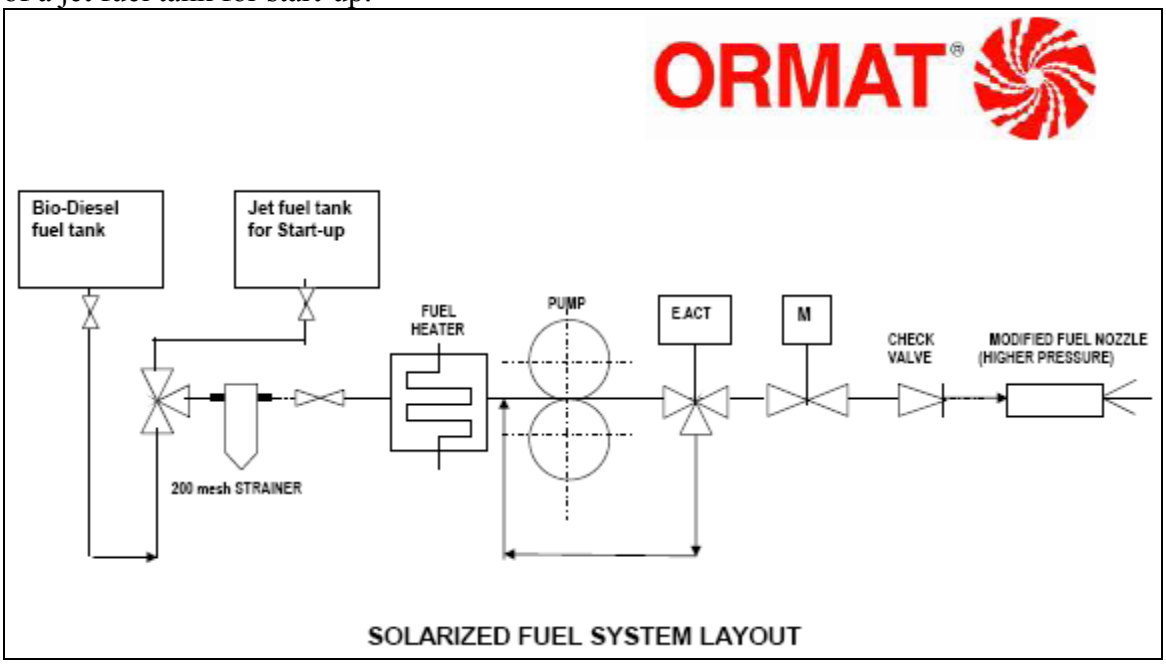

Figure 24 Scheme of solarized fuel system layout

2.4 Solar Component Qualification Test

2.4.1 Objectives

- Component and system test of a hybrid Biodiesel combustor system
- demonstrate solar-hybrid test system operation at 100% renewable energy sources
- collect more O&M data on solar-hybrid system components

The test setup (see Figure 25) used for testing the biofuel combustion system was the arrangement that had been implemented during the SOLGATE project. It consists of a 250kW

Allison turbine and 3 receiver modules serially connected. This setup was mounted in the CESA-1 tower at Plataforma Solar de Almeria (Figure 26, Figure 27).

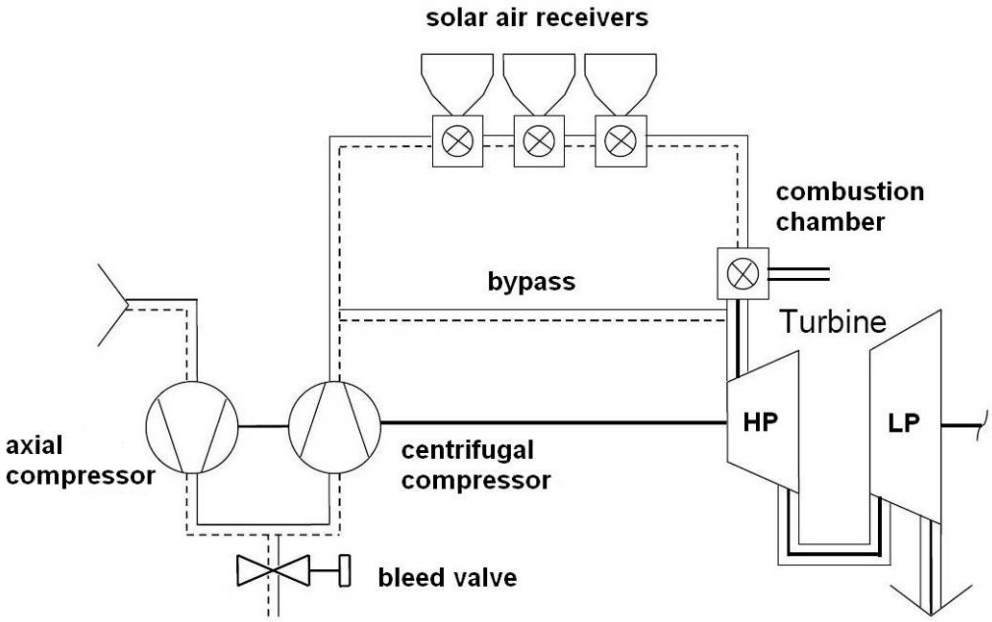

Figure 25 Scheme of the SOLGATE test setup at CESA-1-tower

Figure 26 CESA-1 tower (r.) and detailed view on receivers (l.)

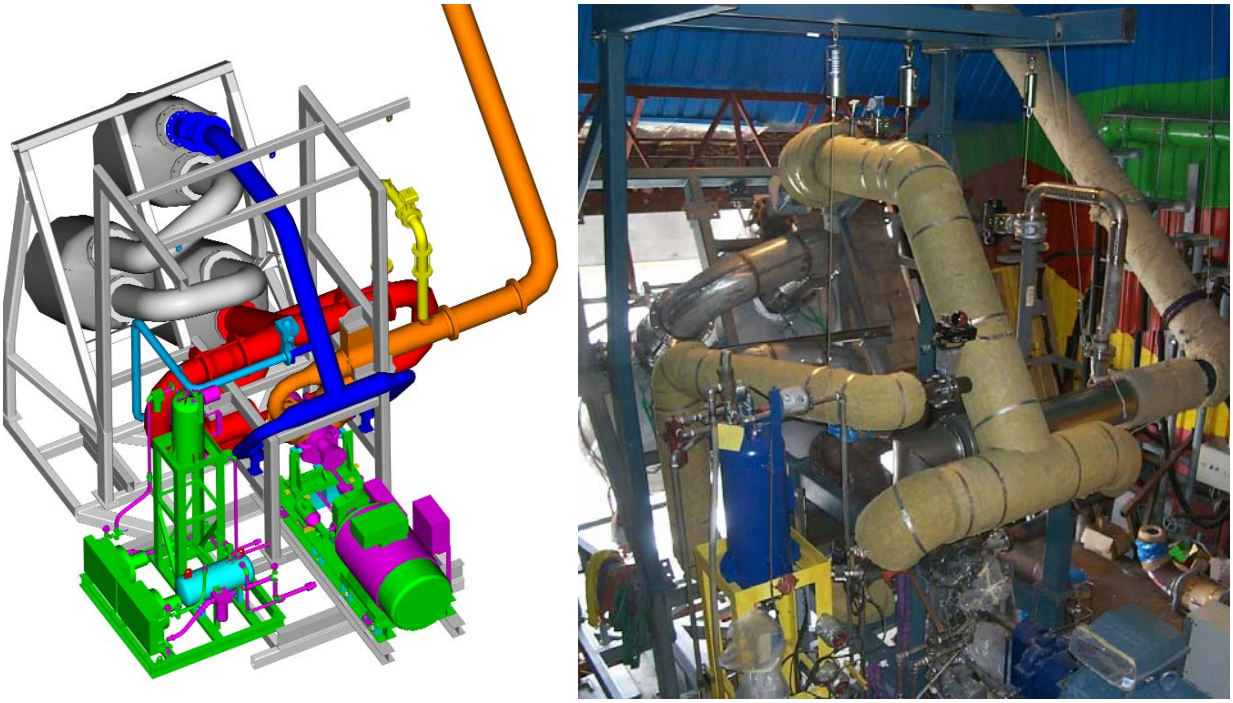

Figure 27 Solgate setup: artificial view (left) and photo (right)

2.4.2 Solar operation with kerosene

Resumption of operation with kerosene

Before the resumption of solar operation a lot of preparation work had to be done, like ongoing repair of water leaks of the secondary concentrators, preparation of the data acquisition system, cleaning of the secondary concentrators and windows, moving of the system into the working position, opening of the emergency pipe, closing of radiation gaps, and electrical connection of the main fuel valves. Especially the cooling water system repeatedly suffered leaks due to ageing of the rubber hoses. Finally, more than 5 years after the last solar operation, on March 11th, 2008, the first solar operation within the SOLHYCO project was done. After about one hour, a water cooling line broke free and forced an immediate shutdown of the cooling water pumps followed by a controlled shutdown of the turbine. Except of this incident, the operation went well, only minor problems were detected. Maximum receiver temperature achieved was a moderate 413°C producing an electrical output of 80 kW.

Then, additional preparation was done, including installation of the flux sensor, repair of ESD electronics, repair of the external platform, test and repair of the auxiliary fuel tank and line, installation of a tracer gas sampling line with cooler (see below), preparation of data quick analysis, and purging of fuel lines. On April 23rd, 2008, the second solar operation was done. Receiver air outlet temperature was above 600 ºC, and the maximum electric power was about 115 kW. Due to a clogged cooling water channel, the mirrors of one panel of a secondary concentrator cracked. Thereupon, the cooling water line was cleaned.

First operation with bio fuel

The commissioning of the bio fuel system was done in May 2008. On May 1st, fuel supply was switched for the first time to operation with bio fuel. It worked completely flawlessly. There was no way to see the change in the measured data. After some tests with the switching,

solar operation with bio fuel was done for more than two hours. 760 ºC in the air produced up to 187 kW of electric power. Operation went very well.

A test of a turbine start with bio fuel instead of kerosene was performed, which showed that the control system adapted to kerosene was not able to start the engine. This confirmed the strategy taken by Ormat, to do the start with kerosene and then switch to bio fuel during operation. Adaption of the control system in principle is possible, but this would have required several weeks of work and tests which was not possible in this project.

Turbine air mass flow measurement

During the month of June, the installation of an improved air mass flow measurement system based on rotameters and the devices for the tracer gas measurement of the turbine air mass flow was completed. A long lasting problem of the solar gas turbine project at PSA is the question of the exact air mass flow through the system. The existing device, a ram pressure sensor, gives a somewhat (around 10-20%) too low value for the air mass flow. This is known because the measured efficiency of the receivers is too low, while the efficiency of the turbine is too high. It was planned to measure the air mass flow with two additional and independent devices, the rotameters and a tracer gas method.

The rotameters are mechanical devices similar to a Roots-pump. They were installed in the suction part before the inlet of the turbine. As the used devices only were able to run up to 0.5 kg/s, two have been installed in parallel (see Figure 28). Nevertheless, this limitation to 1 kg/s only allowed operation up to around 84% of the maximum turbine speed.

In the tracer gas method (Figure 29), a small amount of an easily detectable gas (the tracer gas, here SF_6) is dosed with high precision into the main air stream before the compressor. After very well mixing, samples are taken after the compressor. From the concentration of the tracer gas in these samples, the overall air mass flow can be calculated. This method is not limited to any air mass flow, but it is more delicate than the rotameters. Due to this, it was carefully calibrated with the help of the rotameters.

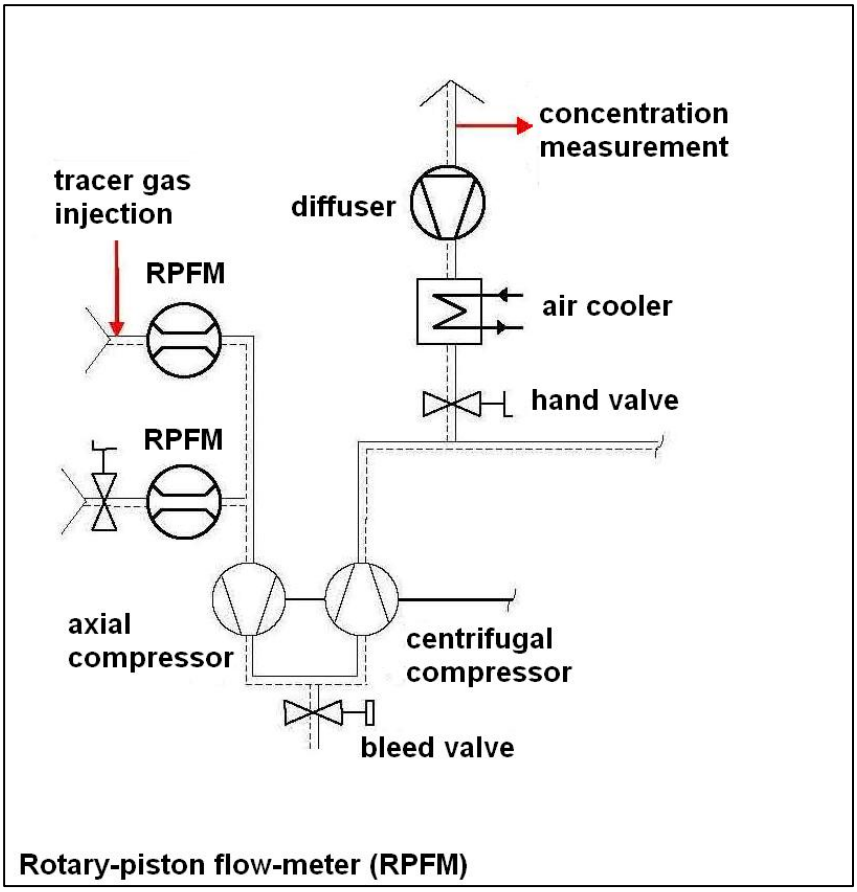

Figure 28 Scheme of rotameter arrangement

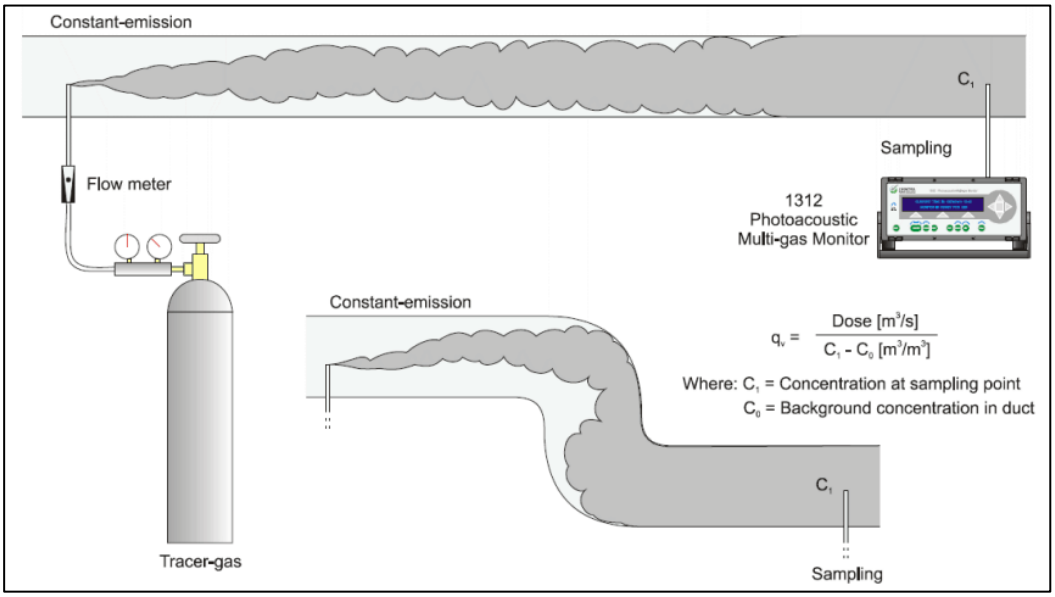

Figure 29 Improved mass flow measurement based on the tracer gas method

On June 26th, the first solar operation with the rotameters was performed. Exhaustive comparison between rotameter and tracer gas mass flow measurement was done. Several ways of injecting of the tracer gas and sampling of the air were tested. Finally it was achieved that the two methods gave the same results within 1%. Then the rotameters had to be dismantled to run the turbine at high power.

Operation with bio fuel at high power

Between Aug. 11th and Sept. 16th 2008 tests with higher power were realized. After solving many problems on the way, the last operation day was successful when the receivers, powered by 49 heliostats, reached the record temperature of 791°C during the test campaign. Anyway, the turbine was not able to operate above 94% speed producing only 160 kW electric output. The reason is not yet clear; a possible explanation is the quite high ambient temperature well above 30°C together with the lower energy content of bio diesel compared with kerosene. Unfortunately, after less then two and a half hours of solar operation, the turbine shut down automatically due to an alarm of a metal sensor in the oil system.

After the gap in autumn 2008 due to non availability of the tower facility, it was tried to resume operation from January 2009 on. But technical problems did not allow the start of the turbine until March. From March 8th to 13th, 2009, with staff from Ormat present at PSA, a final effort to reach design conditions was done. March 10th, 2009, (Figure 30) and especially the last day, March 13th, 2009, (Figure 31) were at least partially successful. It was possible to operate at very high receiver air outlet temperatures (Figure 32), with electric power generation above 200 kW, and with the compressor bleed valve closed. But the turbine speed did not exceed 96.8%.

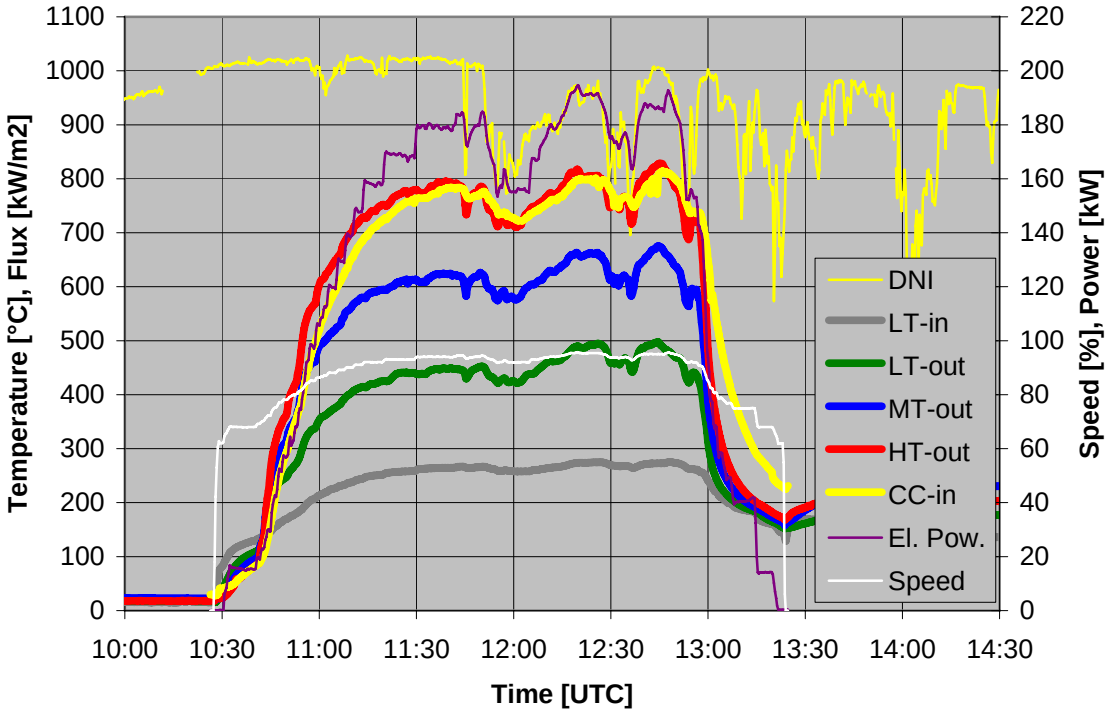

Figure 30 Measured data from March 10th, 2009 (LT/MT/HT = Low/Medium/High temperature receiver, CC = combustion chamber)

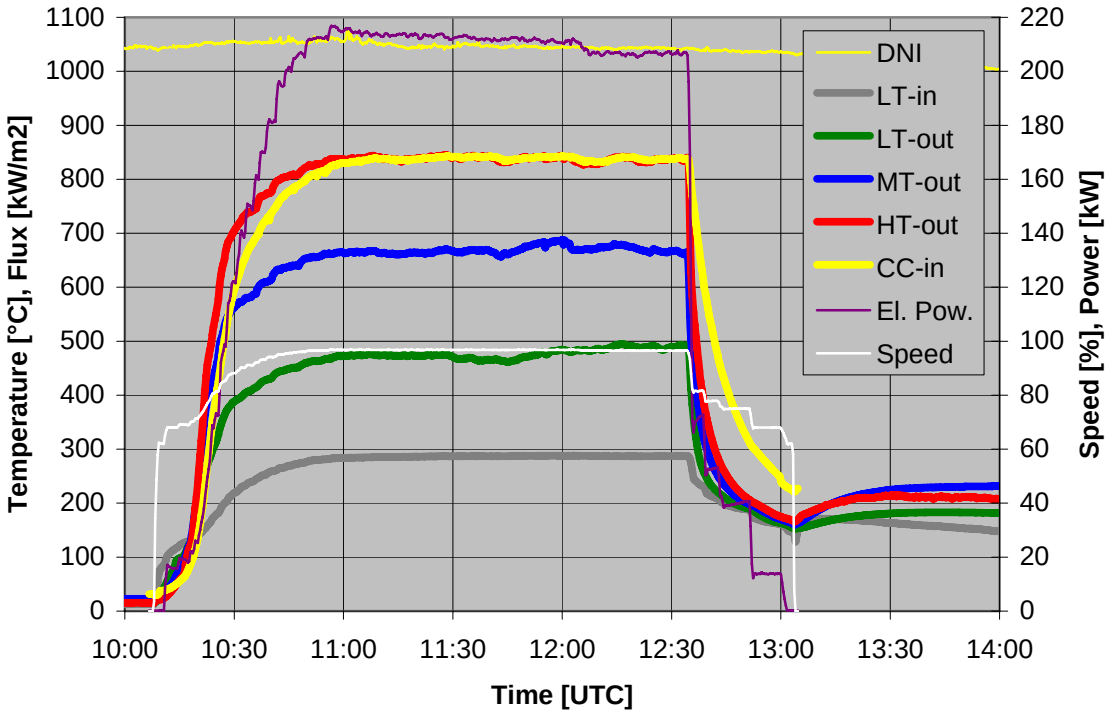

Figure 31 Measured data from March 13th, 2009 (LT/MT/HT = Low/Medium/High temperature receiver, CC = combustion chamber)

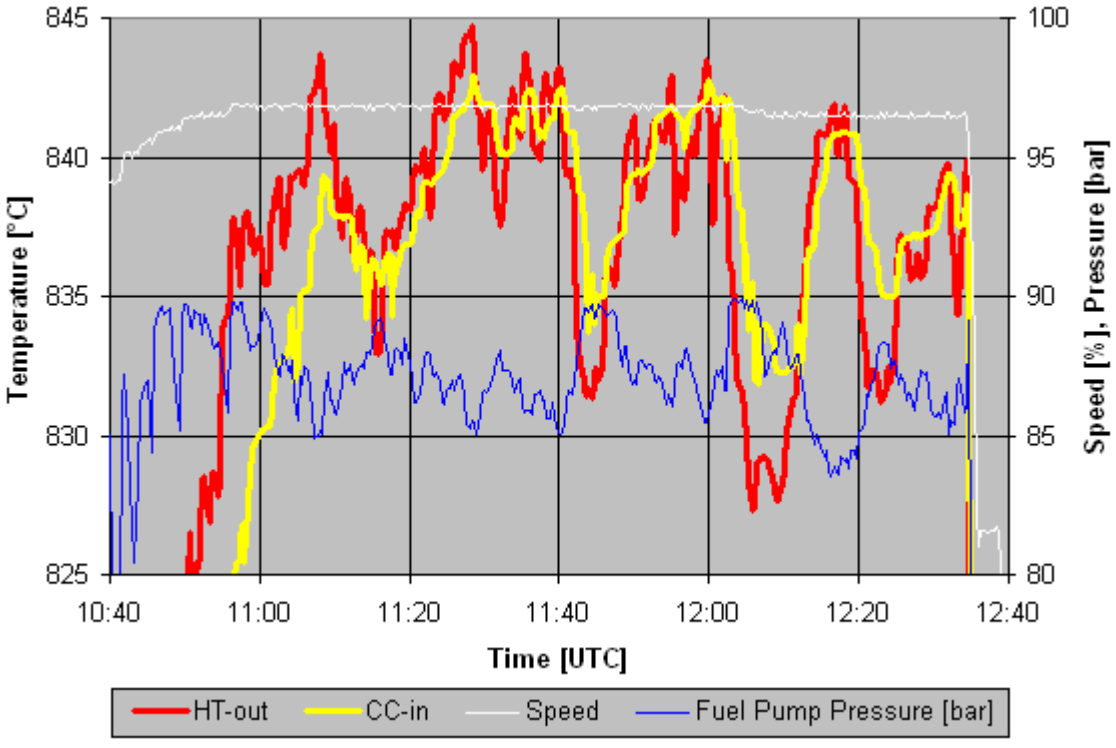

Figure 32 High temperature operation at March 13th, 2009 (HT = High temperature receiver, CC = combustion chamber)

Dismantling of the system

In April 2009 the complete system was dismantled, because the new tube receiver and the Turbec microturbine were already waiting for their installation. The system had been installed nearly eight years in the Cesa-1 tower of the PSA.

2.4.3 Test summary

The goal of 100 operation hours was achieved with the turbine system in start up, fossil, solar and hybrid mode. Of these, 57 hours of solar operation could be accumulated. Main reasons for the limited solar operation hours were technical problems with the gas turbine, which very often interrupted the operation early during the test days. Other reasons were the limitations given by the installation and calibration work with the rotameters in summer 2008, and several more like delayed fuel availability or schedule conflicts in the use of the solar tower. Anyway, the SOLHYCO WP3 operation is considered a success, because it was possible to demonstrate that a commercial helicopter turbine can be operated not only with solar radiation, but also with bio diesel, hence generating close to 100% of the power from renewable energy sources. It also was shown that the pressurized volumetric solar receivers still worked fine after more than six years.

2.5 Development of Solar-Hybrid Microturbine Cogeneration Unit

2.5.1 Objectives

- develop a prototype 100 kWel solar-hybrid microturbine unit for cogeneration purposes
- layout, design and manufacturing of a 350 kWth receiver

2.5.2 Analysis of system configuration and specification of solar-hybrid system

The Turbec T100 is a commercial 100 kW microturbine usually used with natural gas in combined heat and power (CHP) applications. Because of the possibility to attach an external combustion chamber this turbine can be used in a solar (hybrid) system. To meat the overall target of 100 kW output at full load condition in solar-hybrid mode, modifications of the standard microturbine configuration had to be analysed and specified. Main changes compared to the standard unit were:

- Inlet temperature into the combustion chamber is 800ºC compared to 600ºC
- Fuel is Diesel or if possible full Biodiesel compared to Natural Gas
- A new external flow path for integrating the Solar Receiver had to be integrated
- Completely new software for control of two parallel heat sources

2.5.3 Modification of Microturbine unit

After finishing the design of the microturbine flow path with the integration of the solar receiver Turbec conducted tests with the interface for solar application. The test-rig was equipped with the standard Diesel combustor, but it was also fitted with a second, parallel combustor that was controlled independently, this combustor hence acted as “the sun” and was enabling to test all possible scenarios from “zero sun operation” to “zero fuel operation”.

The largest challenge was how to control if the heat supplied is coming from the "sun" or from the Diesel combustor, i.e. detection of flame.

The test went very well but the match with theoretical studies previously made was not perfect, the turbine showed a better result during test for the re-ignition during operation with a lot of heat coming from the "sun".

After the initial test it was also found that heat-shields had to be designed and added to avoid overheating of the internal insulation. The interface system designed by Turbec does not give any large backpressures and the T100 could be run without any compensation for backpressure.

Turbine hardware-design and calculations

After a pre-study was made we discovered some crucial issues that would impact the combustor and turbine design of the solar-hybrid unit. The high inlet air temperatures linked with the possibility to combust fuel was proving to provide more difficulties than originally thought. Basically the original idea for the design was not able to handle properly the increased combustion air temperature used for the Diesel fuel combustor.

In 2006, complete housings to facilitate hot air from the solar receiver to be fed to the turbine were designed. They had to be designed completely from scratch and it had been a challenge to keep temperature high and differential pressure low. Also different ways of cooling critical parts such as igniter have been reviewed.

The design also had to encounter the demand for ease of maintenance support and inspections. Even if this is not one of the major design factors it has to be acknowledged that the need for inspections and status control of the internal flow path can be of importance to understand and troubleshoot the internal combustion process.

Fuel system design and assessment

The fuel system has also gone through assessment to be able to handle Biodiesel. On this task the work needed had been underestimated. We have had some experience with prototypes operating on fossil Diesel but valves and control equipment had to be re-evaluated to obtain a control that could be accepted by the system. Running the solar-hybrid system in all possible scenarios and mixtures of solar power and Biodiesel requires a very stable and accurate control. To find and adapt standard fuel-valves to cope with the fuel flows we need had been a challenge that brought a lot of new experience to us and our partners. Late 2006 we achieved a stable acceptable operation with our third choice of valve supplier. The system still needed adaptation and tuning before the test with the hot air application but our judgment based on the tests in the double combustor rig proved that the system is stable.

Control system

During the development of the fuel-system several control parameters were considered and changes were done to adapt the software to the new fuel-valves. A feedback from TOT (Turbine Outlet Temperature) has been implemented for improved fuel control during start-up. This reduced the problem with start-up smoke. Flame-out problem still exists but has been drastically reduced by extensive testing of different software solutions. A very accurate timing is needed in the start-up sequence to avoid flame-out when switching from pilot to main fuel injection. Controlling the injector air support is the most vital part in this sequence and a lot of effort has been put into this work to get a reliable operation.

2.5.4 Layout, design and manufacturing of receiver

Layout of receiver

Due to the high outlet temperatures of the planned receiver it was necessary to simulate in detail the expected tube temperatures. Therefore it was necessary to know the real flux distribution on the tubes. Thus a tool was developed to estimate the local heat flux distribution on a finite element model. Using this heat flux distribution together with other thermal boundaries like forced convection and radiation exchange gave the opportunity to design the tube receiver much closer to the reality then before. The aim of the development was to have an integrated design tool witch allows the simulation of several tube receiver configurations to figure out the best design.

Therefore a ray-tracing code so called FEMRAY (**F**inite **E**lement **M**esh **Ray** Tracing) was developed (see Figure 33). The code uses the geometric data and the optical properties of each finite element of a predefined mesh to calculate the expected heat flux distribution using a simple ray-tracing algorithm. Direct absorption as well as grey diffuse solar radiation exchange is considered.

On the inner side of the tubes forced convection had been considered. The heat transfer coefficient and the fluid temperature along the tubes were implemented using the macro language of the FE program. Therefore the transferred heat was summed up along the circumference of each ring using the area and temperature of the predefined elements. The fluid temperature, the temperature dependent fluid properties and the heat transfer coefficient of the next ring were calculated using the transferred heat of the previous ring of the tube. The temperature dependent material properties (solid and fluid) were updated while iteratively solving the problem (Figure 34).

Radiation exchange of the tubes and the cavity, radiation exchange inside the tubes as well as radiation to ambient was considered using the radiosity method. Last but not least the resulting flux distribution on the aperture from the ray-tracing calculations of the heliostat field had been applied on the outer surface of the finite element mesh.

The results of the heat flux and the tube temperature distribution for one exemplary receiver design are shown in Figure 35.

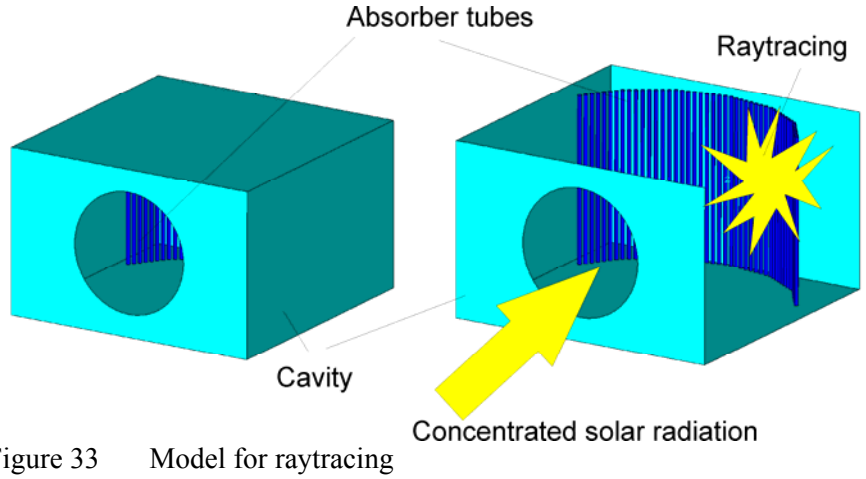

Figure 33 Model for raytracing

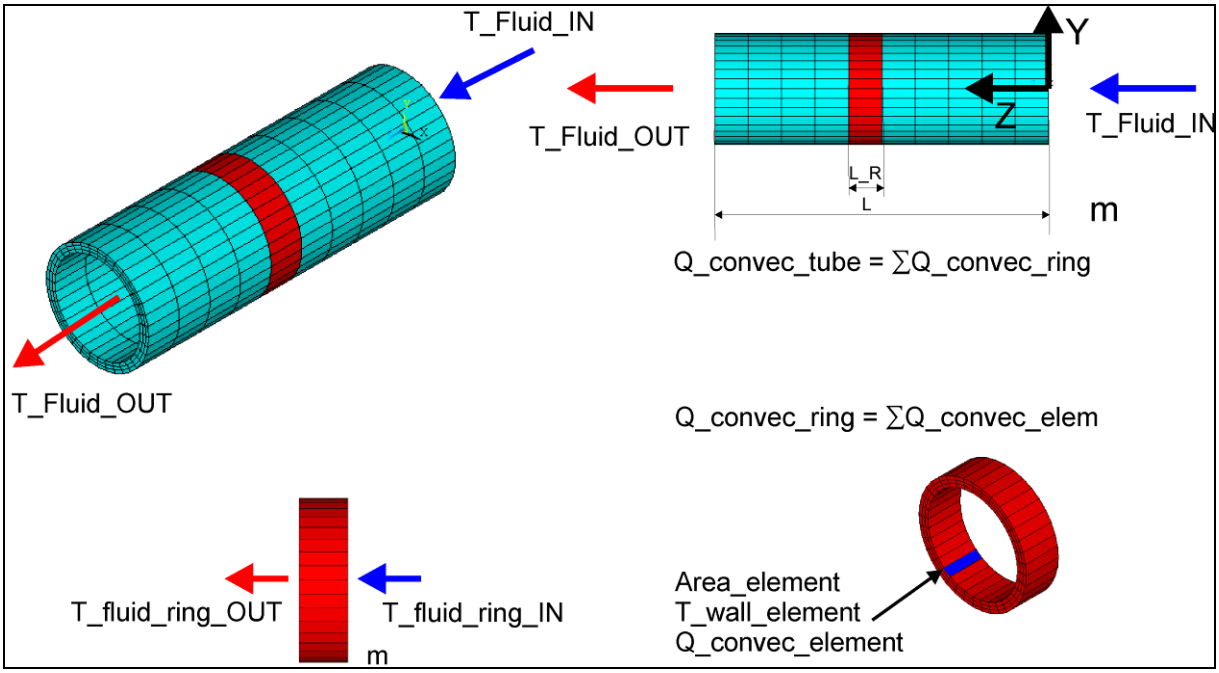

Figure 34 Heat transfer model

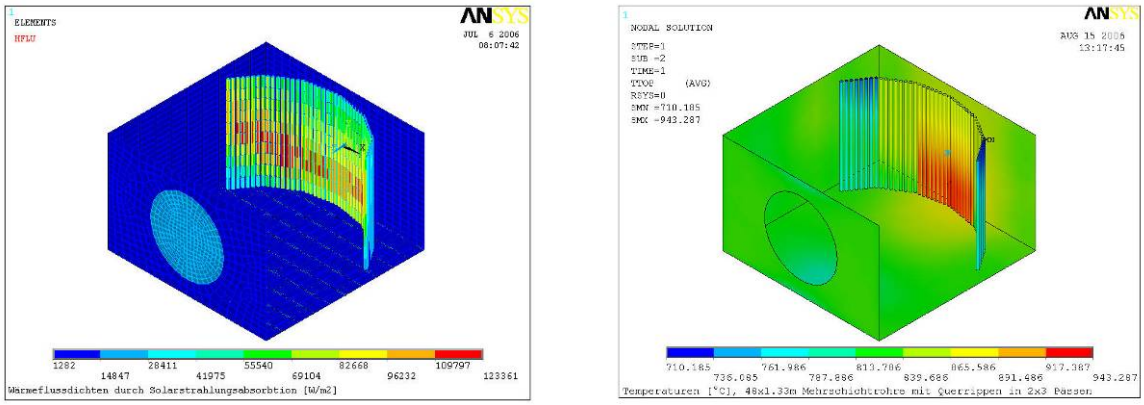

Figure 35 Heat flux distribution onto tubes (left) and tube temperature distribution (right)

With this tool several receiver designs had been investigated.

Design of the receiver

Based on the FEM simulations four pre-designs were made (see Figure 36). Every design variation fulfilled the design aims. Basically the headers were designed considering hydraulic and installation space boundaries. Costs of these design sets were estimated and the best suited design selected. A drawing of the selected design is shown in Figure 37.

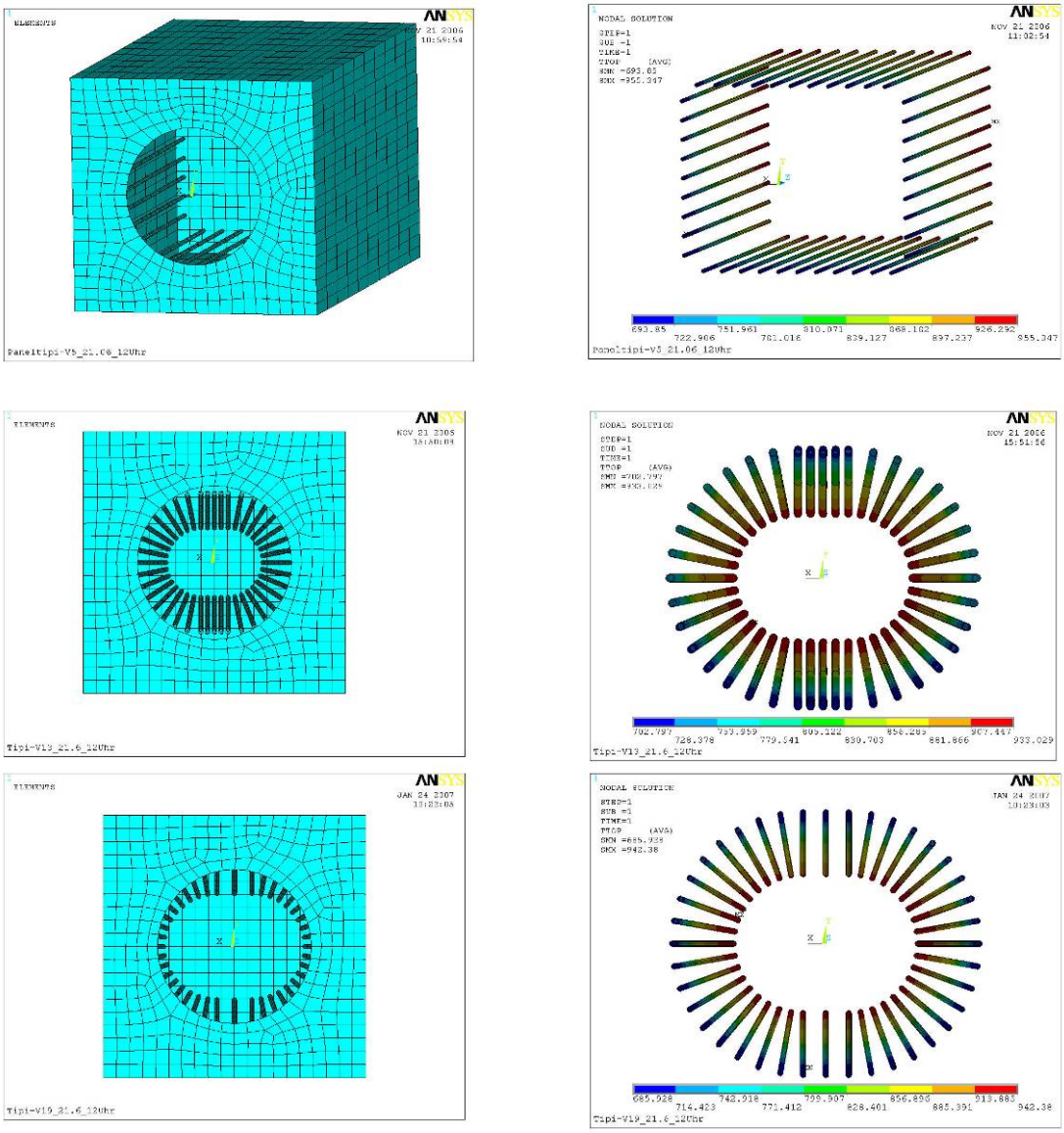

Figure 36 Results for several pre-designs

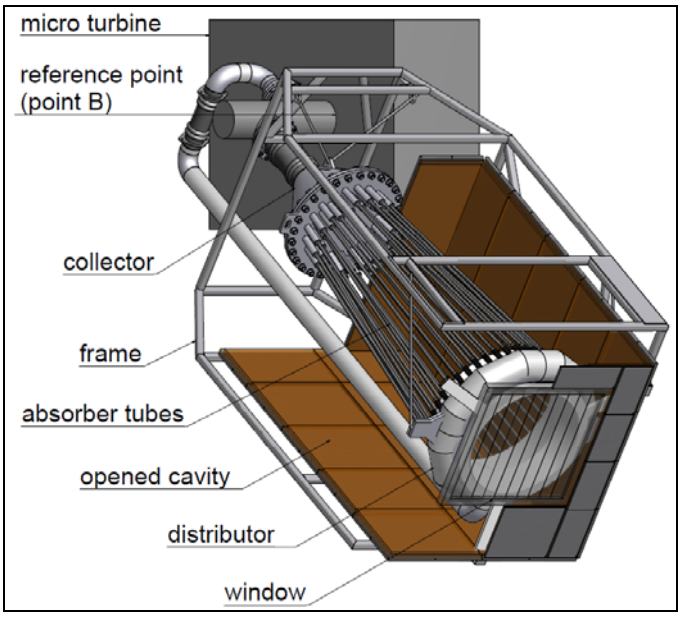

Figure 37 Selected design for receiver and system

Manufacturing of the receiver

After the design-freeze of the receiver system containing receiver, receiver frame and cavity the manufacturing of the receiver was started in February 2009.

The air distributor was partly pre-fabricated by an external company and was not delivered as ordered as a curved tube but made of straight segments. Anyway it could be used without modifying other parts of the assembly. The inner insulation of the weld-on nozzles was mounted already at GEA side. Each absorber tube was equipped with a thermocouple at the outlet of the tube (Figure 38).

Connections for the later installation of measurement equipment like a weld-on tube for the Pitot tube and fittings for the differential pressure were integrated already into the receiver to avoid additional welding afterwards. After finishing the receiver was cleaned and pressure tested with water.

Then the assembly was shipped to a specialized insulation company for doing the inner insulation. The whole receiver was assembled and mounted into the receiver frame. This frame was used both for a safe transportation and as mounting structure later on the tower. All parts that were used only for transportation were painted in yellow (Figure 39).

The receiver was shipped to the Plataforma Solar, Spain, for the final preparation (Figure 40). Some additional small inner insulation parts and some outer insulation had to be mounted. Thermocouples were fixed on the surface of the absorber tubes, in each case five thermocouples in the inlet and outlet of the receiver and more than 20 on different parts like weld-on nozzles and collector to monitor the temperatures (Figure 41). As the last step before lifting the receiver the absorber tubes were painted black with Pyromarc to increase the absorption coefficient. In parallel to the receiver preparation (see finished receiver in Figure 42) the cavity was preassembled on the ground (Figure 43).

Figure 38 Thermocouples in absorber tube outlet

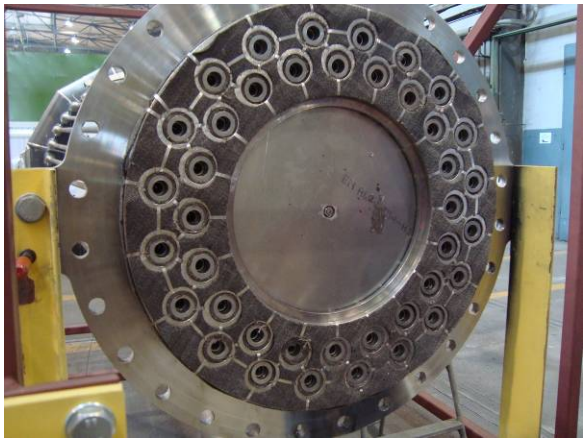

Figure 39 Front side of collector

Figure 40 Receiver delivery to PSA

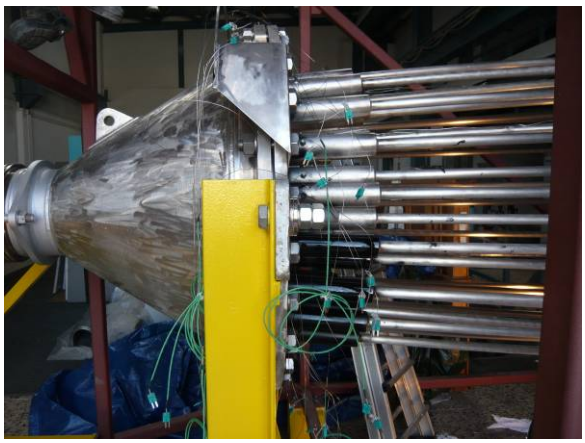

Figure 41 Installation of thermocouples

Figure 42 Finished preparation of receiver

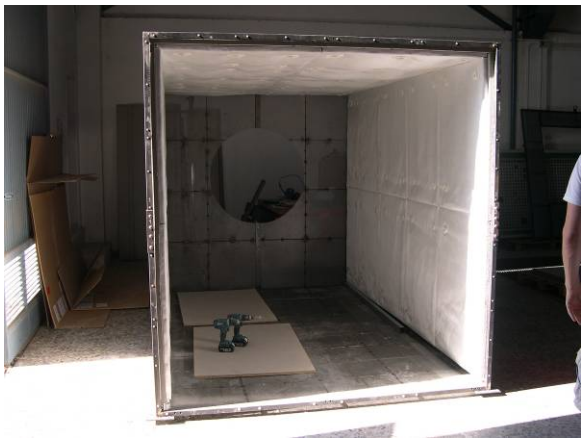

Figure 43 Preparation of cavity on the ground

The turbine had been shipped in spring 2009 and was lifted to the test platform after preparation of the platform (see **Error! Reference source not found.**). Then the receiver was lifted to the tower and the external housing mounted between receiver and turbine. The suspensions of the receiver were installed and the receiver with the external housing aligned to the desired inclination of 35°. After that the support structure was mounted. Contrary to the first planned mounting procedure the cavity was assembled not on the ground but on the tower. This was necessary due to a critical weight of the receiver frame and due to the high porosity of the insulation material of the cavity that required a careful handling. 20 more thermocouples were installed on the cool side and in between the two insulation layers. Air inlet and exhaust gas piping were connected and all measurement equipment installed.

2.6 Cogeneration Unit System Test and Evaluation

2.6.1 Objectives

- Preparation of test bed and installation of all components for solar-hybrid microturbine test
- Test of the solar-hybrid microturbine system

2.6.2 Preparation of test bed

The new solar-hybrid cogeneration system based on the commercial T100 microturbine had to be installed and tested at the CESA-1 tower facility at the Plataforma Solar de Almeria.

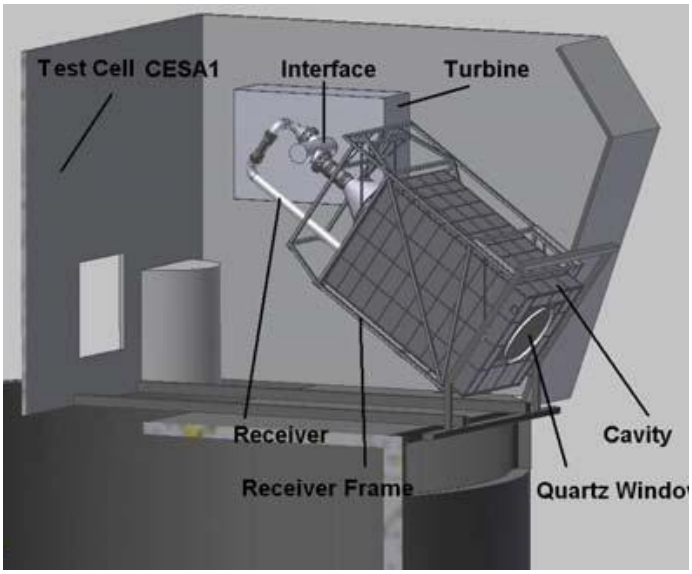

Figure 44 System Overview

Error! Reference source not found. gives an overview over the new system showing the mayor components of the turbine/ receiver assembly that had to be build up in the test bed.

Planning phase

Quite early in the project it was decided that for budget reasons the test bed for the new 100 kW system was not to be installed in the room in the tower in 70 m height as originally planned, but in the same room the tasks of WP 3 were executed, i.e. at the 60 m level. Thus subsystems like the moving bar, fast shutter, fuel and water connections could be further used and other parts and pieces could be reutilized with some modifications, resulting economically beneficial. Interfaces between all the system components had to be defined and drawings of all components had to be elaborated.

Test bed preparations

At the test bed, the rails, motor drive and bottom support structure for the receiver and turbine could be reused as a base for the new support structure described below. Parts of the exhaust piping could be used with little modifications. Grid connection cables from tower base to the test bed and fuel piping from storage tank at the tower base to the test bed could be reused and just had to be extended inside the test room to reach the new points of connection.

Mounting structure

As mentioned above the movable cart from WP 3 was used as a base to mount all major components on it to be able to drive the whole assembly back and forth in the test room. The big benefit of a movable system is to be able to protect the system better from ambient conditions during assembly or periods without operation and most important to allow easy access from the front side.

In order to withstand the total receiver weight of the approximately 2.5 tons the support legs for the receiver assembly were designed to be six pillars of structural steel . These legs were constructed vertically and welded to horizontal cross bars beneath them in order to connect them with the right-hand wagon beam.

The design of the support structure for the turbine turned out to be more sophisticated due to the height the turbine had to be put up. In order to support the turbine well, two support legs made of structural steel were chosen. Special care was taken with the distribution of the turbine weight over both wagon beams. To achieve it both of the legs were diagonally attached to the other wagon beam. Horizontal cross bars were introduced and a platform under the turbine feet was constructed. To assure a good accessibility to the turbine a ladder was provided with an attached platform on top to allow maintenance works to take place. Since the turbine runs at nominal speed with 70000 rpm no significant impact on the support structure was expected due to resulting vibrations. However, to prevent the turbine from displacement side bars were attached to the turbine structure to avoid any possible movement resulting from start-up or failure situations.

Connections

The piping connections had to be designed to be easy to disconnect when the wagon was moved. Gas turbine efficiency highly depends on the air temperature used by the turbine. Therefore it was decided to install an air inlet duct and use air from outside the test room. The installation of the air inlet ducting was the most difficult to perform due to a piece of piping having to be removed for the turbine being able to move backwards. For this operation the air inlet piping was designed with a sleeve connection in order to free the turbine and make it movable. The air inlet pipe can be lifted up and down with a rope (see Figure 45). The exhaust gas piping was connected the same way like in WP3 with a sleeve coupling. Being supported by steel cables the piping can be attached to the turbine without transmitting any loads to the turbine flange. By detaching the sleeve coupling the turbine and receiver system can safely be driven backwards.

The turbine package has a big ventilation fan attached that sucks a huge amount of ambient air through the housing to prevent overheating of the components inside the package and to supply fresh air for the gas turbine process. No ducting was needed for the outlet of this fan because it was pointing upwards directly towards the room ventilation system.

In order to connect the turbine to the electric grid, care had to be taken with the turbine specification and the existing installation. Since the electrical power of this turbine is much less than the former turbine, no problems with the existing cables were expected. Since the electrical cabinet from the former installation had been dismantled, the cables coming from the turbine had to be connected to the cables running up the tower. Due to the cables being oversized for the new turbine, the maximum voltage drop threshold of 5V was complied with. The existing circuit breaker for the grid connection has a nominal current rating of up to 1000 A and breaks short circuit currents of 15 kA. These characteristics are suitable for the Turbec turbine specifications of a rated continuous output current of 173 A and a maximum

Figure 45 Air Inlet and exhaust gas piping

allowed short circuit current from the grid of 35kA.

The fuel installation from WP3 could be reused and just had to be extended to the new turbine location on the support structure. A combination of flexible hose and fix tubing was used. Electrical and mechanical shutoff valves and a metering device were introduced into the line.

Front protection


Figure 46 Front Protection

Although the front protection was mounted at the end of all installation works it is considered part of the test bed and will be explained in this part of the report.

To protect the receiver housing, the tower structure and of course the test room a front protection had to be installed in front of them. Materials in consideration were refractory ceramics made of different mixtures out of AL_2O_3, SiO_2 and CaO or consisting of different organic refractory materials. Due to the temperature gradient inside the ceramics only the front layer has to withstand temperatures of up to 1200 ºC. The other layers of the front protection were chosen to be made of material with a classification temperature of 1000 ºC.
In order to fix the ceramic boards to the wall made of sheet metal that was mounted on a support structure, special fixation systems had to be used. These systems had to be designed to withstand the high temperatures on the front side, heavy wind loads as expected at the test site in Almería and other weather influences. Various system concepts have been analyzed and the best suited one was chosen. To have an additional benefit of the tests several material combinations and fixing methods were installed to be able to make a comparison after the test campaign as seen in Figure 46.

System Installation

The key component which defined the system installation schedule was the delivery of the receiver which was delivered later than scheduled due to several design and production difficulties. The turbine was lifted into the test bed in June 2009 (see Figure 47, left). The receiver and turbine support structure as well as in- and outlet piping were ordered, assembled and brought up to the test room. With the turbine support structure in place, the turbine could be lifted on top and all the external connections could be done. Having connected the turbine to the grid, first control system tests could be done in July 2009.

The receiver was delivered and then lifted up to the test room at the beginning of September 2009 (see Figure 47). During this time sensors were attached to the absorber tubes, the receiver was painted with high temperature paint (Pyromark 2500) and assembly of the receiver housing (cavity) started.

Figure 47 Lifting and installation of turbine and receiver

After lifting the receiver into the test bed structural works could be done adapting the receiver structure in a way that turbine and receiver could be connected smoothly without risking any misalignment. This connection had to be done very carefully since the allowed forces on the turbine flange were very limited. (see Figure 48). To be sure different load cases had to be simulated considering different system states (temperatures, pressure, solar, fossil). A a concept for the receiver support and holding had to be found. To allow thermal expansion without introducing high forces or moments on the turbine interface the receiver was mounted hanging in the receiver support structure. The turbine, turbine interface and the mounted receiver hanging in the receiver support structure can be seen in Figure 49. After the installation of the big components the test room could be closed with the front protection. Inside the test room the cavity was build up and all systems were connected.

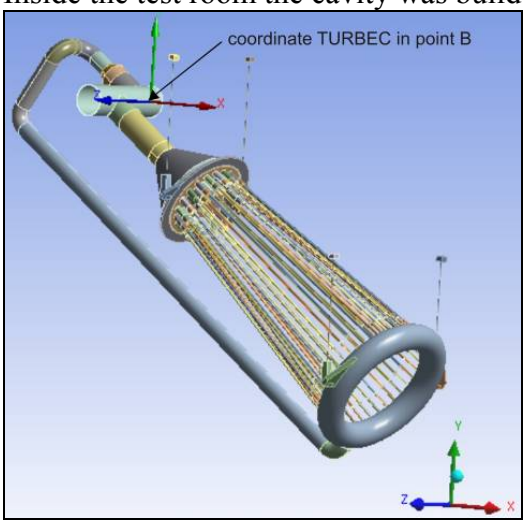

Figure 48 Receiver fix point

Figure 49 Receiver mounted

Cavity

The receiver housing (cavity) is an important functional element of the receiver system. Main purpose of the housing is the thermal insulation of the solar absorber. In the case of the SOLHYCO-Receiver it is also an optical element equalizing radiation load on the absorber tubes by re-radiating visible and thermal radiation to the 'back-side' of the absorber tubes. The cavity was build up of a cubic frame were the sides are closed with single 'door elements' made of wrapped insulation boards mounted on a sheet metal back structure. The ceiling of the cavity can be seen in Figure 49. For fixing the insulation boards to the back structure the same fixing method was used as for the front protection ceramics. The back side of the cavity where the tubes are leaving needed a special solution as well as the front side where the concentrated solar radiation has to enter through an aperture. The components of the cavity were manufactured on PSA and assembled after the installation of the turbine and the receiver in the test room.

At the front side of the cavity an aperture cone (visible in Figure 46) was installed to protect the distribution ring that distributes the air from the compressor/recuperator to the single absorber tubes from direct radiation. Each absorber tube has an own compensator that also had to be individually protected from radiation. On the back side of the cavity an isolated plate was installed inside the ring of absorber tubes to protect the collector plate where all the tubes are ending. This detail later caused big problems as explained in section 2.6.5 (Solar tests)

Data Acquisition and Control

The standard turbine comes with a complete control system that allows safe operation of the system. It is able to receive basic commands from different sources like switching on/off or setting the desired power using a Web-Interface. For the operation of the solar receiver with the gas turbine a special interface was defined for communication between the data acquisition and control of the complete system and the turbine control. The solar version of the turbine control defines different operation modes (fossil, hybrid or solar only) and allows switching between these modes following external commands. For the communication a standard bus communication protocol was used (Modbus) that had to be implemented by the turbine control system and the DAS computer. In Figure 50 a screenshot of the graphical user interface (GUI) to the turbine control is shown. Programs for the control and DAS computer were implemented using the Labview programming environment (see Figure 51).

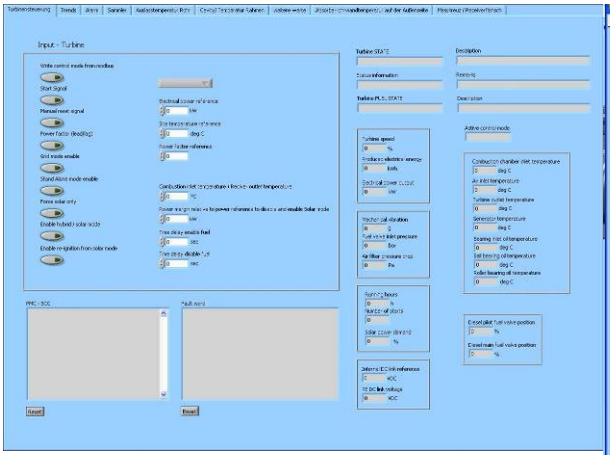

Figure 50 Turbine control GUI

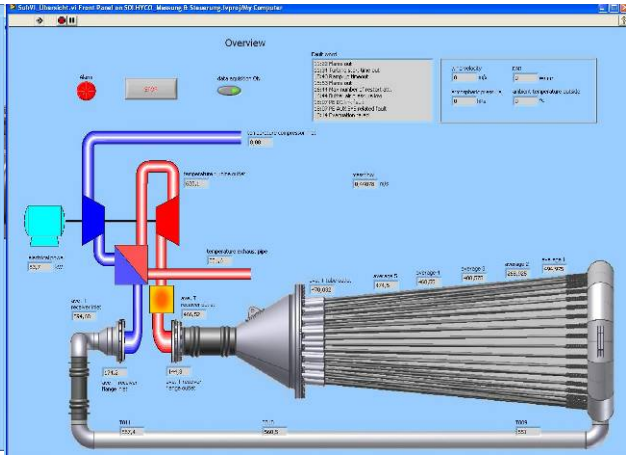

Figure 51 Screen shot system overview

The data acquisition system consisted of about twenty modules for AD conversion with a resolution of 16 bits. Since a high acquisition rate was not necessary relatively low cost

modules could be selected to build up the system. All modules were connected to a RS-485 network and distributed over two electric cabinets. More than 200 signals (including the turbine values) were monitored and recorded by the system. Figure 50 shows a system overview screen that is usually shown on one of the two monitors in the control room where the most important values can be seen. The DAS program later has separate screens (tabs) with a detailed view of the sensors of most sub-systems.

Most sensors were temperature sensors for the supervision of a safe system operation. Special attention was paid to a good measurement of the air mass flow through the solar receiver which caused problems in many other projects. The Pitot sensor (Itabar) was installed in the long straight tube going to the air distribution ring at the receiver front side. Having such a long straight tube there should be no disturbance in the flow and a perfect profile should be developed until the measurement point. This measurement location therefore should allow high precision measurements with an error below 1%. A precise temperature and pressure sensor is located close to the Pitot tube for the necessary calculation of the air density.

The solar flux density measurement at the SOLHYCO test plant is performed with a measurement system named PROHERMES (programmable heliostat and receiver measurement system) which was developed at PSA. In this concept a diffuse reflecting white surface (Lambertian target) is put into the beam path in form of a moving bar mounted in front of the receiver module. It performs a circular (90°) movement downwards and then back to the upright position. The directed solar radiation from the heliostat field hit the target surface where the radiation is diffusely reflected. A remote controlled CCD-camera located in the heliostat field records a series of images of the moving bar with a frequency of about three pictures per second. There are four black markers mounted behind the white plates in order to facilitate the recognition of the moving bar position in the images by the evaluation software. The sequence of images can then be composed to a result image covering the whole aperture area (see Figure 52).

The picture evaluation was done up to now in a custom-made macro in the image processing software OPTIMAS that is not supported anymore. Therefore for the SOLHYCO project a new evaluation tool with a graphical user interface (GUI) was created in the Matlab environment.

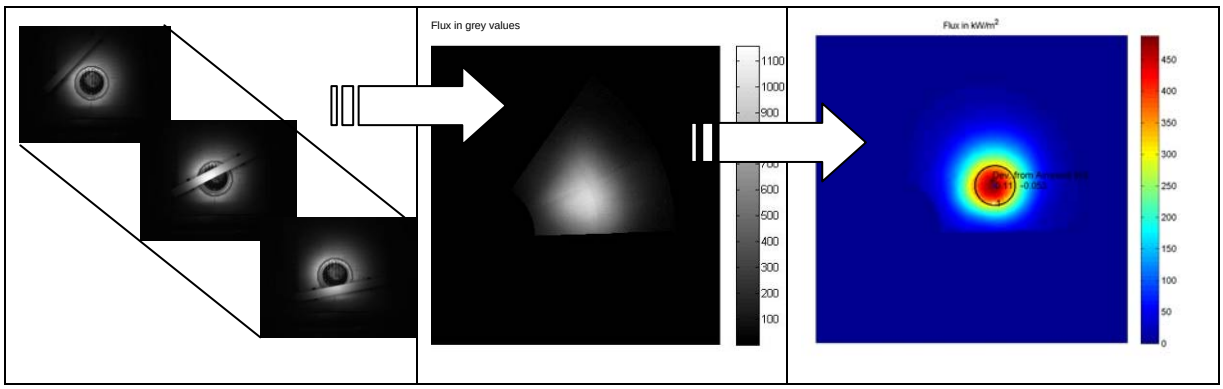

Figure 52 Result picture and calibrated flux map out of a sequence of single moving bar images

The result image consists of a light intensity distribution over the measured area that is linearly proportional to the flux density. From the measurement of a reference spot with a radiometer, it is possible to assign physical flux densities to the corresponding intensity (gray) values of the images. This results in a quantitative flux density distribution over the whole measurement area. With this information the input power in the moving bar plane can be

calculated. The flux image, all measurement parameters and the results from the image evaluation are then exported to a standardized Excel evaluation sheet.

An infrared camera was provided for measuring temperatures on the absorber tubes. Two openings in the receiver housing were installed to be able to view and grab images of the tubes. After some tests with the system it was found out that there is not much benefit compared to the measurements with the temperature sensors and just for supervision of the IR system was not very practical.

Ambient condition like solar radiation, temperature, wind, etc were measured with sensors of the CESA-1 facility and included in the SOLHYCO DAS using OPC communication. Since the sensors were not calibrated the data later was post processed and ambient data was included from a DLR high precision station located on PSA.

2.6.3 Test Plan

A test plan was elaborated defining the test phases during the project progress. The operation period was divided in fossil start-up, fossil operation, solar start-up and solar-hybrid operation phase. In the test plan the goals for the phases were defined and procedures were elaborated for the safe operation of the system. Additionally, check lists were defined that should later be followed and refined during the operation phases.

2.6.4 Turbine commissioning/ fossil start up

First turbine starts showed unsatisfactory combustion behavior, noticeable by high amount of smoke coming out of the escape pipe during light-up. After the first tests the maximum power reached during operation decreased and turbines surges occurred while changing control parameter or during shut down procedure.

For troubleshooting an analyzer for the exhaust gases was installed. After ignition problems the delivered cooled ignitor was found to be broken and had to be replaced by a standard one. After cleaning the fuel injection nozzles and considerable changes in the control software a first run with 90 kW_{el} was achieved. NOx values several times higher than normally were detected that indicated too high combustion temperatures. Therefore the combustion chamber was dismounted. A high amount of unburned carbonized diesel was found. The flame tube showed a small damage caused by overheating (see Figure 53 and Figure 54).

Figure 53 Damaged flame tube

Figure 54 Unburned diesel

Figure 55 Eccentric position of external flame tube

Through the open combustion chamber it was possible to check the positioning of the extension flame tube. As the mounting procedure of this tube was quite difficult there were doubts that it was centered well (Figure 55). And in fact it was one of the problems that could be solved by accessing through the combustion chamber and moving it slightly to get it into the right position.

Measurements showed low absolute system pressure and low mass flow through the receiver compared to the expected values by Turbec. Turbec analyzed the data and came to the following approaches that might be the problem

- Strange air distribution due to air leakage somewhere in the system
- Wrong delta-T over the combustion chamber
-

To be able to go on with the troubleshooting additional measurement equipment was necessary (pressure sensor for the pilot/main air of the combustion chamber, pressure sensor for the fuel, endoscope) and a new flame tube had to be ordered. The new sensors were installed and the connections to the combustion chamber were checked. During one start attempt it was not possible to reach electrical generation and a lot of flame out occurred during ramp up (from 28 to 75 %). The combustion chamber was dismantled again but nothing strange could be noticed. After reassembling the system electrical generation could be reached. After the test another time Diesel was observed in the pilot injection air pipe. The measured fuel and injection air pressure seemed to be reliable. It was observed again that air mass flow and pressure of the receiver were quite low and the fuel consumption seemed to be too high.

The detailed analysis of the data after the tests showed a very high temperature drop over the receiver. At that time not all insulation parts of the cavity were installed yet so that even after heating up the system a drop of about 260 K (from 620 °C receiver inlet to 360 °C outlet temperature) was reached. This led to increased fuel consumption as the T100 control system needed to compensate the low combustion inlet temperature to be able to keep the temperature set point of the turbine outlet temperature (TOT). In one of the test runs the load on the combustion chamber reached 460 kW while 350 kW is the limit to be able to keep the emissions in an acceptable value and 400 kW is the design limit.

To reduce the temperature drop over the receiver the missing insulation parts were installed in the following weeks. But since during start up and heating up of the system there is no possibility to avoid the low combustion chamber inlet temperatures the control system had to be modified. A maximum allowed temperature difference between the combustion inlet

temperature and the TOT was implemented. Since the combustion air temperature is not measured by the turbine control system the average temperature of the absorber tubes outlet was sent via Modbus to the turbine control.

Several turbine tests with remote control from Turbec/Sweden were done, observing unstable control and surges during operation and during normal shut down. These problems could not be solved before a one month break in December 2009 that had been scheduled to refurbish the low voltage distribution system of the CESA-1 tower. A new flame tube was installed. The low air flow through the receiver could be indicating an air by-pass through the external housing; therefore the springs and the correct position of the extension flame tube were checked again. To resolve the doubts about the absolute pressure measurement the sensor was replaced by a new one. To decrease heat losses over the receiver the aperture of the receiver was closed with insulating material. The assembly of the combustion chamber was checked again and everything was cleaned. With an endoscope a slight damage could be detected on a blade of the stator of the turbine (Figure 56). This might had been caused by the overheating of the combustion chamber or by small particles or a loose piece in the receiver loop and was identified as the main reason for the compressor surges. Since there are possible work-arounds it was decided not to proceed with a very costly repair at this moment.

During the further commissioning focus was given to adapt the control systems behavior to the damaged turbine nozzles. After solving the problem with the combustion chamber overload the target was now to avoid the surge phenomena during normal operation through the decrease of ramp change rates of reference values. Furthermore some extra protection was added to detect flame-out during running with the combination of solar and fuel power. Within several days of tests and software modifications the turbine could be commissioned successfully.

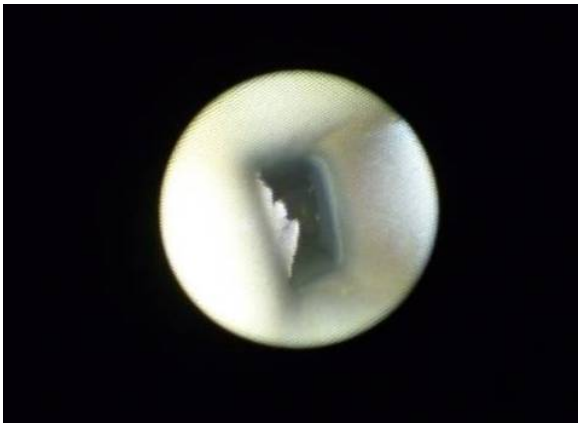

Figure 56 Damaged turbine nozzle

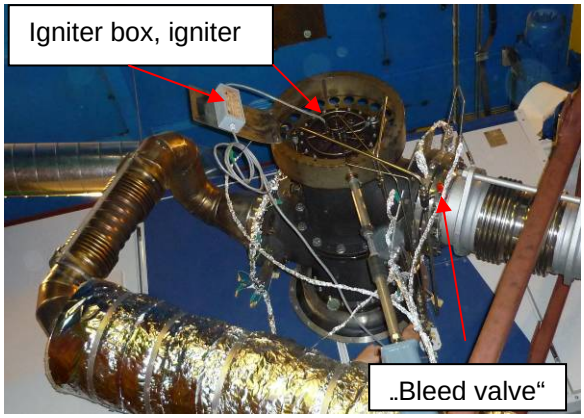

Figure 57 External housing

Another possibility to avoid surges was to reduce the pressure after the compressor and increase mass flow by using a bleed valve. Several tests were made with different operation parameters and using the existing piping to the external housing for bleeding (see Figure 57). The bled mass flow seemed to be too low and surges occurred even with the valve totally open. Finally the plan was to install a new bleed valve in a piping at the compressor outlet in the turbine package. But as during first tests another solution could be found (see next chapter), no more modifications were made. The initial concern that a damaged stator will limit the maximum reachable turbine power was disproved when on March 31st, 2010 the turbine reached 99 kW.

Fossil only test

After first experiences with the turbine and receiver control several procedures were implemented to improve the operation. To shorten the long start-up time of the turbine system caused by the high thermal inertia of the receiver, the receiver was preheated every test day with few heliostats.

It was found that compressor surges during operation could be avoided adapting the operation strategy to run with high turbine speed (> approx 93 %). The limitations through the reachable work points of the systems were at this time expected to be rather low but as we will see on the next pages, this assumption was not completely correct.

The design point for the solar receiver was selected at maximum turbine power (100 kW) with a TOT of 645 °C. According to data delivered by Turbec the recuperator outlet temperature (≈ receiver inlet temperature) should then be about 600 °C, air mass flow 0.77 kg/s and absolute system pressure 4.3 bars. However during the tests 600 °C receiver inlet temperature were already reached with a TOT of about 610 °C. During the first tests this inconsistency was not noticed.

Since the material of the receiver inlet tube is only a high temperature steel with approval up to 600 °C and not a nickel alloy like the absorber tubes, this temperature should not be exceeded. Therefore TOT reference had to be limited to 610 °C which reduces the reachable power output. One explanation for this could be that compressed air was bypassing the recuperator or the receiver.

At the end of April 2010 several light-up problems appeared. Finally a new box with a cooled ignitor was installed. After three test days with receiver outlet temperatures of up to 750 °C the light-up problems appeared again. The ignitor was checked and incorrect sparkling observed. The inner insulation was probably broken again. Therefore, the “old” un-cooled ignitor with the “new” ignitor box was installed. All remaining tests were run successfully without any further light-up problems with the un-cooled igniter with receiver outlet temperatures of up to 805 °C and more than 100 hours of solar operation.

Solar Startup

The first solar test was done focusing some few heliostats on the receiver without operating the turbine (Figure 58). The heliostat aim point was checked. Organic binder of the alumina of the front protection was burned out slowly, receiver and cavity heated up for a first time and all connections and ducts of receiver and cavity checked for light tightness. During the following tests the turbine was always operated and the number of heliostats increased step by step. The heliostat field operator was instructed in the planed tests.

Figure 58 First solar operation

On the fifth test day on March 26th 2010 650 °C receiver outlet temperature was reached and 700 °C on the following test day. Consecutive temperature increase was done slowly to avoid overheating of components and to gain more operation experience.

In the design heliostat field layout 29 heliostats were foreseen to reach maximum receiver power at 800 °C receiver outlet temperature at 825 W/m² of direct insolation. The first tests showed that a much higher number of heliostats were necessary to reach the desired temperatures. The maximum number of heliostats focused on the receiver during the tests without window was 59 (see Figure 59) with approximately 780 °C receiver outlet temperature at more than 900 W/m² DNI. After installing the quartz window this number was reduced significantly to a maximum of 39 at similar DNI conditions and with a reached temperature of 805 °C. From the complete CESA-1 heliostat field a total number of 60 heliostats were selected for use during the solar tests. One reason for the high number of necessary heliostats was that all odd-numbered rows of the heliostat field were out of service during the whole test period due to a scheduled replacement of there gear boxes and the installation of new control circuits. This constrained the selection of the heliostats and therefore the ideally distribution of them. Also a time extensive cleaning of the heliostats and problems with the tracking led to the high number of heliostats.

After gaining some experience fixed heliostat groups were defined to allow an easier operation and a faster start up. Each group – in total 11 - consisted of four heliostats and was arranged in a way that a homogenous distribution of the receiver temperature was achieved. After focusing all groups single heliostats were added to optimize the desired test conditions.

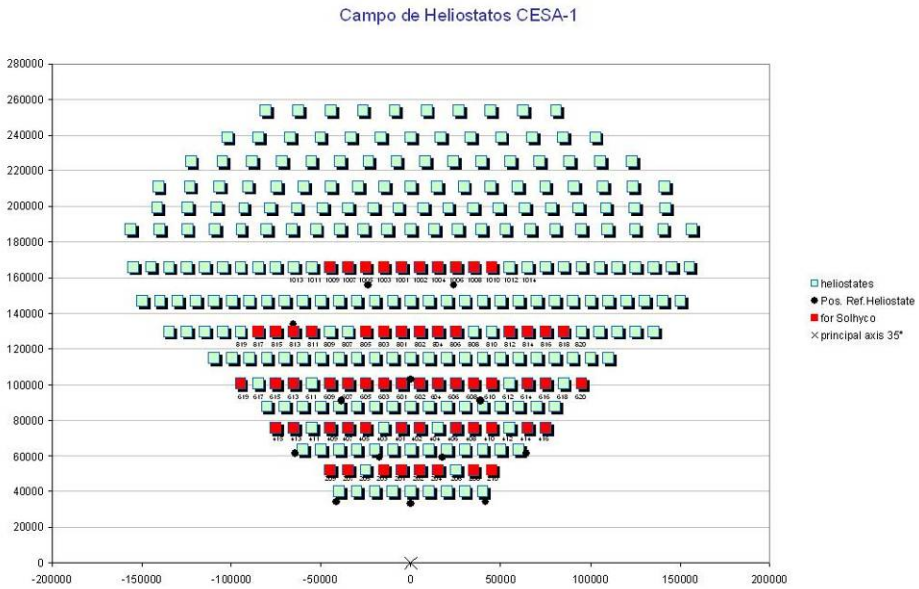

Figure 59 CESA-1 heliostat field with heliostat used for SOLHYCO

2.6.5 Solar tests

Solar tests were carried out each time the weather was good enough (wind forecast < 50 km/h, few clouds) and no technical problems had to be solved first. Main objective was to reach a receiver outlet temperature of 800 °C at maximum air mass flow.

One observation during the tests was the high sensitivity of the surface temperature of the absorber tubes from the distribution of the focused heliostats. One single heliostat, especially from the second and forth row, could cause temperature peaks on the absorber tubes. On the other hand this behavior permitted to select a specific heliostat to increase the temperature in a specific region of the receiver. As the heliostats of the nearest rows have a significant smaller focus the temperature on the upper part of the receiver, where these heliostats are focused on, were quite high. With few heliostats the needed input power for this receiver part could be achieved. The lower part of the receiver, where heliostats from the row eight and ten were focused on, had much lower absorber surface temperatures. Heliostats from these rows have a very big focus compared to the small aperture of 900 mm and therefore high spillage losses. Even when focusing all centre heliostats from these rows the absorber temperature reached was much lower than on the upper part of the receiver.

Due to the insufficient input power from the back part of the heliostat field and due to a very high sensitivity against wind the temperature distribution of the receiver was not as equal as desired. This was one of the reasons why the limit of the surface temperature of some upper absorber tubes was reached before the average maximum receiver outlet temperature of 800 °C could be achieved.

During the test phase without the quartz window the highest average outlet temperature was 798 °C for a short time before the surface temperature of one absorber tube exceeded the limit of 910 °C and heliostats had to be removed. During the further progress of the work package the limit for the absorber surface temperature was slightly increased to be able to reach higher temperatures. Every time the limit was increased the effect on the receiver had to be checked carefully after the test. But even with higher limits steady state conditions could only be reached for receiver outlet temperatures around 780 °C.

The temperature distribution could be equalized significantly after installation of the quartz window. With reduced convection losses steady state operation at 800 °C receiver outlet temperature was easy to achieve. No major problems with the receiver could be observed during operation.

In total the turbine was operated more than 165 hours with more than 100 hours of solar operation including 30 hours of operation with the quartz window. However, as described above design conditions could not be reached totally due to the limited receiver inlet temperature and the lower than predicted mass flow. The cavity has been identified as the most critical component in the setup. Already during the first solar tests temperatures higher than expected were measured on the collector plate of the receiver. This plate is located just behind the back wall of the cavity where all absorber tubes are ducted through the cavity wall and merged together into the collector. Both collector and cavity are insulated on the hot, inner side. The maximum temperature for the collector was estimated to be 200 °C but finally values up to 340 °C had to be permitted to allow operation. All other temperature sensors on the backside of the collector showed values as low as expected.

Four causes for exceeding temperatures and heat losses were found:

- On one hand the weld-on nozzles of the absorber tubes heated up the air and on the other hand prevented that air could pass easily over the collector plate surface to cool it down.
- The insulation material used where the absorber tubes were ducted through the cavity turned out to be partly light-conductive (Figure 60). So direct solar irradiation passed the insulation and heated up the collector.
- The insulation material used for the cavity showed higher heat shrinkage than expected. Hot air passed through the gaps between the insulation boards, heated up the test room and the collector (Figure 61).
- The support structure for the insulation plates made of folded metal panels was not manufactured within the specified limits. Therefore several gaps had to be filled with small metal plates and bars but were not stiff enough and deformed specially on the top of the cavity once they were heated up (see Figure 62).

Solar irradiation on the collector could be blocked by installing thin Inconel sheets inside the cavity where the absorber tubes passed trough the cavity wall (see Figure 64 and Figure 65). The temperatures could be reduced substantially by installing several small fans close to the weld-on nozzles (Figure 63). Anyway, the temperatures remained quite high and in some cases solar operation had to be interrupted for approx. one hour when temperatures higher than 340 °C were reached. When dismantling the system an inspection with an endoscope should be done to check the status of the inner insulation of the collector.

The flange between external housing and receiver inlet also in some cases exceeded the limit of 200 °C. One cause might have been the missing inlayer of the inner insulation that could not be installed due to a change of the mounting procedure. As the gaskets of the flanges are designed for 600 °C just a small fan was installed for additional cooling.

The bending of the absorber tubes that was observed caused by the high temperature and gravity was no problem during this test phase but should be investigated further to avoid long term problems.

The PT100 of the Pitot tube used for the calculation of the receiver air mass flow got broken during the test phase and had to be replaced.

At the end of the project an area of about 100 mm x 100 mm with annealing color was detected on the eastern part of the compensator on the receiver outlet (Figure 66). When dismantling the system or the external housing the inner isolation of this part should be checked with an endoscope.

Other observation made on the receiver was a movement of the receiver front side to the east while heating up and therefore expanding. At increasing temperatures the head of the shackle of the receiver suspension touched the frame and had to be removed (see Figure 67).

Figure 60 Radiation coming through back side of cavity

Figure 61 Gaps in cavity wall after aprox. 45 hours of operation

Figure 62 Top of cavity with overheated metal sheet

Figure 63 Additionally installed cooling fans

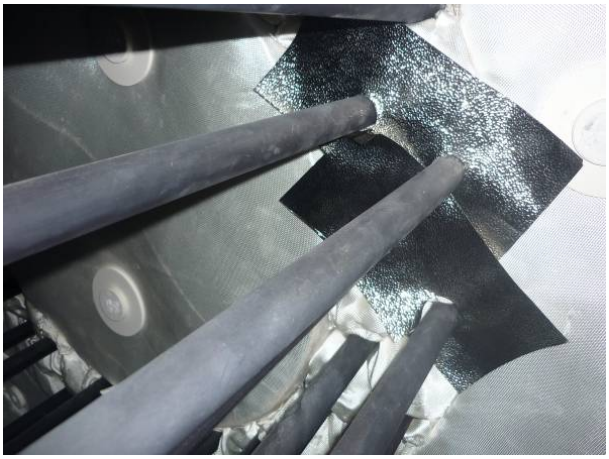

Figure 64 First Inconel sheets on back side of cavity installed

Figure 65 All sheets installed

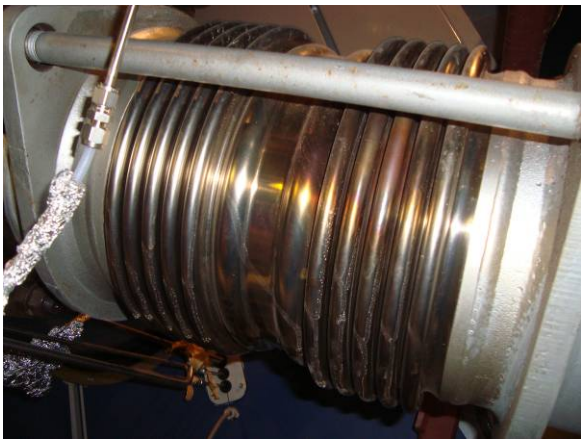

Figure 66 Annealing color on compensator of receiver outlet

Figure 67 Shackle of receiver suspension touching the frame structure

2.6.6 Quick diagnostics

In parallel to the detailed data processing, a data processing campaign was carried on with the aim to:

1. Check for fails in the sensors and outliers cleaning
2. Re-sample of the time series from the original one-second sampling to 10 seconds data series.
3. Complete the re-sampled data sets with a reliable measurement of the meteorological magnitudes (direct normal irradiation, etc.) taken from an other Data Acquisition System with the same sampling interval and synchronising both data sets for all the test days
4. Reduction by principal components analysis (PCA[3]) of the time series measuring a "same" magnitude (for instance the outlet air temperature from receiver, measured with several sensors in different positions of a section in the outlet pipe, to a single time series)
5. Carry out energy balances and main diagnostics in the system.

All this processing was carried out by developing scripts under Matlab 7.0.

Approach:
As during commissioning and start up not all sensors were already installed and the flux measurement system did still not run properly only the last 31 daily files from the 64 test days were evaluated more in detail. The continuous recordings of the (about 200 channels) for this daily files were received from the DAS system. Data processing of each

[3] Principal component analysis (PCA) is a mathematical procedure defined as an orthogonal linear transformation that transforms the data to a new coordinate system such that the greatest variance by any projection of the data comes to lie on the first coordinate (called the first principal component). This principal component is equivalent to the mean time series if all the magnitudes are covariant. But if, for instance, one of the sensors fails or is quite noisy, this technique gives a low weight to that sensor so that the resultant time series from this reduction is more representative of the true magnitud. This technique of reduction is carried out at this step of quick analysis (with programmed scripts in Matlab for Solhyco-WP5 data analysis) for all the selected magnitudes for the further energy balances which are carried out in the last step.

daily test data sheet was carried out to produce a “quick diagnostic” document containing a summary of plots and tables aimed for such a “quick diagnostic (qD)” of the test day (see Figure 68). The plots and tables included in each qD report are:

- A summary table of the main (or maximum) test conditions
- Information on the heliostats used during the test
- Plots on the receiver gained power and the produced electric power
- Plots on meteorological conditions
- Plots on concentrated solar flux measurements
- Plots on the temperatures evolution in the inlet and outlet air across the system
- Plots on the temperatures evolution in the receiver tubes
- Plots on absolute pressure and pressure drop across the receiver
- Temperature evolution in the set of sensor located in the tubes surface of the receiver
- The turbine efficiency

-

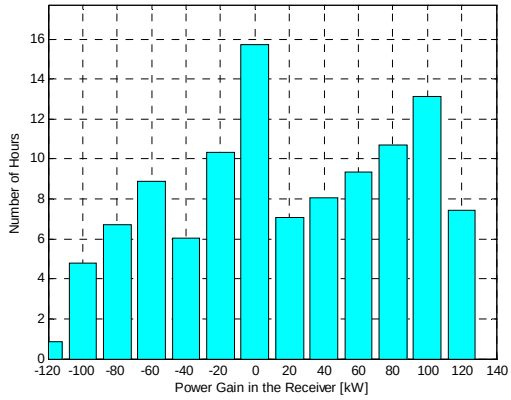

Frequency distribution of power gains in the receiver

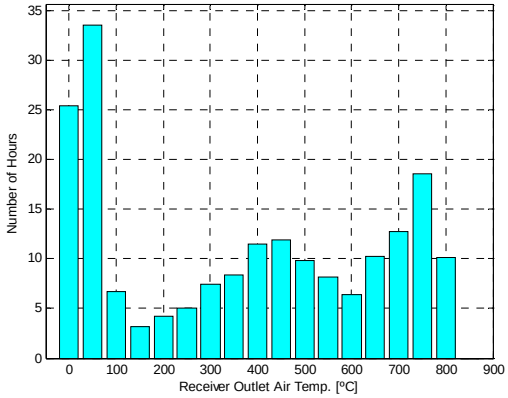

Frequency distribution of receiver outlet air temperature

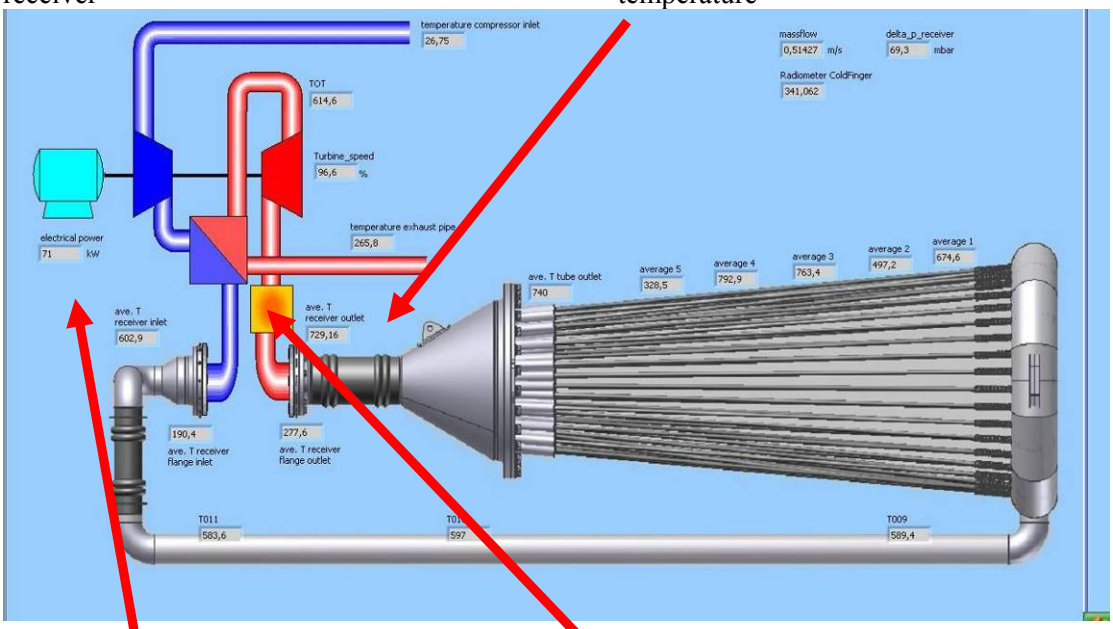

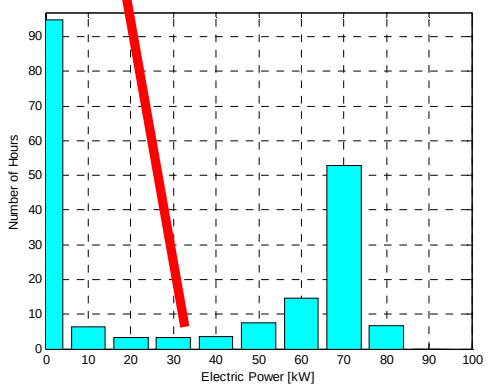

Frequency distribution of Electric Power

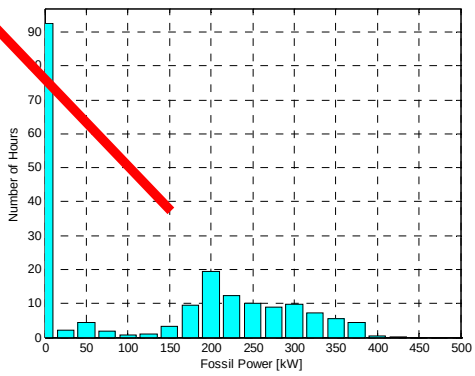

Frequency distribution of fossil power contribution

Figure 68 Quick diagnostic document: overview of power and temperatures in test phase

Summary of Results

After the test campaign the collection of data sheets were again processed altogether to produce an analysis summarising the overall test conditions of the test phase by frequency distributions. These summaries are based on the data starting on 19th of April 2010.

2.6.7 Evaluation

During the test phase of the project a total of 207 concentrated solar flux measurements were carried out on 17 different test days. The peak flux of the concentrated solar radiation on the receiver aperture ranges from 145.5 kW/m² to 672.4 kW/m². The mean flux over the receiver aperture ranges from 124.1 kW/m² to 504.3 kW/m² with a mean value of 328.2 kW/m².

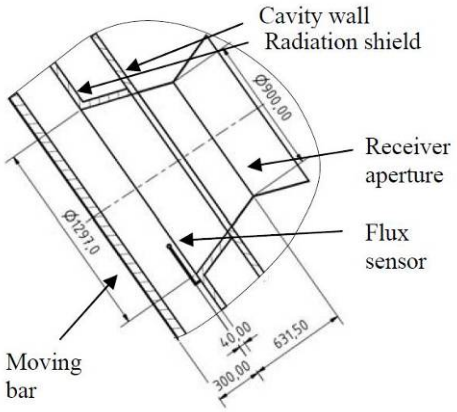

Figure 69 Cross section of aperture

As the moving bar, the receiver aperture and the flux sensor are not located in the same plane (see Figure 69) the incoming solar radiation can not be directly calculated from the measured flux map. Compared to a configuration where the moving bar is directly in front of the aperture as well as the flux sensor additional errors are introduced. Ray-tracing calculations using deflectometry data of all heliostats and the geometry of the radiation shield have been used to determine the solar receiver input power and the error of this evaluation. A diffuse reflectivity of 95 % of the white ceramic radiation shield material (conical aperture) is assumed for the ray-tracing calculations. The concentrated sun light hitting this shield is diffusely re-radiated and contributes to the input power of the receiver. The high tracking error of the heliostat field had to be modeled in the ray-tracing process which further contributed to the errors of the evaluation method.

The receiver input power is determined according to the following steps:

1. Determination of the average aim point: In the ray-tracing process all heliostats are set on the same aim point and this aim point is changed until the calculated flux map in the moving bar plane shows the same center as the measured flux map. It is assumed that the aim point is in a plane orthogonal to the north direction in the receiver aperture middle.
2. Tracking error: A statistical tracking error with a Gaussian distribution is imposed on the aim points of the heliostats and the standard deviation is changed until the best conformity with the measured distribution is achieved.
3. Moving bar evaluation diameter: The diameter in the moving bar plane from where solar radiation enters the aperture in the radiation shield is determined using ray-tracing runs with the statistical deviation from the second step.
4. Ray-tracing runs: A sufficient number of ray-tracing runs with different sets of statistically distributed aim points is performed and the power into the receiver, into the flux sensor, into a projection of the flux sensor onto the moving bar plane and into the diameter on the moving bar plane from step 3 are calculated.
5. Intensity calibration factor: The ratio of the flux sensor flux and the flux at the projection onto the moving bar plane and the standard deviation of the ratio are determined from the calculations in 4.

6. Evaluation of the measured flux map: the measured flux map is calibrated with the intensity calibration factor ratio and the power through the moving bar plane diameter is calculated.
7. Receiver input power: All ray-tracing runs from step 4 are calibrated to have the same power into the moving bar evaluation diameter and then the mean power into the receiver aperture and its standard deviation are calculated.

For both set ups with and without quartz window in front of the aperture steady state operation points were evaluated at different part loads of the thermal power of the receiver. Measurements at receiver outlet temperatures of 650, 700 and 750 °C and two points at maximum achieved temperatures were chosen. The turbine power was always constant at 70 kW_{el} like the turbine outlet temperature (610 °C set point) and therefore the receiver inlet temperature (approx. 600 °C).

Table 7 gives an overview of the receiver efficiency and the steady state conditions. Measured receiver efficiencies of 39.7 % for the open receiver at 782 °C outlet temperature and 43 % at 803 °C outlet temperature for the configuration with the window are much lower than the expected values due to design flaws in the cavity insulation and a too low mass flow from the turbine. This is also the reason why solar to electric efficiency is far below the expected value. System simulations for the SOLHYCO setup presented by Uhlig[4] showed efficiencies of 67.7 % for the open aperture configuration and 80.8 % for the quartz window configuration under full load conditions. The measured efficiencies of 39.7 % and 43 % are significantly below these values. Although the losses in the collector and the cavity wall were not considered in the publication above, the discrepancy is very high.

Two reasons for this were found:
1. The heat loss through the cavity walls was much too high. According to the simulations und design conditions the whole cavity should lose about 10 kW assuming an average wall temperature of 780 °C. During the fossil only tests the cavity loss was determined to be more than 70 kW when the aperture was closed with insulation and the turbine was operated only with a receiver inlet temperature of 550 °C. At higher operation temperatures under solar conditions this loss must be significantly higher.

Design flaws concerning the cavity were identified as:
a) Use of insulation material without previous heat treatment and
b) Weak external mounting structure.

When the cavity was heated up for the first time after the construction the insulation material started to shrink and as the temperatures at the front side was higher then on the back, a stronger shrinkage at the front bent the insulation sheets inwards, thus opening gaps. The weak mounting structure allowed the gaps to open up even more. The perforated sheet metal (used to save weight) could not block convection through the gaps also contributing to the high losses.

2. The second reason for the poor system performance was identified in the fact that the turbine didn't deliver the expected mass flow of about 0.77 kg/s minus the small burner mass flow, but only about 75 % of this value. The back pressure from the damaged turbine nozzles is one possible reason but also an internal leakage in the turbine or the external housing is suspected as reason.

[4] Uhlig R., Amsbeck L., Helsch G., Röger M. , Development of a Broadband Antireflection Coated Transparent Silica Window for a Solar-Hybrid Microturbine System, Solarpaces 2009, Berlin, Germany

	without window			with window		
date YYMMDD time	**100519 12:50**	**100524 15:13**	**100610 13:34**	**100623 12:48**	**100629 13:45**	**100623 15:24**
DNI [W/m²]	940.5	931.8	875.9	922.7	851.7	916.0
number of heliostats [-]	46	44	32	38	34	28
wind velocity [m/s]	3.8	4.8	5.3	5.9	2.2	4.3
wind direction [°N]	213.8	108.8	237.7	101.9	103.4	109.4
turbine power [kW]	69.98	69.88	69.62	69.96	69.93	69.16
turbine revolutions [%]	96.60	96.43	95.53	97.90	98.20	98.13
receiver inlet temperatur [°C]	597.7	598.4	599.7	594.2	603.4	604.1
receiver outlet temperatur [°C]	782.2	782.7	749.0	803.2	790.3	745.5
average absorber tube outlet temperatur [°C]	790.2	789.7	753.7	816.2	807.5	751.3
absolute humidity [g/kg]	1.72	1.31	3.55	4.34	1.39	2.63
receiver pressure [bar]	3.75	3.75	3.69	3.84	3.84	3.80
air mass flow [kg/s]	0.516	0.515	0.504	0.526	0.523	0.523
pressure drop [mbar]	70.4	71.8	67.5	73.3	71.8	69.2
solar input [kW]	272.8	284.8	190.7	291.5	271.6	185.0
thermal receiver power [kWth]	108.3	107.8	85.6	125.4	111.1	84.5
receiver efficiency [%]	39.7	37.8	44.9	43.0	40.9	45.6
solar to electric system efficiency [%] (turbine efficiency * receiver efficiency)	9.9	9.4	11.18	10.69	10.07	10.86
fuel volume flow [ml/s]	4.81	4.82	5.4	4.35	4.8	5.70
fossil power [kW]	173	173	194	156	173	205.84
density fuel (t) [kg/m³]	846.3	846.3	843.15	846.3	849.8	849.8
turbine efficiency [%] (turbine power / (fossil power + thermal receiver power))	24.9	24.9	24.9	24.86	24.61	23.82

Table 7. Overview of detailed evaluated data

2.6.8 Outlook

Considering the test behavior the developed solar hybrid cogeneration system can be seen as an important step forward to a commercial system. Certainly, not all objectives could be reached because the problems described above could not be solved in the project due to time and budget limitations. But this is not seen as an obstacle for the technology as they can be solved easily in the future. The consortium will try to get new funds to correct the identified problems and to demonstrate the full capabilities of the system.

2.7 Commercial System Layout and Cost Analysis

For cogeneration systems a preferred system configuration was chosen and a cost analysis for small series with 10 and 100 units was done. The dependency of the cost for electricity generation on the fuel cost, especially, if a high capacity factor is desired, and the influence of the plant location was analyzed, since also the radiation level is influencing the economical situation. The data necessary to evaluate the plant performance, cost and annual yield was elaborated and implemented in a simulation programme. It should be noticed that all uncertain cost estimations (i.e. cost reduction of the window, inner insulation, etc.) are chosen very conservative.

Solar hybrid without cogeneration:

The results for the investment cost without cogeneration are shown in Figure 70. It can be seen that the total investment cost for a small series production of 100 units per year is 344,000 € per unit. The largest cost share is the receiver cost with approx. 90 k€. Since it is a system without cogeneration, no heat exchanger cost is considered.

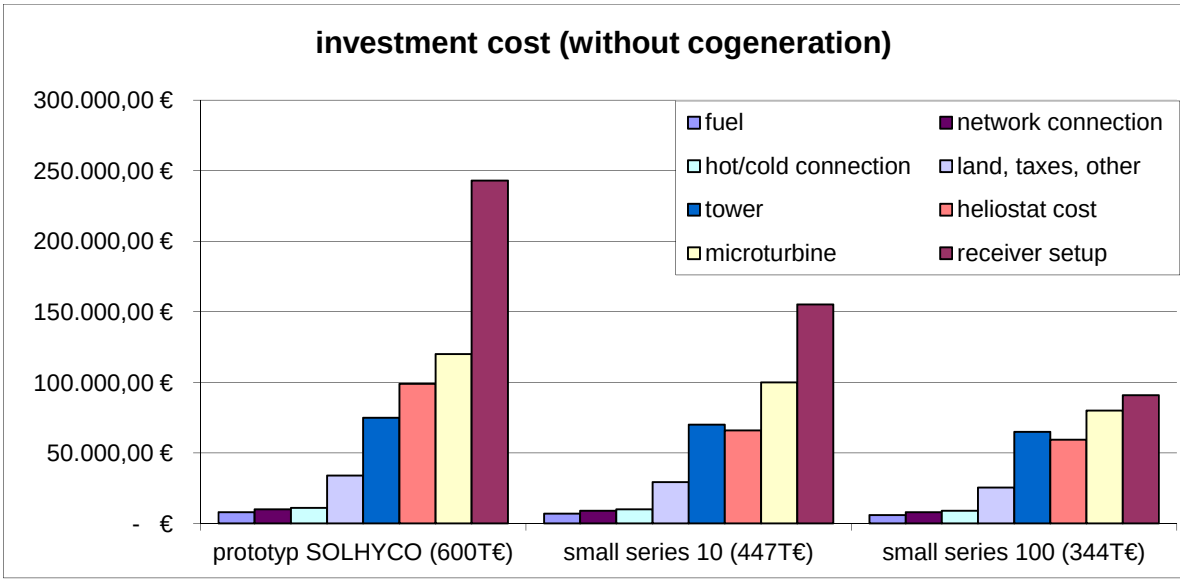

Figure 70 Investment costs of the system components without cogeneration

The annual cost for the solar-hybrid systems is composed mainly of investment, operating and maintenance costs. All following calculations are based on the numbers of the diagram "small series 100". With an interest rate of 6 % and a period of amortization of 20 years, the investment costs amount to 32,167 €/year. Operation and maintenance is assumed with a fixed rate of 31,000 €/year for personal and consumables, plus the cost for the fuel that depends on operating conditions. To evaluate the economic performance, the cost are analysed for the site of Spain (PSA) and Algeria. The utilized site data are given in Table 8.

Table 8. Site data for Spain (PSA) and Algeria

	Spain	Algeria
annual solar irradiation [kWh/m^{2}a]	2000	2200
gas tariff [€cent/kWh]	2,06	0,15

The following Figure 71 shows the LEC of the standard receiver layout for Spain and Algeria.

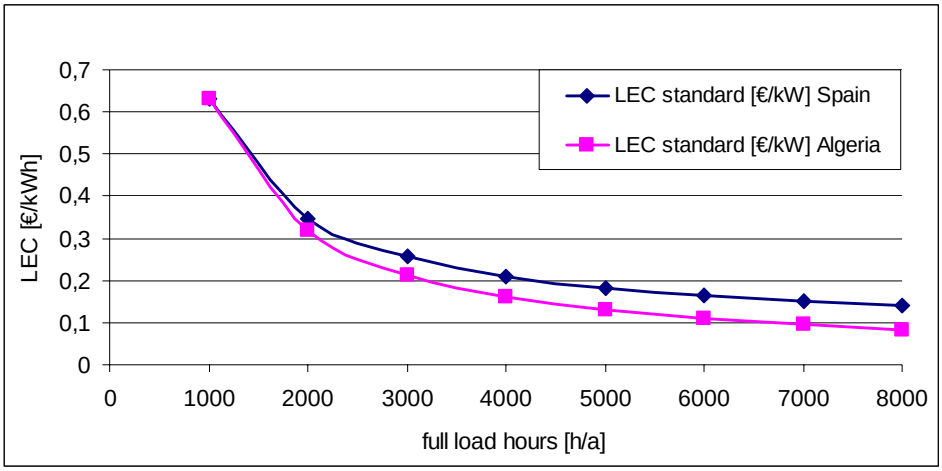

Figure 71 Levelized electricity costs of the system without cogeneration

The system is not making use of the thermal excess heat of 182 kW since no cogeneration is assumed. Figure 72 shows the cost for the unused heat power depending on full load hours. Thereby it is assumed that 182 kW has to be supplied by other technologies with an efficiency of 90% and a gas tariff of 2.06 €cent/kWh for Spain and 0.15 €cent/kWh for Algeria.

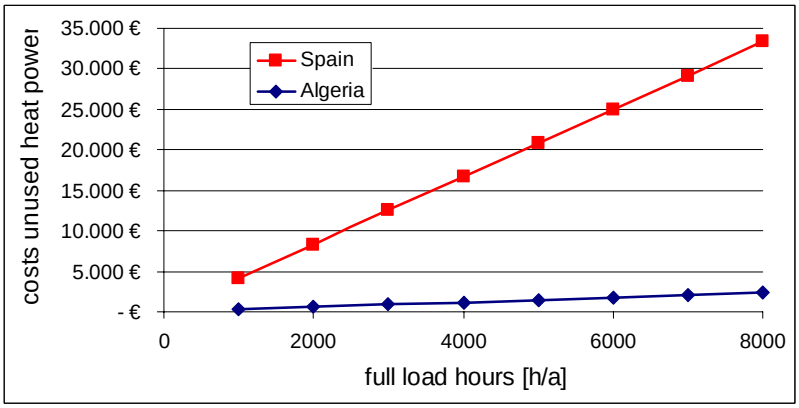

Figure 72 Cost of unused heat power (standard layout)

Solar hybrid with cogeneration:

In order to evaluate the economic performance of the solar hybrid system with cogeneration the additional investment cost for the heat exchanger for cogeneration is considered with an amount of 80 k€ (Figure 73). For the following calculations an electrical refrigerating machine with a COP of 3 and an electricity tariff of 9.09 €cent/kWh (Spain) is assumed as the reference system.

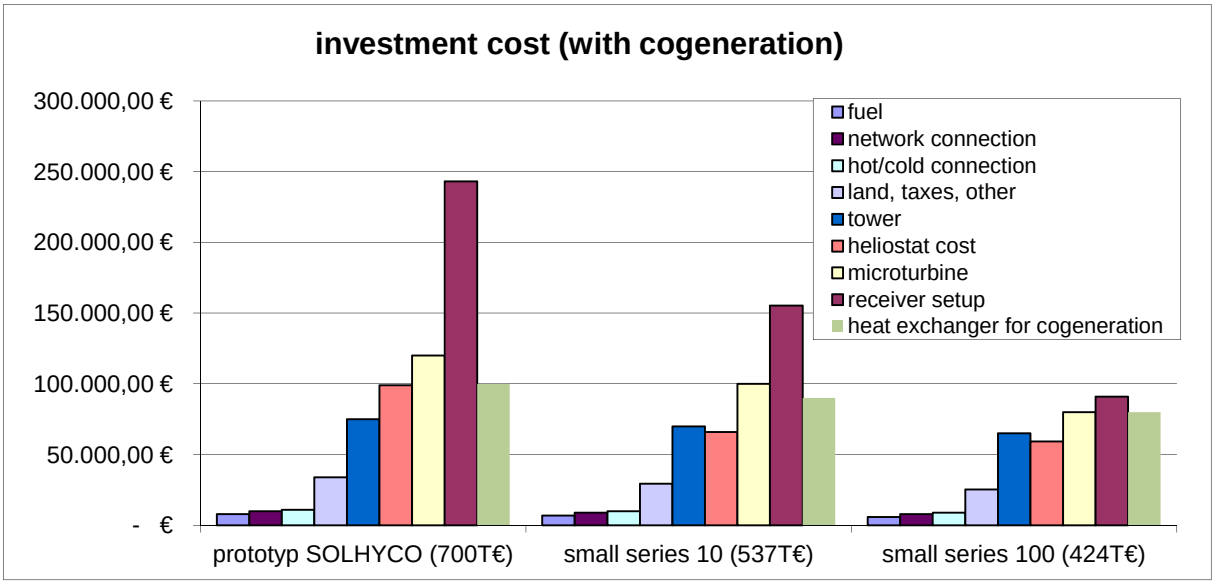

Figure 73 Investment costs of the system components with cogeneration

The following Figure 74 shows the LEC of the solar hybrid system with cogeneration for Spain and Algeria.

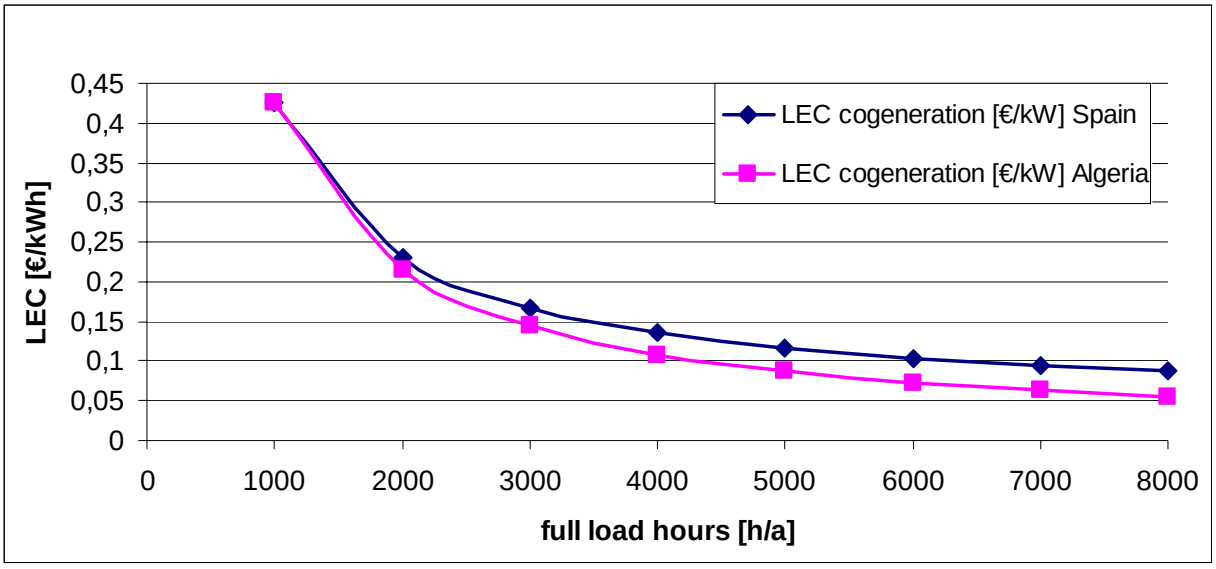

Figure 74 Levelized electricity cost with cogeneration (Spain and Algeria)

Comparison of solar hybrid systems without and with cogeneration:

The following Figure 75 illustrates the levelized electricity cost for systems with and without cogeneration.

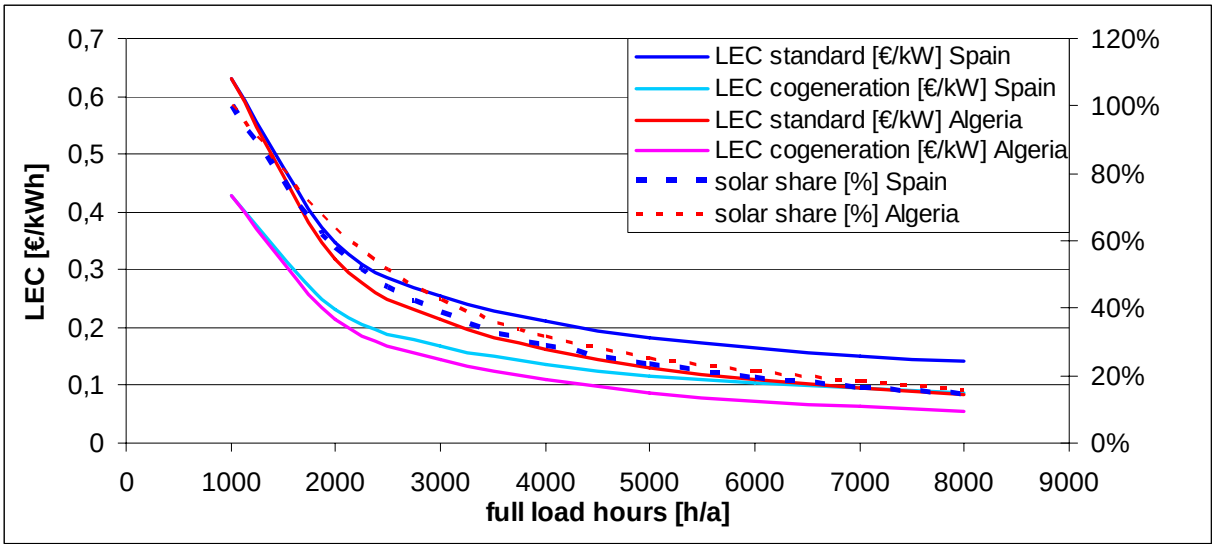

Figure 75 LEC with and without cogeneration (Spain and Algeria)

It can be concluded, that the cost for electricity generation is highly depending on the fuel cost, especially, if a high capacity factor is desired. Another factor, but less important is the solar radiation level which may lead to variations of around 10 % in the generation cost between a reasonable and a good solar site.

The cost for electricity generation for a good solar site in Algeria is 0.16 €/kWh in a mid load operating scheme at 4000 hours. For higher capacity factors the plant would be able to generate electricity at a cost of 0.09 €/kWh, but the solar share would then be only 15 %. For low capacity factors and high solar shares the generation cost are naturally higher (0.32 €/kWh at 64 % solar share).

Large systems

For power levels >20 MW the preferred configuration was selected and evaluated. Cost data and the financing scheme were selected and system simulations run. The results of the study show that solar-hybrid power can be generated at attractive cost, compared to other renewable energy solutions. However, the original goal of solar-hybrid LEC of 5 €Cent/kWh can not be met with the current cost predictions. For a plant operated at base load conditions (8000 h/a) the LEC was calculated to be 7.8 €Cent/kWh. Nevertheless, this plant is very close to be economically viable in the Algeria market.

2.8 Market assessment Mediterranean

2.8.1 Objectives

- identify appropriate market niches for first commercialisation of the solar hybrid cogeneration unit
- identify future market potential for solar hybrid power plants (>20 MWe)
- develop a standardised accounting scheme for solar-hybrid power generation
- improve public awareness about the technology

The market assessment activity is based on existing possibilities and the development of renewable energies in the region of MENA. The study was limited to four representative countries (Egypt, Morocco, Tunisia and Algeria) and the following topics were studied.

- Energy situation
- Solar thermal Applications
- Promotion of Renewable Energy Utilisation
- Policy Framework
- National Institutions in charge of energy

The Mediterranean market was studied in detail to elaborate the market potential for the SOLHYCO technology. The market assessment showed that in most countries the market for hybrid systems is not very well prepared since feed-in regulations, if existing, prefer storage against hybrid solutions. The most promising market for hybrid systems was identified as Algeria, where the feed-in tariff requires solar shares >25 % to get 200 % of the market price. Thus, solar hybrid systems must reach electricity generation cost below 0.08 €/kWh to be competitive. If the small system (100 kW) is operated with a 25 % solar share at a good solar site in Algeria, the generation cost are 0.10 €/kWh. To be competitive generation cost must drop by 20 %, which is seen to be generally possible by introducing some technical improvements in the system. Especially the receiver cost may come down as the design could be improved cost wise.

For larger systems (5 MW) the Algerian market is even more attractive, where our cost study showed a LEC of approx. 0.085 €/kWh for 25 % solar share. The selected 21 MW plant would generate the electricity at 0.078 €/kWh as base load plant, but then it would be not eligible for the preferred feed-in tariff.

2.8.2 Dissemination activities

During the SOLHYCO project three web sites were created in English, Spanish and Portuguese language. They are hosted by CEA, IIE and FUSP/USP. These web sites are containing the project results and much information on the technology. It is foreseen to maintain these sites also after the project end.

During the course of the project a total of 15 papers or articles were published on the development of the SOLHYCO technology.

2.9 Technological and market assessment – Brazil

2.9.1 Objectives

- Introduce a reliable renewable cogeneration system that reduces CO_2 emissions through decentralized power generation systems by 40 % (short term) and up to 100 % (long term) using solar energy and biomass
- Enhance both financial stability and market sustainability of medium or small-sized agro-industries for which the proposed SHM system should be suited for power and heat generation
- Identify appropriate market niches for first commercialisation of the solar hybrid cogeneration unit and also future market potential for solar hybrid microturbines (≤ 100 kW) to Brazilian agro-industries
- Improve public awareness about the technology

2.9.2 Introduction

Brazil has the political goal to increase the use of renewable energy and improve energy efficiency to reduce CO_2 emissions. Brazil has in several regions high solar irradiation levels which can efficiently be used in solar plants. In addition, the Brazil agro-industry is searching for environmentally friendly methods of energy production, including the efficient use of residues of its production processes (e.g. sugar production). There is a variety of small agro-industrial consumers that require reliable supply of power and heat in this industrial sector.

For example the fact that Brazil has a rapid growth in milk production, emerging today as world's sixth largest milk producer and growing at a 4 % annual rate. Brazil produces 66 % of the total milk produced in the South American Common Market. The future implementation of the proposed system technology on a larger scale will assist in providing renewable energy supply and increase the energy efficiency. On the other hand the solar-hybrid cogeneration systems can be built with a significant share of local products and work because the regions with high solar radiation coincide with low economic development status; development of the plants can be an important factor to improve economic and social conditions.

Programs focus on reducing greenhouse gas (GHG) emissions and on long-term sustainable development are appreciated in the governmental and private sector. On the other hand initiatives to support the increase of energy efficiency and to improved electricity access in rural areas are important programs of federal government. For that reason, actions like cogeneration from sugar-cane bagasse, wind energy and small-size hydroelectric power plants have been encouraged in Brazil. Yet, such actions are not able to reach medium or small-sized agro industries and fulfill their energy requirements to heat or electricity.

In this way a new technology for solar-hybrid microturbines developed in the SOLHYCO, using solar assisted co-generation of power and heat, like co-firing with biofuel is welcome in the Brazil energy matrix; the system ensures full power availability (power on demand) and represents a good opportunity to introduce a solar concentrated concept in the Brazilian market.

To introduce the SOLHYCO in Brazil the study is divided in three parts: The biofuel potential, solar radiation potential at selected areas for case studies and the study of technical issues for future pilot plants.

2.9.3 Biofuel Study

Biodiesel may become a prospective energy alternative because it is yielded from renewable biomass sources. Considered as an "ecologically correct" fuel, it significantly reduces emission of pollutants such as carbon monoxide, carbon dioxide and unburned hydrocarbons. In addition, it is almost free from sulphur and aromatic carcinogenic substances.

Benefiting from a large territory as well as from proper climate and soil, Brazil is a country presenting favorable conditions for biomass exploitation as food, chemical and pharmaceutical purposes and energy generation. In view of that, besides representing a strategic option to decrease the dependence upon oil products (with desirable and welcome advantages to the environment), biofuel use in Brazil corresponds to a new market for several oleaginous crops. It is certainly a valuable product for exportation as well. Given a diversity of raw material in the country different plants specialized in the production are distributed by all regions.

Biofuel is a biodegradable fuel derived from renewable sources. Chemically speaking, it can be obtained through different processes like cracking, esterification or transesterification. There are dozens of vegetables oleaginous species in Brazil from which it is possible to produce Biodiesel, including (but not restricted to) “mamona”, “dendê” (palm tree), sunflower, “babaçu”, peanut, tame nut and soy. The Brazilian diversity of raw material to Biodiesel production is an advantage for possible regional development and especially to the northeast where the production of this biofuel is incentivized with agricultural familiar program (see Figure 76).

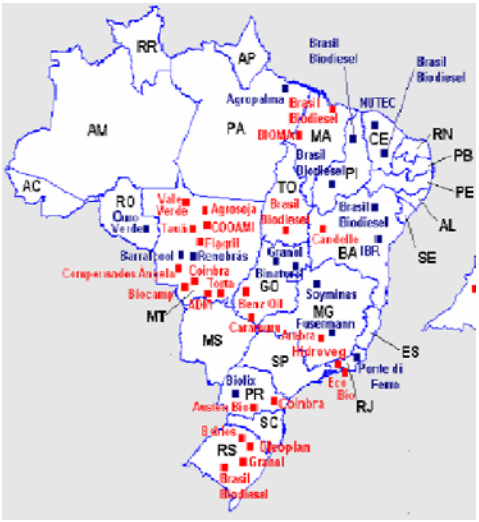

Figure 76 Brazilian distribution of Biodiesel plants.

The regions with the best solar radiation are northeast and center-west of the country. They are also Biodiesel producers. The possibilities to integrate the solar-hybrid concentrated technology with the agroindustrial chain for the biodiesel crops is a good market opportunity for the SOLHYCO technology.

2.9.4 Solar Radiation potential

The mission in Brazil is to evaluate potential places for solar plants. To analyze the potential data collected from the project SONDA (National Organization System for Environment Data), SWERA Project (Solar and Wind Energy Resource Assessment) and from Astronomy, Geophysics and Atmospheric Science Institute of USP (IAG) of three different regions in the country were used.

The System of National Organization of Environmental Data (SONDA) is a project of the Brazilian National Institute for Space Research (INPE) aiming at implementing physical infrastructure and human resources so as to raise and improve Brazil’s solar and wind power resources database and through the Division of Climate and Environment (DMA), the Center for Weather Forecasting and Climate Studies (CPTEC / INPE) is responsible for coordinating project activities in Brazil and in Latin America.

The SWERA project was initially managed by the United Nations Environment Program (UNEP), more specifically, by its Division of Technology, Industry and Economics (DTIE), in collaboration with more than 25 partners around the world. Due to the success of the project within 13 pilot countries in 2006 SWERA expanded itself into a full program. Its mission is to provide high quality information suitably formatted on renewable energy

resources for countries and regions around the world, along with the tools needed to apply these data in convenient way so as to facilitate renewable energy policies and investments.

In the following the results of the SONDA stations as well as the geographic details for each of the 3 studied regions are presented (see Figure 77).

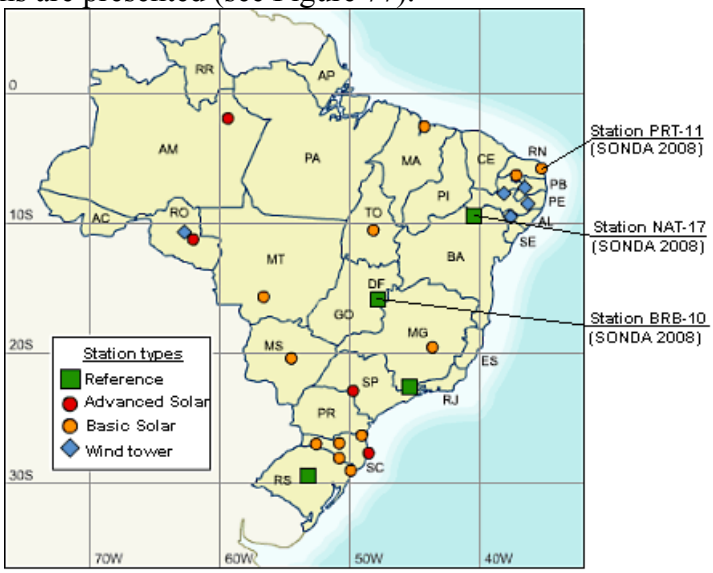

Figure 77 Location of SONDA stations (SONDA, 2008).

Details of each station are provided as follows:

Brasília station:
Identification: BRB – 10
Location: latitude 15° 36’ 03’’ S; longitude 47° 42' 47" O; altitude 1023 m
Time Zone: GMT-3
Data since: March 2006

Petrolina station:
Identification: PTR-11
Location: latitude 09° 04' 08" S; longitude 40° 19' 11" O; altitude 387 m
Time Zone: GMT-3
Data since: July 2004

Natal station:
Identification: NAT-17
Location: latitude 05° 50' 10" S; longitude 35° 12' 27" O; altitude 50 m
Time Zone: GMT-3
Data since: July 2007

Monthly data from the Sonda project in the three positions (cities) and two regions (Brasilia (centre-west region), Petrolina (northeast region) and Natal (northeast region)) and annual data from IAG (Sao Paulo southeast region) were used, as presented in Table 9 -Table 12.

Table 9. Brasilia's station: monthly normal direct radiation average

Year	Month	Average of normal direct radiation (W/m²)
2006	March	123.85
	April	161.12
	May	253.34
	June	270.21
	July	265.79
	August	286.50
	September	197.52
	October	---
	November	127.13
	December	134.67
2007	January	116.13
	February	133.38
	March	272.22
	April	184.97
	May	281.09
	June	273.26
	July	249.62
	August	295.26
	September	297.22
	October	196.18
	November	136.95

Table 10. Petrolina's station: monthly normal direct radiation average.

Year	Month	Average of normal direct radiation (W/m²)
2004	July	252.10
	August	232.10
	September	346.82
	October	355.92
	November	360.90
	December	362.89
2005	January	*
	February	183.93
	March	490.57
2007	January	*
	February	-8
	March	*
	April	712.15
	May	654.60
	June	588.66
	July	370.68

*Fail of data series.

Table 11. Natal's station: monthly normal direct radiation average.

Year	Month	Average of normal direct radiation (W/m²)
2007	July	243.44
	August	353.21
	September	395.84
	October	376.36
	November	380.50
	December	351.35
2008	January	207.23
	February	393.28
	March	339.37
	April	144.55

Table 12. Data from IAG for São Paulo: annual direct radiation average.

Year	Direct radiation (W/m^2)
1998	91.5383
1999	101.6219
2000	99.7075
2001	111.8147
2002	107.3439
2003	101.7900
2004	91.5683
2005	91.1333
2006	103.9844
2007	106.9103
2008	92.4039

The data show the potential difference between the regions of the country. For the Northeast region the potential of DNI is bigger than in the centre–west and southeast, but these regions have better conditions to Biodiesel crops, particularly the southeast region that is the mean economical region of the country. To analyze the feasibility of the SOLHYCO technology the Northeast and Southeast regions were elected, the first one because of the solar resource and the social goal, since this region is the one with the worst social indicators in the country, and the second one due to its economical importance.

Technical Issues

Data initially mined demonstrate the possibility of implementing at least three cases in order to gather further data to study and to check the economic feasibility of the proposed SOLHYCO technology under Brazilian conditions.

Data-mining was accomplished in three regions with large application potential of such technology in Brazil due to either climate or by strategic reasoning or finally due to a considerable impact on the social development of regions lacking energy production or distribution, so that they are case evocative to be followed during SOLHYCO Project. Such case choice was based on the goal set in terms of implementing distributed energy production and cogeneration sites, in a Brazilian region lacking energy offer; this way justifying all necessary investment.

One may summarize those follow-up proposals for the three different places as follows:

Case 1: Climate and market data acquisition for Brazil's northeast backwoods region in Rio Grande do Norte state, in a place where GEAGRO-USP has been already conducting another project named "Portal dos Ventos" (www.usp.br/unicetex). The idea was to analyze the feasibility of a pilot implementation allowing at the same time technology dissemination and interest raise from private and public companies, towards the development of a region lacking social and economic power.

Case 2: Climate and market data acquisition for Brazil's northeast region locally presenting great agribusiness development (based on rational use of irrigated tropical fruit crops) near Petrolina in the Pernambuco state. In this case, climate advantages are present and electricity demands occur provided that companies (packing houses) rely on fruit processing and refrigeration, aiming at internal and external market supply.

Case 3: Climate and market data acquisition for Brazil's southeast region at Lins, a countryside town in São Paulo state, which comprises a strategic region in terms of agroindustrial development and biomass production (ethanol and Biodiesel). A close relation is suggested with JBS Cold Store, a company that already employs cogeneration based on Biodiesel.

In the basic scheme to agro industrial application shown in Figure 78, the proposed system provides electricity and heat by cogeneration and refrigeration using a chiller, the sources are solar radiation and a biofuel for sunless periods. For each case the use of heat or cold can be estimated according the agro industrial application. This was done in a simulation.

Figure 78 Schematic representation of industrial application in agro industries.

Specific in the case 3 (Lins) is that the system can include the biodiesel factory to improve sustainability of the global process, like in the Figure 79. The chain in the picture shows a complete process cycle including the reduction of greenhouse gas emission and the possibility to improve the system profitability obtaining credits from Clean Development Mechanism (CDM). In this way the system has three inputs: an economical by CDM, raw material and an energy input by solar radiation. Outputs are the final product (beef), biofuel (Biodiesel) and electricity. Internally, the solar plant supplies cold, heat and electricity to the system (slaughterhouse and Biodiesel factory). In Brazil there exist similar systems using sugar-cane bagasse as energy source.

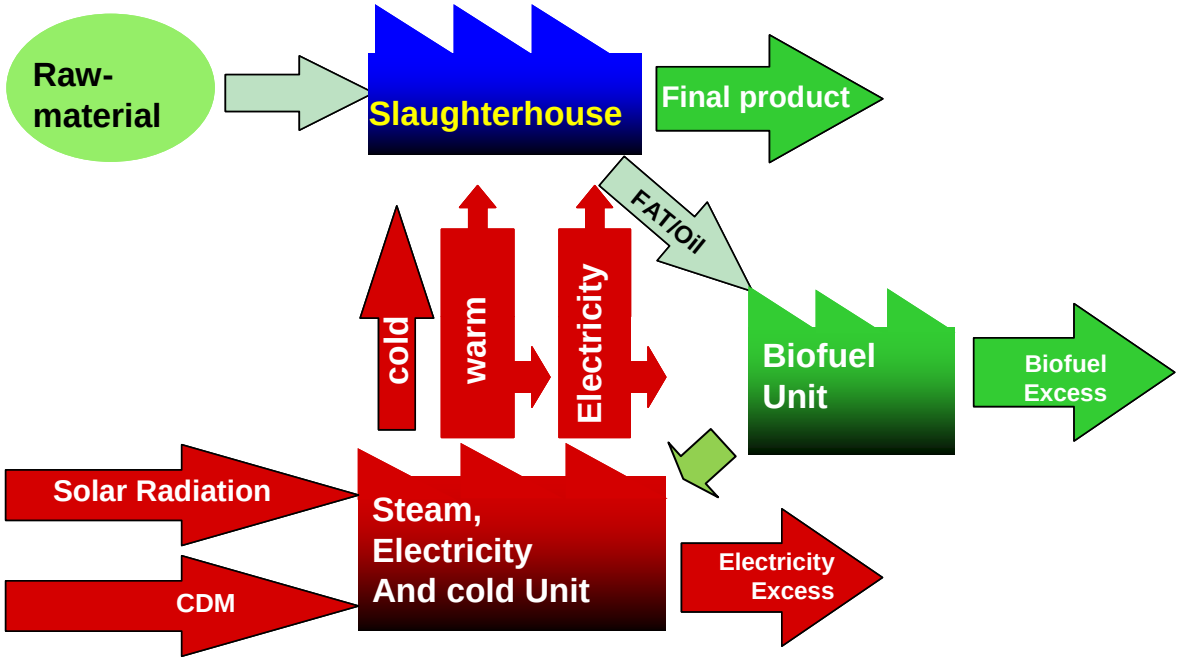

Figure 79 Concentrated Solar Power in beef production chain, Clean Development Mechanism (CDM).

Each case was simulated and the results are shown in the follow tables considering the system as presented in the Table 13.

Table 13. Data for simulating case 1-3

Case	Energy Demand					Annual Temperature Average (ºC)	DNI
	Electrical (MWh/year)	Heat (Mcal/year)	Heat (Kcal/hour)	Cold (Mcal/year)	Cold (Kcal/hour)		Annual (kWh/m^2*a)
1	5,096	50.7360	5.8398	714.84	82.2790	28.0	1,999
2*	252					26.7	2,041
3	5,760	41,273,602.75	4,750,644.88			23.3	2,065

* Only electrical demand.

Case 1 – Caiçara do Rio do Vento, RN.
Radiation data from Natal were used, the Table 14 shows the simulated results of the system.

Table 14. Performance to Case 1: Dairy in Caiçara do Rio do Vento (northeast region).

SOLHYCO performance		
engine output	357.14	[kW]
Electric power	100	[kW]
η_{el} Performance (real)	28.0%	
Solar thermal degree of efficiency per annum	47.0%	
Full load hours	4,000	h/a
Solar radiation	1,999	[kWh/m²a]
Mirror total surface	388.8	m²
Field degree of efficiency	63.41%	
Receiver degree of efficiency	77.7%	
Heat flow volume per year	1,428,571	[kWh]
Solar generated heat	382,929	[kWh]
Fossil generated heat	1,045,643	[kWh]
Solar share	27	[%]
Solar full load hours	1,072	[h]
Total electric revenue per year	400,000	[kWh]
Solar electric revenue per year	107,220	[kWh]
Biofuel electric revenue per year	292,780	[kWh]
heat losses without cogeneration		
Heat power	177.30	kW
Inlet temperature cogeneration system	280.00	°C
Outlet temperature cogeneration system	50	°C
Mean fluid temperature	165.00	°C
Heat capacity, air @ 1bar	1,027.80	J/KgK
Annual revenue of cogeneration system	709,182	kWh
micro gasturbine		
Engine output	357.14	kW
Electric power	100	kW
Mass flow	0.75	kg/s
Outlet temperature recuperator	280	°C
cogeneration system input		
Heat power	108.47	kW
Inlet temperature cogeneration system	280	°C
Outlet temperature cogeneration system	140	°C
Mean fluid temperature	210.00	°C
Mean fluid temperature	483.15	K
Heat capacity, air @ 1bar	1,033.01	J/KgK
Heat capacity, air @ 4.5bar	1,031.48	J/KgK
η Efficiency of cogeneration system	20	%
Engine power	21.69	kW
Annual revenue of cogeneration system	86,773	kWh
heat losses with cogeneration		
Heat power)	69.05	kW
Inlet temperature cogeneration system	140.00	°C
Outlet temperature cogeneration system	50	°C
Mean fluid temperature	95.00	°C
Heat capacity, air @ 1bar	1,023.02	J/KgK
Annual revenue of cogeneration system	276,214	kWh

In this case 100 % of the generated energy from the SOLHYCO system is used by the dairy. The configuration uses the maximum power (100 kW electrical) and operates on 4,000 full load hours. These conditions represent a good option for this region from the technical point of view. Despite some technical considerations this model takes into account the generation of new formal jobs and economic growth to local farms.

Case B – Petrolina - PE

Radiation data from Petrolina and in agreement with studies of CEPEL (Brazilian Electricity Research Center). Table 15 shows the simulated results of the system applied to a packing house.

Table 15. Performance to Case B: Packing house in Petrolina city (Northeast region).

SOLHYCO performance		
Engine output	357.14	[kW]
Electric power	100	[kW]
η_{el} Performance (real)	28.0	%
Solar thermal degree of efficiency per annum	47.0	%
Full load hours	4,000	h/a
Solar radiation	2,041	[kWh/m^2a]
Mirror total surface	440	m^2
Field degree of efficiency	60.5	%
Receiver degree of efficiency	77,7	%
Heat flow volume per year	1,428,571	[kWh]
Solar generated heat	422,155	[kWh]
Fossil generated heat	1,006,416	[kWh]
Solar share	30	[%]
Solar full load hours	1,182	[h]
Total electric revenue per year	400,000	[kWh]
Solar electric revenue per year	118,203	[kWh]
Biofuel electric revenue per year	281,797	[kWh]
heat losses without cogeneration		
Heat power	340.41	kW
Inlet temperature cogeneration system	280.00	°C
Outlet temperature cogeneration system	50	°C
Mean fluid temperature	165.00	°C
Heat capacity, air @ 1bar	1,027.80	J/KgK
Annual revenue of cogeneration system	1,361,629	kWh
Cogeneration SYSTEM performance		
micro gasturbine		
Engine output	357.14	kW
Electric power	100	kW
Mass flow	1.44	kg/s
Outlet temperature recuperator	280	°C
cogeneration system input		
Heat power	208.25	kW
Inlet temperature cogeneration system	280	°C
Outlet temperature cogeneration system	140	°C
Mean fluid temperature	210.00	°C
Mean fluid temperature	483.15	K
Heat capacity, air @ 1bar	1,033.01	J/KgK
Heat capacity, air @ 4.5bar	1,031.48	J/KgK
η Efficiency of cogeneration system	20	%
Engine power [kW]	41.65	kW
Annual revenue of cogeneration system	166,603	kWh
heat losses with cogeneration		
Heat power)	132.58	kW
Inlet temperature cogeneration system	140.00	°C
Outlet temperature cogeneration system	50	°C
Mean fluid temperature	95.00	°C
Heat capacity, air @ 1bar	1,023.02	J/KgK
Annual revenue of cogeneration system	530,332	kWh

In this case the system doesn't supply 100 % of the packing houses demand, but represents a good solution since electricity from the grid is available. Despite that the cogeneration has been used in the simulation, its use is not considered in the real model, because the system uses only cold from electricity. Thus the analysis of viability of cogeneration is impaired. Here the implementation of a solar technology is a new step of development process in the region inside the semi-arid zone of the country.

Case 3 – Lins – SP

Radiation data from São Paulo, IAG system. Table 16 shows the simulated results of the system applied to a slaughterhouse.

Table 16. Performance to Case 3: Slaughterhouse in Lins city (Southeast region)

SOLHYCO performance		
engine output	357.14	[kW]
Electric power	100	[kW]
η_{el} Performance (real)	28.0	%
Solar thermal degree of efficiency per annum	47.0	%
Full load hours	4,000	h/a
Solar radiation	2,065	[kWh/m^2a]
Mirror total surface	440	m^2
Field degree of efficiency	60.5	%
Receiver degree of efficiency	77.7	%
Heat flow volume per year	1,428,571	[kWh]
Solar generated heat	427,119	[kWh]
Fossil generated heat	1,001,452	[kWh]
Solar share	30	[%]
Solar full load hours	1,196	[h]
Total electric revenue per year	400,000	[kWh]
Solar electric revenue per year	119,593	[kWh]
Biofuel electric revenue per year	280,407	[kWh]
heat losses without cogeneration		
Heat power	340.41	kW
Inlet temperature cogeneration system	280.00	°C
Outlet temperature cogeneration system	50	°C
Mean fluid temperature	165.00	°C
Heat capacity, air @ 1bar	1,027.80	J/KgK
Annual revenue of cogeneration system	1,361,629	kWh
Cogeneration SYSTEM performance		
micro gasturbine		
Engine output	357.14	kW
Electric power	100	kW
Mass flow	1.44	kg/s
Outlet temperature recuperator	280	°C
cogeneration system input		
Heat power	208.25	kW
Inlet temperature cogeneration system	280	°C
Outlet temperature cogeneration system	140	°C
Mean fluid temperature	210.00	°C
Mean fluid temperature	483.15	K
Heat capacity, air @ 1bar	1,033.01	J/KgK
Heat capacity, air @ 4.5bar	1,031.48	J/KgK
η Efficiency of cogeneration system	20	%
Engine power [kW]	41.65	kW
Annual revenue of cogeneration system [kWh]	166,603	kWh
heat losses with cogeneration		
Heat power	132.58	kW
Inlet temperature cogeneration system	140.00	°C
Outlet temperature cogeneration system	50	°C
Mean fluid temperature	95.00	°C
Heat capacity, air @ 1bar	1023.02	J/KgK
Annual revenue of cogeneration system	530,332	kWh

In this case the model considers a Biodiesel factory side by side with the solar plant and the possibility to refrigeration by the cogeneration system upgraded with a chiller. The slaughterhouse is close to the energy complex (solar plant and Biodiesel factory). There is a high degree of sustainability in this model since the fat used in the Biodiesel factory is a big environmental problem. Some big slaughterhouses have excess of fat (normally used to make soap). The Clean Development Mechanism opens the possibility to apply projects on energy efficiency, thus reducing methane and the consumption of fossil fuel. In any of our cases CDM can be applied, because the results led to best energy efficiency, reduction on fuel in the Biodiesel process and reduce the consumption of grid electricity, which is also generated from thermal plants from fossil fuels (although Brazil has a high RE share).

Adapting the conceptual system design to the commercial conditions and Brazilian cases, it is proposed to provide the heliostat field by a commercial producer, but with the possibility to be made in Brazil. The receiver, insulating cavity and the tower can also be manufactured in the country by either a SOLHYCO partner or by other national suppliers. Until reaching a high market volume being attractive for local productions, the microtubine and control system certainly would still have to be imported from European countries to supply the Brazilian projects.

2.9.5 Conceptual design of SHM system prototype available for potential market insertion in Brazilian rural areas

The system based on the SOLHYCO technology adapted to commercial conditions and Brazilian cases could be defined as:

Equipments

Turbine
Turbec T100

Heliostats
Considering the potential of solar radiation in the three regions studied and the estimated demand of a system of 100 kW electrical, a heliostat field with 388,8 m² of total mirror area ir required which is composed of 27 heliostats with 14.4 m^2 each. The model considered is similar to a commercial model made by Brightsource. This or similar commercial models may be provided in a near future, including the possibility of local manufacturing in Brazil.

Receiver
The receiver could be manufactured in Brazil by GEA (partner in SOLHYCO project). GEA has a factory in Brazil providing all conditions for a serial production of receivers.

Receiver cavity/ radiation shield
The cavity is a highly insulated structure to minimize heat losses of the receiver. The inner side has to withstand temperatures up to 1000 °C and the heat loss through the wall should be less than 10 kW at an average temperature of the inner side of 800 °C. The wall has to be airtight. Especially challenging is the area where the absorber tube leaves the cavity. The cavity in the SOLHYCO project was made of two overlapping layers of 25 mm microtherm sheet with a silica textile around the inner layer.

The cavity could be manufactured in Brazil if a suitable company is found.

Tower
The function of the tower is the positioning of the receiver (height and aperture angle) according to the heliostat field layout. Here, the aperture angle is chosen as 80° and the aperture diameter as 0.798 m, considering the position in Caiçara do Rio do Vento (latitude 5.70°, longitude 36.06°).

A further question concerning a tower construction is the mounting of the receiver and the turbine. The non-availability or high renting costs of a mobile crane would justify a fixed crane on the tower. For example, a triangle tower concept (1) and the tripod concept (2) (see Figure 80) could be equipped with a simple cable winch that moves the whole receiver room up. Due to the optical requirements a 22.0 m tower is necessary.

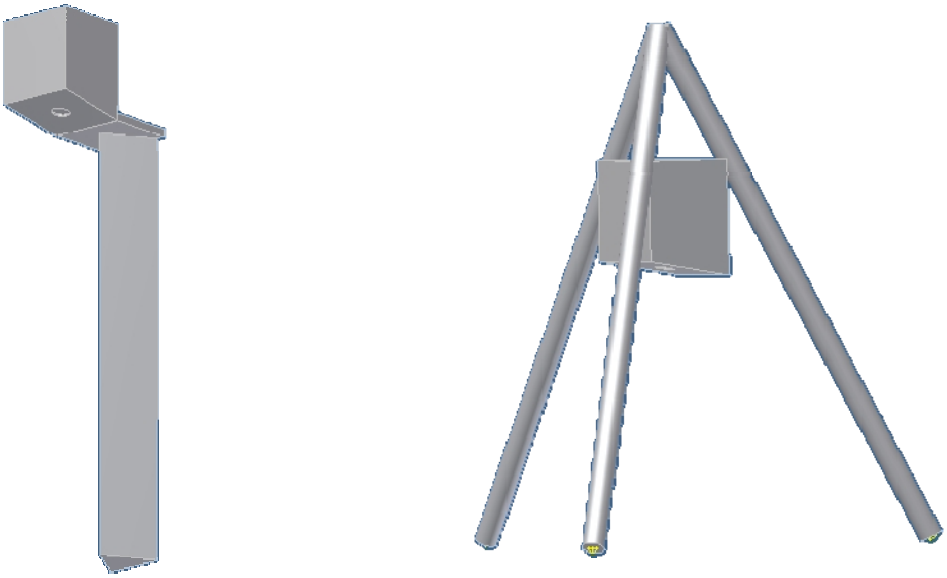

Figure 80 Tower concept 1 (Triangle tower), Tower concept 2 (Tripod).

System layout
In the solar-hybrid mode fuel is used in the combustion chamber to heat the hot air from the receiver further. By this the maximum turbine inlet temperature (TIT) is 950 °C and therefore the maximum power of about 100 kWel (depending on the ambient temperature) can be achieved at any time. The 950 °C TIT results in about 650 °C turbine outlet temperature (TOT) which heats the air from the compressor to about 600 °C (receiver inlet temperature). With an airflow of about 0.75 kg/s through the receiver this results in a thermal power of the receiver of 180 kWth. A resume of the conceptual design of the system is given in Table 17.

Heliostat field layouts
For the system described above the heliostat field with the layout considering 14.4 m² per heliostat and design point receiver power 180 kWth (solar-hybrid) is presented in Figure 81.

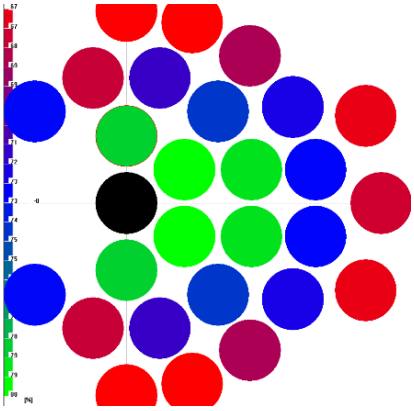

Figure 81 Heliostat field layout

Table 17. Resume of conceptual design of SHM system.

Total heliostat number [-]	Total mirror area [m2]	Optical tower height [m2]	Aperture diameter [m]	Aperture angle [°]	Total field efficiency [-]
27	388.8	22.044	0.798	80	0.6341

2.9.6 Institutional report and report on market assessment of Brazil

The market assessment study was divided in three steps to create an organized model to introduce the CSP technology in Brazil. First, two workshops were organized to introduce and discuss the SOLHYCO technology with specialists from the government, private sector and academy. Second, the official plans of the government to the energy matrix were compiled and third, international documents on the CSP technology were consulted.

The many important discussions upon solar thermal energy and cogeneration production conducted during the SOLHYCO dissemination activities revealed some new perspectives for the Brazilian society accustomed to think of solar energy only from the photovoltaic perspective. A large application potential of such technology in Brazil was acknowledged due to either climate or by strategic reasoning or finally due to a considerable impact on the social development of regions lacking energy production or distribution. The discussion also pointed to a near future economic feasibility of the proposed technology. Some companies and governmental sector knew about the technology and showed interest in international projects as mean conclusion from the workshops.

As a main benefit of the established partnerships, one should mention a proposal for a climate initiative project named SMILE-pro (Solar-hybrid Microturbine systems for rural electricity production. This project based on SOLHYCO includes the design and erection of two modular solar-hybrid microturbine systems for small grid / off-grid power and heat generation and the use of biofuels for fully CO_2 neutral operation.

From the official documents three different statements can be deducted for Brazil:
- Brazil has made changes in its energy policy in order to promote greater diversification in the electricity generation matrix;
- Alternative energy sources in Brazil have been introduced by means of incentive policies, based on the formation of a market, using the state purchasing power as its principal stimulus;
- The value of kWh generated was not yet competitive with the sources traditionally used in the Brazilian energy matrix, and the process of expansion planned by the government

envisages a gradual increase in the use of energy from fossil fuels or nuclear power, which leads on one hand to values higher than for the hydro sources (accounting for more than 90% of the current generation level), on the other hand it also increases interest in sustainable sources that can maintain the current level of low emission of electricity supply.

For the Brazilian government solar systems need a drastic cost reduction to be competitive with the hydro electricity and in near future with the wind power. Although international trends are to reduce costs as presented in the CSP road map and others document of the International Energy Agency (IEA), Brazil won't go to participate in these favorable scenarios if not taking part in research and technological development.

.

In this scenario the market assessment for technology can be concluded that:

- Changes in the Brazilian energy matrix leading to an increase in the emission of greenhouse gases represent an opportunity to clean technologies.
- The international expectative on a cost reduction can be a factor of stimulus for new investments in solar plants in Brazil.
- the agribusiness sector as consumer of electricity and thermal energy is a market niche for cogeneration based on solar energy.
- Finally, Brazil's government and the private sector need to stimulate research and development for the Hybrid Solar participating in the global market to introduce solar power plants in the country.

2.10 Market Assessment Mexico

2.10.1 Objectives

- Identify appropriate market niches for first commercialisation of the solar hybrid cogeneration unit;
- Identify future market potential for solar hybrid power plants (>20 MWe);
- Improve public awareness about the technology.

2.10.2 The Solar Resource in Mexico

For the electricity and heat generation the fuel becomes an important factor and it determines in great measure the economy of the plant. The cost of the different fossil fuels constitutes a fundamental factor for the taking of decisions on the localization of a conventional plant. For the solar thermal power plants the "fuel" is free of cost. Mexico has a territory with an area close to 2 million square kilometers. Solar energy is an abundant resource in Mexico, more evenly distributed over the national territory than wind, biomass or hydropower. The Instituto de Investigaciones Electricas (IIE) has a geographical information system (GIS) as tool for handling of information on the resources and the technologies of renewable energy. Among the tools GIS is available for the evaluation of the solar resource. The information presented by the GIS was generated from most advanced modeling tools with input data from satellite images. An analysis was carried out to determine the distribution of the monthly average Direct Normal Irradiance (DNI) in kWh/m^2-day with the purpose of determining the territorial distribution of the resource. Yearly average DNI in the whole territory is shown in Figure 82; different colors indicate the intensity of the resource, corresponding in red the areas of highest intensity and in yellow the area of lowest intensity.

Figure 82 Territorial distribution of Solar Resource

Detailed exploration of the country to identify state by state the levels of average DNI per year (kWh/m^2-year) was also carried out. The analysis showed areas in the country with DNI levels between 2157 and 2800 kWh/m2-year including: extensive portions of the Baja California peninsula and Sonora, smaller portions of the states of Chihuahua, Coahuila, Durango, Guerrero, Nayarit, Michoacán, Sinaloa and the peninsula of Yucatan. Areas of DNI between 1750 and 2156 kWh/m2-year include portions of the states: Aguascalientes, Campeche, Chiapas, Colima, Hidalgo, Guanajuato, Mexico state, Jalisco, Morelos, Nuevo León, Puebla, Querétaro, Quintana Roo, San Luis Potosí, Tabasco, Tamaulipas, Tlaxcala, Yucatan and Zacatecas. Areas with less than 1750 kWh/m2-year constitute relatively little territory, corresponding in portions of the states of: Veracruz, Oaxaca and Puebla. The analysis concludes that there are zones in the country that potentially are suitable for deployment of CSP mainly in the northwest, north and central-north portions, which are considered having low precipitation and high percentage of clear days through the year.

2.10.3 General Methodology for the Market Assessment

In Mexico, studies have been carried out by the National Commission for the Efficient Use of the Energy (CONUEE, Comisión Nacional para el Uso Eficiente de la Energía) to determine the potential of cogeneration. However, these studies have not considered the possibility for integrating an additional source of heat like the concentrated solar energy to the cogeneration system. The methodology for the evaluation of the cogeneration potential for the SOLHYCO technology is based on the information from the National Balance of Energy published by the Energy Secretariat of Mexico identifying the type and quantity of fuel used by different sectors, following the next steps:

- Review of the current state of the primary energy production, the net balance of the energy, the internal offer of primary energy, the gross production of secondary energy, the national consumption of energy and the final consumption by sectors.
- By economic sectors the demand of fuels (type and quantity) is determined. The corresponding portion to the electricity consumption coming from Federal Electricity Commission (CFE, Comisión Federal de Electricidad) is excluded.
- By means of analysis of the different sectors is determined which sector or sectors are the most appropriate for the implementation of the cogeneration systems assisted with concentrated solar radiation.
- It is assumed that the consumed fuel is fed to a cogeneration system and transformed in thermal and electric energy.

- It is assumed that the cogeneration system will have a global efficiency of 70 %, corresponding to 30 % in the electricity generation and 40 % in the efficiency of conversion of useful thermal energy.
- The operation of the cogeneration system would be 100 %
- Establish scenarios based on the described assumptions and evaluate finally the cogeneration potential .

Primary Energy Production (PEP) includes those energy products that are extracted or captured directly from natural resources as the mineral coal, crude oil, condensed, natural gas, nuclear energy, hydro-energy, geothermal energy, wind energy, sugarcane trash and firewood. PEP is used as input to obtain secondary products or it is consumed in direct way. In 2008, PEP was 10,500 Petajoules (PJ=10^{15} Joules). Hydrocarbons still remain as the main source, when contributing 89.1 % of the PEP. Inside the hydrocarbons, the biggest participation is given by the crude oil with 69.7 % and natural gas with 29.3 %. After hydrocarbons, primary electricity follows in importance contributing with 5.4 % of the PEP, 68.2 % corresponds to hydroenergy, 18.8 % nuclear, 12.4 % geoenergy and 0.5 % wind energy. The production of coal was 2.2 % and the production of biomass 3.3%.

Total Final Consumption (TFC) is the energy and the raw material dedicated to the different sectors of the economy for their consumption and is divided in non-energetic and energetic consumptions (5,101.2 PJ). Non-energetic consumption registers the consumption of primary and secondary energy as raw material in the processes of non energy commodities (286.3 PJ), for example: Petrochemical PEMEX (Mexican Petroleum Company) uses dry gas and oil derived to elaborate plastics, solvents, polymers, rubber, among others.

Energy final consumption refers to the fuels used by different sectors as follows (4,814.9 PJ):

- **Transport sector**: is the first energy consumer of the country, 2,472 PJ, 50.4% and is constituted by fuels used as: Auto-transport, Aircrafts; Railroad, Marine, Electricity.
- **Industrial sector:** is the second consumer of energy with 1341.7 PJ, 27.9 % and includes all the productive processes of the industry in which 16 branches stand out: iron and steel industry, petrochemical of Pemex, chemistry, sugar, cement, mining, cellulose and paper, glass, fertilizers, beer and malt, automotive, beverages, construction, aluminum, rubber and tobacco in the country.
- **Residential, commercial and public sector:** is the third energy consumer of the country, 900.8 PJ, 18.7 % and is constituted by 3 subsectors, residential, commercial and public. Residential register the consumption of fuels in the urban and rural homes. Commercial is the energy consumption in local commercial, restaurants, hotels, among other, and Public service includes the energy consumption in the public lighting, pumping of potable water and waste waters.
- **Agricultural sector:** is the smallest consumer with 144.7 PJ, 3 %, energy is consumed to carry out all the related activities directly with the agriculture and the cattle raising.

At this point it is being important to define which sectors are the most suitable for concentrating solar power applications. Transport sector is the biggest energy consumer but its activity is incompatible with the CSP technology. The sector that would be very interesting is the agricultural. However, this sector, thanks to the government support, receives an extraordinary subsidy in the electric tariff. The residential, commercial and public service sectors have a strong use in urban areas where a competition would exist for the land use. However, rural areas, as well as in other nations, are characterized also in Mexico by low population density, lack of services (including electricity and potable water mainly), and low income people, not familiar with modern technology. Therefore it is a segment that could be

an interesting market for new generating technologies. Another appropriate sector would be the industrial sector. There might exist incompatibility for the land use in some cases, but in general the industrial parks are located outside of the urban areas. In this study the cogeneration potential will only be considering the industrial sector and the segment of rural population.

2.10.4 Industrial Sector Potential

A list of industrial branches and the type of the consumed fuel are shown in Table 18. It contains the most intensive branches in energy use with 68 % of the total consumption of the industry. The other branches consume 32 % (428.88 PJ) of the energy of the sector. In this concept they group the rest of the less intensive industries of the country like: foods (milk, coffee, etc), tobacco, textile, wood, leather, ceramic products, manufacture of furniture and industrial equipment, etc.

Table 18. Energy Consumption Industrial Sector (PJ), 2008

	Coal	Sugarcane	Coal coke	Oil coke	Gas LP	Diesel	Fuel oil	Dry gas	Electr.	Total
Total	7.59	97.5	93.11	144.67	42.64	58.11	83.56	431.06	383.56	1341.79
PEMEX Petrochem						0.47	0.22	26.97	0	27.66
Iron-Steel			86.08	6.87	0.01	1.28	8.63	139.99	30.44	273.29
Chemical				13.97	0.82	5.37	9.39	54.08	18.78	102.41
Sugar		97.26				0.04	6.03		0.36	103.68
Cement	7.59			90.41		0.28	28.21	7.66	16.34	150.48
Mining			7.02		3.69	5.39	5.96	33.89	20.93	76.88
Celluose-paper		0.24			0.46	1.42	11.28	28.5	9.91	51.8
Glass				0.01	0.14	0.16	4.2	45.98	4.26	54.74
Malta-beer					0.7	0.14	7.12	8.41	3.23	19.59
Fertilizers						0.15		3.34	0.55	4.05
Automotive					0.4	0.6		2.24	7.05	10.29
Beverages					1.18	3.96	1.54	3.21	3.05	12.95
Construction						10.47			1.7	12.18
Rubber					0.01	1.7	0.58	4.2	1.64	8.13
Aluminum					0.04	0.01		1.17	3.11	4.34
Tobacco							0.01	0.22	0.2	0.43
Other branches				33.41	35.21	26.66	0.4	71.21	261.99	428.88

Note: 16 industrial branches corresponding to the most intensive (68%) + other branches (32%)
Other branches include industries: food, milk, textil, wood, etc

In order to determine the potential of the industrial sector three scenarios were established.

- High scenario, it is taking into account the entire industrial sector but excluding electricity given by CFE
- Medium scenario, including all the industrial branches but excluding electricity, oil coke as fuels, and all the intensive industry (except beverages and rubber)
- Low scenario, same conditions as medium scenario, but excluding gas drying..

High Scenario: according to the Table 18, if electricity is suppressed, the total energy consumption of the industrial sector would become 958.23 PJ. All the energy would be available for cogeneration purposes. Also it is assumed that the total consumed fuel is fed to a cogeneration system transformed in thermal (40 % efficiency) and electric energy (30 %) and operation of the cogeneration system 100 % around the year. The final result would be **9090 MWe** (electrical energy) and **12,120 MWt** (thermal energy available for process). However,

this scenario although impressive only proves that potential is quite interesting and potentially could be demanded by the industry. In accordance to studies made in the past by the CONUEE more realistic potential could be defined if different sectors are eliminated as a consequence of that they do not use steam or utilization is minimum. Such industries are the iron-steel, cement, glass, automotive, construction and mining industries. Under this assumptions the cogeneration potential could be reduced to **4374 MWe** and **5832 MWt**. This scenario could be a very interesting opportunity to the projected SOLHYCO technology at big scale with plants of more than 20 MWe displacing natural gas. This power is taking into consideration the tendency in the Mexican industry using cogeneration systems.

Medium Scenario: this takes into account the same assumptions for efficiencies and operation hours, but rejecting electricity and oil coke as fuels and all intensive industry (except other branches, beverages and rubber). The energy consumption of the reduced industrial sector would become 149.87 PJ, translated to power it would be **1421 MWe** and **1895 MWt.** The medium scenario is suitable for cogeneration systems from 1 to 20 MWe where the displaced fuels are mainly natural gas and fuel oil.

Low Scenario: It uses the same assumptions as in the medium scenario but excluding dry gas. The energy consumption of the reduced industrial sector would become 71.25 PJ, translated to power it would be **675 MWe** and **901 MWt.** It would be ideal for starting the SOLHYCO technology in the industry especially at small industry where diesel and liquefied gas are used more intensively.

In summary in Table 19 all above discussed different scenarios are presented. The scenarios presented determine the cogeneration potential for the whole national territory according to all assumptions discussed. Three zones (northwest, north and central-north) comprising seven states were selected as candidates for this purpose. With the purpose of defining the potential for these areas starting from the national potential and taking into account the low scenario that is the most appropriate as start-up of the technology SOLHYCO in the country, the following considerations were made:

- The Total Final Consumption (**TFC**) of energy by region was identified. Each region corresponds to the definition of the National Balance of Energy.
- Each region has different consumptions, it also includes consequently other states that are not considered in the study, a demand factor was determined ($\mathbf{f_d}$)
- The Demand by each of selected States (**DS**) includes the consumption of all the sectors; a factor by sector is defined ($\mathbf{f_s}$).
- Defined the Demanded Energy (**DE**) by the industrial sector a scale factor ($\mathbf{f_{sc}}$) was determined and comparable according to the demanded energy at national level in the low scenario.
- Total energy demanded by the "reduced industrial sector" (**RIS**) is estimated.
- Finally potential of cogeneration for the three selected zones, through the RIS and with convenient unit conversion, is determined

The results of this procedure are summarized in Table 20. The last column shows what might be considered as the potential for the cogeneration generating capacity that could be supported with the energy contents of the solar resource using the technology SOLHYCO. The total potential reported **(124 MWe, 165 MWt)** is roughly equivalent to 2.5 times the current installed capacity for cogeneration in the selected states.

Table 19. **National Potential of Cogeneration (Industrial)**

Scenarios	Electrical energy (MWe)	Thermal Energy (MWt)
Low	675	901
Medium	1,421	1,895
High	4,374	5,832

Table 20. **Industrial Cogeneration Potential in Mexico (low scenario)**

Region	TFC (PJ)	f_d (%)	D_s (PJ)	f_s (%)	DE (PJ)	f_{sc} (%)	RIS (PJ)	Cogeneration Potential MWe	MWt)
Northwest	499.94	80	399.95	28	111.98	5.3	5.93	56	75
Northeast	797.14	41	326.82	28	91.50	5.3	4.84	46	61
Central-West	970.91	16	155.34	28	43.49	5.3	2.3	22	29
Total	**2267.99**	-	**881.49**	-	**246.97**	-	**13.07**	**124**	**165**

2.10.5 Rural Area Potential

According to population's national count carried out by the INEGI (National Institute of Statistics and Geography) by the year 2005, the electric power supply arrives to near 137 thousand towns (133,345 rural and 3,356 urban) and the national population has the service (96.64 %). The total population of Mexico in 2005 was nearly 103 million inhabitants from which near to 15 million are living in the three study regions as is shown in Table 21. The study regions show approximately 2.74 % without electricity which is equivalent to 402,366 inhabitants. These numbers are considering urban and rural population. According to the statistics, rural population amount is not defined. However, the degree of electrification of the country indicates that most of the urban areas are electrified. Therefore, in order to make an estimation of the rural population we are taking 90 % of the inhabitants without electricity and living in rural areas, that is 362,000 inhabitants.

Table 21. **Level of Electrification of the Study Area**

		Inhabitants			
		Total	With Electricity	W/o electricity	Not specific*
Region	**Mexican states**	100,028,461	96,663,124	2,469,642	895,695
NorthWest	**Baja California**	2,604,782	2,526,478	38,301	40,003
	Baja California Sur	483,686	463,679	13,751	6,256
	Sonora	2,314,698	2,250,409	42,915	21,374
North	**Coahuila**	2,450,186	2,415,266	18,831	16,089
	Chihuahua	3,078,953	2,920,843	130,671	27,439
Central North	**San Luis Potosí**	2,380,536	2,237,654	132,251	10,631
	Zacatecas	1,352,911	1,318,470	25,646	8,795
	Total	14,665,752	14,132,799	402,366	130,587

*Inhabitants without information according to INEGI

According to the national network of electricity there are certain areas without service, mainly rural areas. These areas could be a good niche for the SOLHYCO technology especially for off-grid applications and can be anticipated as follows:

- Mini-grids for village power (domestic and public service)
- Village productive applications such as: water desalination and pumping, ice making and refrigeration, machine shops and agro-industries

The above described applications constitute the core of the off-grid market for the SOLHYCO technology applied in the rural environment. An estimation of the size of such market was

made using the following assumptions. Non electrified rural population of 362,000 inhabitants was determined in the previous paragraph and distribution among the three regions as shown in Table 22. Average consumption per inhabitant per year was estimated from the value of the average national consumption which is 80 GJ/inhabitant-year, rural population consumption is much less and it was assumed as 30 GJ/inhabitant-year. This value is comparable to the value reported in other studies. Under these considerations the last two columns show the estimated potential for the rural population. The power required to electrify total rural communities inside the study regions is around **103 MWe with 137 MWt** available as thermal energy. The implementation of the cogeneration system could be through localized mini-grids with thermal energy useful for productive activities as was mentioned above.

Table 22. Rural population; estimated potential of cogeneration

		Inhabitant					
		Total non electrified population	**Non electrified rural population**	**Average Consumption per inhabitant (GJ/year)**	**Total consumption (PJ/year)**	**Estimated Potential**	
						MWe	**MWt**
NorthWest	**Baja California**	38,301	34,471	30	1.03	9.81	13.08
	Baja California Sur	13,751	12,376	30	0.37	3.52	4.70
	Sonora	42,915	38,624	30	1.16	10.99	14.66
North	**Coahuila**	18,831	16,948	30	0.51	4.82	6.43
	Chihuahua	130,671	117,604	30	3.53	33.47	44.63
Central North	**San Luis Potosí**	132,251	119,026	30	3.57	33.87	45.16
	Zacatecas	25,646	23,081	30	0.69	6.57	8.76
	Total	402,366	362,129	30	10.86	103.06	137.41

2.10.6 Value Market Potential

The SOLHYCO technology proposed is using solar energy and fossil fuel operating in hybrid mode. Inside the calculations it is important to know how the DNI value is influencing the energy cost. As known the output energy is a function of such value and the energy cost is inversely to the DNI value. The selected regions have values of DNI which are from 2200 to 2800 kWh/m^2-year. Figure 83 shows the influence of the DNI value on the Levelized Energy Cost (LEC). These numbers were determined for the comparison of the SOLHYCO system operating under different scenarios (with or without cogeneration unit). The LEC value is running from a minimum value of 0.148 €/kWh until 0.151 €/kWh corresponding to a SOLHYCO system with cogeneration and from 0.185 €/kWh to 0.189 €/kWh when SOLHYCO would be operated without cogeneration unit. As a rule, minimum LEC values mainly are correlated with the states located at the northwest region. At industrial level the energy cost is variable and depends on the time consumption and the size of the industry. In 2008, the tariff of electricity was from a minimum of 0.05 €/kWh to 0.11 €/kWh covering as well the small as the big industries. At this level of energy cost the SOLHYCO technology can be seen as non competitive. However, fewer subsidies are announced by the government and when fuel costs are increasing industries will be forced to seek other alternatives. At rural level the case is much more promising since there are zones completely isolated where the cost of the energy with Diesel generators is around 0.16 €/kWh. Thus the SOLHYCO technology could be deployed in Mexico; the market is very interesting as shown in Table 23.

A market of more than 2000 SOLHYCO units and an investment of almost 800 million Euros was estimated as total potential for Mexico. For the near term, the rural market to which SOLHYCO is already close to be competitive certainly offers a great chance with 1000 units at 350 million Euros investment.

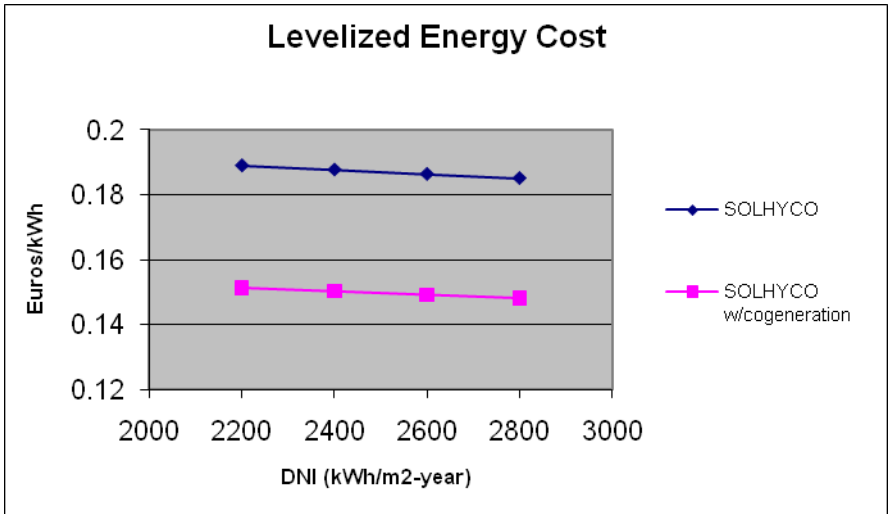

Figure 83 Energy Cost as Function of DNI

Table 23. Market Value of the SOLHYCO Technology

Region	Industrial Sector			Rural segment		
	MWe	Estimated Units	Investment Million Euros	MWe	Estimated Units	Investment Million Euros
Northwest	56	560	192.6	24.5	245	84.3
Northeast	46	460	158.2	38	380	130.7
Central-West	22	220	75.6	40.5	405	139.3
Total	**124**	**1240**	**426.4**	**103**	**1030**	**354.3**

2.10.7 Dissemination Activity

Inside of the activities of the SOLHYCO project a workshop was contemplated. The workshop was carried out with representatives of the government's institutions, industrial and academic of the country whose purpose was to describe the activities and advances of the denominated project SOLHYCO. Unfortunately, the workshop was held after the end of the project due to organization reasons (availability of infrastructure and incompatibility of the attendees' calendar). Nevertheless the results are provided to the project as described later. On July 15th, 2010, in Mexico City at the facilities of the CONUEE (Comisión Nacional para el Uso Eficiente de la Energía) the workshop "Taller de Sistemas Híbridos Solar-Gas para Cogeneración" (Workshop for Hybrid Systems Solar-Gas for Cogeneration) on the Concentrating Solar Power (CSP) with systems of central receiver and solar-hybrid microturbine for electric generation and process heat was held. In this occasion, the event was organized by the Instituto de Investigaciones Electricas, through the Department of Non Conventional Energy, as part of the contribution from IIE to the activities of the SOLHYCO project. Also, the support for the organization of the event from the CONUEE was very important. The event was able to gather more than 30 attendees of diverse entities of the public sector and private, as well as representatives of educational institutions. The conferences presented first the current situation of the CSP technologies, next the situation of the cogeneration in Mexico, later the detailed description of the project SOLHYCO and finally the potential of application of the SOLHYCO technology in Mexico. The presentation

of the CSP technologies was able to wake up interest among the participants Although these technologies have had a strong impulse in some other countries, in Mexico like in many others a lack of knowledge of the CSP still exists. The cogeneration in Mexico with fossil fuels is known but industrial sector made a claim to the government in order to establish better conditions for its exploitation. The presentation of the technology SOLHYCO was received with interest by the participants. They recognized the value of this emerging technology and that its application in Mexico could have a good acceptance, mainly for the use of a fuel that is distributed in the whole country and free of cost like the solar energy. In the presentation of the cogeneration potential in Mexico by means of solar energy, the public recognized, first the technological value of the concept and second that combined efforts should be gathered between government and private sector to undertake projects like SOLHYCO in benefit of the environment and the energy sustainability of the country. For the SOLHYCO project a web site was created and updated in Spanish version (http://www.iie.org.mx:8080/SitioGENC/SOLHYCO/). This web site is containing the project results and general information concerning the technology. Finally, two papers regarding to the project were presented at two different congresses and one more is expected after the end of the project.

2.11 Conclusions

The SOLHYCO project could demonstrate for the first time a dispatchable 100 % renewable electricity generation with a commercial gas turbine based on biofuels. Even the operation of a gas turbine without any fuel, just with solar energy, was shown.

SOLHYCO developed the very promising PML tube technology for solar receivers, which should be implemented and tested to demonstrate high efficiencies at less stresses. Long term behaviour should be further investigated.

The cost study and market assessment showed that the system is very close to be economically viable in markets as Algeria or even commercial markets with high cost levels of higher than 0,10 €/kWh.

First project proposals for the broader demonstration of the microturbine system have been brought on the road. In 2011 the decision for the construction of two units in Brazil is expected. Another demonstration plant based on the SOLHYCO results has been initiated with financial support of the EC. The project SOLUGAS will be a scale-up to 5 MWe based on preliminary results of the SOLHYCO project. It will be constructed at the Abengoa site in Seville in 2011. This will be the biggest tower plant based on gas turbine technology worldwide.

Implication for the SOLUGAS project:

In addition, it should be mentioned that thanks to the extension of the SOLHYCO project several goals could be achieved which can be seen as a significant progress in this technology. Especially the SOLUGAS project will profit from the final results of the SOLHYCO project.

The major achievements of SOLHYCO which can be useful for SOLUGAS are:

- successful test and evaluation of a first prototype of a solar-hybrid microturbine system

- demonstration of stable receiver and system operation at the design outlet temperature of 800°C
- manufacturing of PML sample tubes and demonstration of their superior thermodynamic characteristics in a laboratory-test
- verification of the method for compensating thermal expansion of the tubes for the first time in such configuration
- validation of a new detailed simulation model of the receiver coupling a ray-tracing tool for the solar flux distribution with a Finite-Element-Model (FEM) for the evaluation of temperatures and stresses
- verification of the effectiveness of a quartz glass cover at the cavity entrance for an optimized receiver design, allowing for efficiencies of up to 85 %

It could also be observed that the new developed ceramic receiver cavity was not performing as desired, which should be kept in mind for SOLUGAS.